SEISMIC ASSESSMENT OF A TRADITIONAL RESIDENTIAL BUILDING IN ANTAKYA AFTER 2023 TÜRKİYE EARTHQUAKE SEQUENCE

A THESIS SUBMITTED TO
THE GRADUATE SCHOOL OF NATURAL AND APPLIED SCIENCES
OF
MIDDLE EAST TECHNICAL UNIVERSITY

BY

HASİP ATICI

IN PARTIAL FULFILLMENT OF THE REQUIREMENTS
FOR
THE DEGREE OF MASTER OF SCIENCE
IN
CONSERVATION OF CULTURAL HERITAGE IN ARCHITECTURE

DECEMBER 2024

Approval of the thesis:

SEISMIC ASSESSMENT OF A TRADITIONAL RESIDENTIAL BUILDING IN ANTAKYA AFTER 2023 TÜRKİYE EARTHQUAKE SEQUENCE

submitted by **HASİP ATICI** in partial fulfillment of the requirements for the degree of **Master of Science** i**n Conservation of Cultural Heritage in Architecture, Middle East Technical University** by,

Prof. Dr. Naci Emre Altun
Dean, **Graduate School of Natural and Applied Sciences** _____

Assoc. Prof. Dr. Ayşem Berrin Çakmaklı
Head of the Department, **Architecture** _____

Assoc. Prof. Dr. Pınar Aykaç Leidholm
Supervisor, **Architecture, METU** _____

Prof. Dr. Murat Altuğ Erberik
Co-Supervisor, **Civil Engineering, METU** _____

Examining Committee Members:

Prof. Dr. Neriman Şahin Güçhan
Architecture, METU _____

Assoc. Prof. Dr. Pınar Aykaç Leidholm
Architecture, METU _____

Prof. Dr. Murat Altuğ Erberik
Civil Engineering, METU _____

Prof. Dr. Güliz Bilgin Altınöz
Architecture, METU _____

Assoc. Prof. Dr. Umut Almaç
Architecture, ITU _____

Date: 04.12.2024

I hereby declare that all information in this document has been obtained and presented in accordance with academic rules and ethical conduct. I also declare that, as required by these rules and conduct, I have fully cited and referenced all material and results that are not original to this work.

Name Last name : Hasip Atıcı

Signature :

ABSTRACT

SEISMIC ASSESSMENT OF A TRADITIONAL RESIDENTIAL BUILDING IN ANTAKYA AFTER 2023 TÜRKİYE EARTHQUAKE SEQUENCE

Atıcı, Hasip
Master of Science, Conservation of Cultural Heritage in Architecture
Supervisor : Assoc. Dr. Pınar Aykaç Leidholm
Co-Supervisor: Prof. Dr. Murat Altuğ Erberik

December 2024, 122 pages

Historical structures remain standing for many years, although they are exposed to many effects. One of the critical factors affecting the survival of these structures is earthquakes. Researching how historical structures behave in earthquakes is important for their conservation.

Damages occurring after earthquakes provide important information about the structural behavior of the building. Earthquakes allow obtaining valuable information about the seismic performance of buildings whose pre-earthquake status is known and whose behavior can be observed after earthquake. Knowing the structural earthquake performance of buildings also contributes to the determination of possible interventions that can be applied to structures before possible future earthquakes.

Antakya and its historical city center are among the most affected places in the 2023 Türkiye Earthquake Sequence (Mw=7.7 & Mw=7.6). In this thesis, one of the traditional residential buildings located in the historical city center of Antakya was examined. The building known as Beştek House located in district 3, building lot

587 is a non-engineered, unreinforced masonry building (URM) with architectural and historical values, where changes in construction techniques and materials used can be observed over the centuries. The building was partially collapsed in the 2023 Türkiye Earthquakes.

This thesis aims to perform linear static analysis of a traditional unreinforced masonry residential building, which was partially collapsed by consecutive earthquakes that occurred in Türkiye in 2023, using the SAP2000 software by finite element modelling. The building was documented by the METU Graduate Program in Conservation of Cultural Heritage in 2019 as part of the Design in Architectural Conservation (CONS 506) studio course. After the earthquakes in 2023, the structure was documented by METU Centre for Research and Assessment of Historical Environment (TAÇDAM) within the scope of the project CARE-PACE | Post-Earthquake Damage Assessment, Emergency Response, Conservation, Rehabilitation, and Resilience of Cultural Heritage Assets in Multi-layered City: Antakya, Hatay. In this study, the effects of the earthquake on the structure were examined by comparing the structural analysis results and actual damages. Thus, the results regarding the seismic behavior of the examined structure were presented and evaluations are made on the construction technique, structural order and materials of traditional masonry buildings in Antakya. This study is important in that it reveals the weak features of an original Antakya House, which has seen interventions over time, against seismic effects.

Keywords: Unreinforced Masonry Building, Finite Element Method, Seismic Performance Assessment, 2023 Türkiye Earthquake Sequence, Antakya

ÖZ

ANTAKYA'DAKİ GELENEKSEL BİR KONUT BİNASININ 2023 TÜRKİYE DEPREMLERİ SONRASI SİSMİK DEĞERLENDİRMESİ

Atıcı, Hasip
Yüksek Lisans, Kültürel Mirası Koruma, Mimarlık
Tez Yöneticisi: Doç. Dr. Pınar Aykaç Leidholm
Ortak Tez Yöneticisi: Prof. Dr. Murat Altuğ Erberik

Aralık 2024, 122 sayfa

Tarihi yapılar pek çok etkiye maruz kalmalarına rağmen uzun yıllar ayakta kalmaktadır. Bu yapıların ayakta kalmasını etkileyen kritik etkenlerden biri depremlerdir. Tarihi yapıların depremde nasıl davrandığının araştırılması, onların korunması bakımından önemlidir.

Deprem sonrası oluşan hasarlar, binanın yapısal davranışı hakkında önemli bilgiler vermektedir. Depremler, depremden önceki durumu bilinen ve davranışı deprem sonrasında gözlenebilen binaların sismik performansı hakkında değerli bilgiler elde edilmesine imkan vermektedir. Binaların yapısal deprem performansının bilinmesi aynı zamanda gelecekteki olası depremler öncesinde yapılara uygulanabilecek olası müdahalelerin belirlenmesine katkı sağlamaktadır.

2023 Türkiye Depremlerinde (Mw=7.7 & Mw=7.6) en çok etkilenen yerler arasında Antakya ve Antakya'nın tarihi kent merkezi yer almaktadır. Bu tezde, Antakya tarihi kent merkezinde yer alan geleneksel konut yapılarından biri incelenmiştir. 3. Mıntıka 587 numaralı parselde bulunan, Beştek Evi ismiyle bilinen bina, yapım tekniği ve kullanılan malzemelerde, yüzyıllar içinde yaşanan değişikliklerin izlenebildiği,

mimari ve tarihi değerlere sahip, mühendislik hizmeti görmemiş, donatısız yığma bir binadır. Bina, 2023 Türkiye Depremleriyle kısmen yıkılmıştır.

Bu tezde, 2023 yılında Türkiye'de meydana gelen ardışık depremlerde kısmen yıkılan, geleneksel, mühendislik hizmeti görmemiş, donatısız yığma bir konut yapısının SAP2000 yazılımı kullanılarak sonlu elemanlar modeliyle doğrusal statik analizinin gerçekleştirilmesi amaçlanmıştır. Yapı, 2019 yılında ODTÜ Kültürel Mirası Koruma Yüksek Lisans Programı tarafından Mimari Korumada Tasarım (CONS 506) stüdyo dersi kapsamında belgelenmiştir. 2023 yılında meydana gelen depremlerden sonra da yapı ODTÜ Tarihsel Çevre Değerlerini Uygulama ve Araştırma Merkezi (TAÇDAM) tarafından Çok Katmanlı Kent: Antakya, Hatay'da Deprem Sonrası Hasar Değerlendirmesi, Acil Müdahale, Koruma, Rehabilitasyon ve Kültürel Miras Varlıklarının Dayanıklılığı projesi kapsamında belgelenmiştir. Bu çalışmada, yapısal analiz sonuçları ve gerçek deprem hasarları karşılaştırılarak depremin yapıya olan etkileri incelenmiştir. Böylece, incelenen yapının deprem davranışına ilişkin sonuçlar ortaya koyulmuş ve Antakya'daki geleneksel yığma yapıların yapım tekniği, yapısal düzeni ve malzemeleri üzerine değerlendirmelerde bulunulmuştur. Bu çalışma, zaman içinde müdahaleler görmüş, özgün bir Antakya Evi'nin sismik etkiler karşısındaki zayıf özelliklerini ortaya koyması bakımından önemlidir.

Anahtar Kelimeler: Donatısız Yığma Binalar, Sonlu Elemanlar Yöntemi, Sismik Performans Değerlendirmesi, 2023 Türkiye Deprem Dizisi, Antakya

To the People of Affan, Antakya

ACKNOWLEDGMENTS

I would like to express my deepest gratitude to my supervisors Assoc. Prof. Dr. Pınar Aykaç Leidholm and Prof. Dr. Murat Altuğ Erberik for their guidance, support and patience.

I would like to thank Prof. Dr. Güliz Bilgin Altınöz who is the coordinator of the CARE-PACE project for her support and giving me the opportunity to study my thesis about Antakya.

I would like to thank specially Orhan Mete Işıkoğlu for sharing his knowledge with me. Also, I would like to thank Yavuz Semerdöken, Parnian Nemati and Assoc. Dr. Duygu Ergenç for their support from their field.

Also, I thank to CONS 506 course team who documented and accessed Beştek House in 2019, Buse Melis Alpüren, Ekin Bakır, Nurettin Murat Dörtlük, Parnian Nemati, Ceren Yağmur Yıldırım, Tuğçe Yürük under supervision of Prof. Dr. Neriman Şahin Güçhan, Assoc. Prof. Dr. Pınar Aykaç Leidholm, Pınar Gökçınar Balkan for their labor and productions.

I would also like to thank all jury members of my thesis for their valuable comments, namely, Prof. Dr. Neriman Şahin Güçhan, Prof. Dr. Güliz Bilgin Altınöz, Assoc. Prof. Dr. Umut Almaç and as pre-jury member Assoc. Prof. Dr. Özgün Özçakır.

TABLE OF CONTENTS

LIST OF TABLES

TABLES

LIST OF FIGURES

FIGURES

LIST OF ABBREVIATIONS

ABBREVIATIONS

AFAD	Disaster and Emergency Management Presidency
DD-1	Earthquake Ground Motion Level for which the possibility to be exceeded in 50 years is 2 % (2475 years return period)
DD-2	Earthquake Ground Motion Level for which the possibility to be exceeded in 50 years is 10 % (475 years return period)
EERC	Earthquake Engineering Research Center, METU
ITU	Istanbul Technical University
KOERI	Kandilli Observatory and Earthquake Research Institute
METU	Middle East Technical University
METU CONS	METU Graduate Program in Conservation of Cultural Heritage
PGA	Peak Ground Acceleration
METU TAÇDAM	METU Center for Research and Assessment of Historical Environment
TBSC	Turkish Building Seismic Code
URM	Unreinforced Masonry
USGS	United States Geological Survey

LIST OF SYMBOLS

SYMBOLS

V_{Ed}	Design shear force acting on the wall
V_{Rd}	Design shear force strength in load-bearing masonry walls
V_s30	Average shear-wave velocity to 30 m depth [m/s]
E	Modulus of Elasticity
M_w	Moment Magnitude
R	Response Modification Factor
R_a (T)	Seismic Load Reduction Factor
a*	Spectral acceleration
α_0	Load factor
e*	Mass participation ratio
M*	Effective modal mass

CHAPTER 1

INTRODUCTION

1.1 Definition of the Problem

Traditional buildings are important elements of the culture. They subject to many changes through their lifetime. The change is taking place by human interventions and natural forces. In addition, the structural system of the buildings changes in time with interventions. These alterations affect the structural performance of the buildings, as well. Therefore, they are both sensitive due to factors such as alterations in structural system, modern time pressure and burden of time. On the other hand, conservation of these houses are important not only they constitute an important part of the urban fabric, but also they are the spaces where the culture and life in the region continues.

One of the main threats to the traditional buildings is earthquakes. Earthquakes result in partial or complete destruction of the traditional fabric over time. Türkiye is an earthquake-prone country. Türkiye is under the interaction of Eurasia, Arab and Africa tectonic plates. Antakya is located in the south of Türkiye at the intersection of these tectonic plates. Therefore, the city has witnessed devastating earthquakes since its foundation. The last major earthquake effecting the city was 2023 Türkiye Earthquake sequence (Mw:7.7 & Mw:7.6). Antakya and its traditional houses in historical city center have suffered great destruction in these last major earthquakes.

The structural system of a significant part of the buildings in historical city center of Antakya is masonry in ground floor and timber in upper floor. Residential buildings located in the historical center of Antakya are generally non-engineered, unreinforced masonry (URM) buildings on the ground floor and timber in upper

floor, as well. An example of these characteristics is located in Ülkü Street in Gazi Paşa Quarter, in the historical city center of Antakya. The house is called by its former homeowners' last name, Beştek House. The building has witnessed 2023 Türkiye Earthquake Sequence and partially collapsed with the earthquakes.

In order to understand the damages that occurred after the earthquake, it is beneficial to compare the possible damages before the earthquake with those that occurred after the earthquake. In this study, comparison has been made over the Beştek House which has been studied and documented comprehensively in 2019 by METU Graduate Program in Conservation of Cultural Heritage. By this study, an information about the structural performance of the building is added to the study.

Beştek House was selected for the following reasons. The most decisive was that the building has been documented in detail before the earthquakes. It represents the features of the Antakya houses at the beginning of the 20th century. In addition, it is a transition period structure with the I-profile beams added to the structure in the late 19th century and early 20th century. In the 2023 Earthquake sequence, it is standing even some partial collapse and damages. Partial collapse is going to provide an opportunity for comparative analysis of structural performance of the building, so that weak zones and construction technique mistakes will be visible. Last, it is not seen any intervention in terms of restoration or conservation until the earthquakes.

1.2 Aim and Scope

The main aim of this thesis is to obtain information about the structural behavior and earthquake performance of a traditional, residential, unreinforced masonry building by structural analysis and to compare the analysis results with the real earthquake damage. Structural analysis has revealed deficiencies in construction techniques, structural layout, weaknesses in materials used, and the effects of interventions on behavior over time.

The building suffered significant damage in the 2023 Türkiye earthquakes. Analysis results are close with the actual earthquake damage therefore, it can be stated that the evaluations made regarding the investigated features are consistent. A comparison is available under the effects of numerical seismic calculations on the building as a whole and the load-bearing walls of the building each. Analysis results were evaluated under the conditions recommended by the Guideline for Earthquake Risk Management of Historical Structures (GERMHS, 2017) and Turkish Building Seismic Code (TBSC, 2018). Then, results are compared with damage caused by the earthquake.

The building is analyzed by linear static analysis method. This method will provide a sufficient data set regarding the behavior of structure and the parameters examined. Factors such as the lack of detailed knowledge of the properties of the materials used in the building and the difficulty of mathematically expressing the character of the connections do not allow further studies to be carried out at this stage.

Consequently, fragile zones of the building to the seismic forces are obtained by structural analyses. Results are compared with the real earthquake damage in 2023 Türkiye Earthquake Sequence. Therefore, the thesis aimed to contribute to the conservation of non-engineered, valuable residential buildings.

1.3 Methodology of the Study

The study was carried out in these stages, which are the observations in the field survey, literature research about the seismicity around Antakya and understanding the structural and architectural features of the selected case based on the architectural conservation studio project of CONS 506, modelling and structural analysis.

Field surveys were conducted in June 2023 and September 2023 to observe the buildings geometry, construction technique and damages after earthquakes. The building has been documented after the earthquakes by METU Centre for Research and Assessment of Historical Environment (TAÇDAM) in 2023 within the scope of

the project “CARE-PACE | Post-Earthquake Damage Assessment, Emergency Response, Conservation, Rehabilitation, and Resilience of Cultural Heritage Assets in Multi-layered City: Antakya, Hatay[1] under the execution of Prof. Dr. Ayşe Güliz BİLGİN ALTINÖZ. Thus, deformed shape and damage patterns of the building are documented. This information is used in comparison of the analytical study and real damage.

Literature survey is done about the seismicity of Antakya, construction technique and materials of the Antakya Houses and 2023 Türkiye earthquake sequence. For the Beştek House, literature survey is based on the architectural conservation studio project of CONS 506 course conducted by METU Graduate Program in Conservation of Cultural Heritage. Therefore, more realistic structural modelling and analysis was available.

In the structural analysis stage, macro-modelling technique with Finite Element Method (FEM) is used to analyze the building. To do that, interventions to the building and alterations are considered. Linear static analysis has been applied on the model. SAP2000 Software is used for numerical modelling and structural analysis. Eventually, the weak zones of the building are validated by comparing analytical results and observations after the earthquake.

As a result of the study, the information about critical zones of the building before the earthquake is obtained by linear static analysis. As such, a traditional building in

[1] CARE-PACE | Post-Earthquake Damage Assessment, Emergency Response, Conservation, Rehabilitation, and Resilience of Cultural Heritage Assets in Multi-layered City: Antakya, Hatay. Project Members: Prof. Dr. Güliz Bilgin Altınöz, Prof. Dr. Neriman Şahin Güçhan, Assoc. Prof. Dr. Pınar Aykaç Leidholm, Assoc. Prof. Dr. Özgün Özçakır, Dr. Sibel Yıldırım Esen, Dr. Filiz Diri Akyıldız, Specialist Kemal Gülcen, Assoc. Prof. Dr. Duygu Ergenç Cabanas Rodriguez, Dr. Emine Çiğdem Asrav, Research Assist. Gökhan Okumuş, Research Assist. Merve Öztürk, Research Assist. Simay Cansu Ekici Üner, Research Assist. Elif Miray Kısaer Koca, Research Assist. İrem Diker Gökçe, PhD Student, Parnian Nemati, Master Student Hasip Atıcı, Research Assist. Selen Tuğrul, Research Assist. Özgür Ürey, Prof. Dr. Ahmet Türer, Prof. Dr. Murat Altuğ Erberik, Prof. Dr. Sadık Bakır, Prof. Dr. Tamer Topal, Research Assist. Dr. İlham Sarıkaya, Research Assist. Dr. Nadire Atıcı, Research Assist. Dr. Deniz Erdem, Prof Dr. Hatice Pamir, Assoc. Prof. Dr. Mert N. Rifaioğlu, Manager in Netherlands Institute in Turkey (NIT) Fokke Albert Gerritsen, Institute Researcher (NIT) Aysel Arslan, Geomatic Engineer Kenan Kantarcı

an earthquake prone area with architectural and historical values and also unique characteristics differing from the other buildings nearby, which has witnessed three big earthquakes consecutively has been studied by macro modelling technique with linear static analysis.

CHAPTER 2

BEŞTEK HOUSE AS A TRADITIONAL RESIDENTIAL BUILDING IN ANTAKYA

In this chapter, mainly, a traditional residential structure located in the historical center of Antakya, Beştek House, is described with its architectural and structural features. Beştek House has been studied comprehensively by METU Graduate Program in Conservation of Cultural Heritage in 2019 within the scope of Design in Architectural Conservation (CONS 506) course.

Beştek House was one of the buildings got damage by the 2023 Türkiye Earthquakes in Antakya. The damage to the building was observed on site and documented by METU TAÇDAM after the earthquakes that occurred in Türkiye on February 6, 2023. In the first part of this chapter, seismicity of Antakya was researched from literature. Next, an information about 2023 Türkiye Earthquake sequence is given with a focus on Antakya and Beştek House. At the end of the chapter, the damage status of the building after the earthquake was explained.

2.1 Seismic Activity in Antakya Region

Antakya is an old settlement area that has 2300 years of historical background. The city is located at the intersection of three major tectonic plates, namely Anatolian, Arabian and African plates. East Anatolian and Dead Sea faults intersect in the region (Figure 2.1). Therefore, it has been exposed to many devastating earthquakes throughout history (Figure 2.2) (Beyen *et* al., 2003, KOERI, 2023).

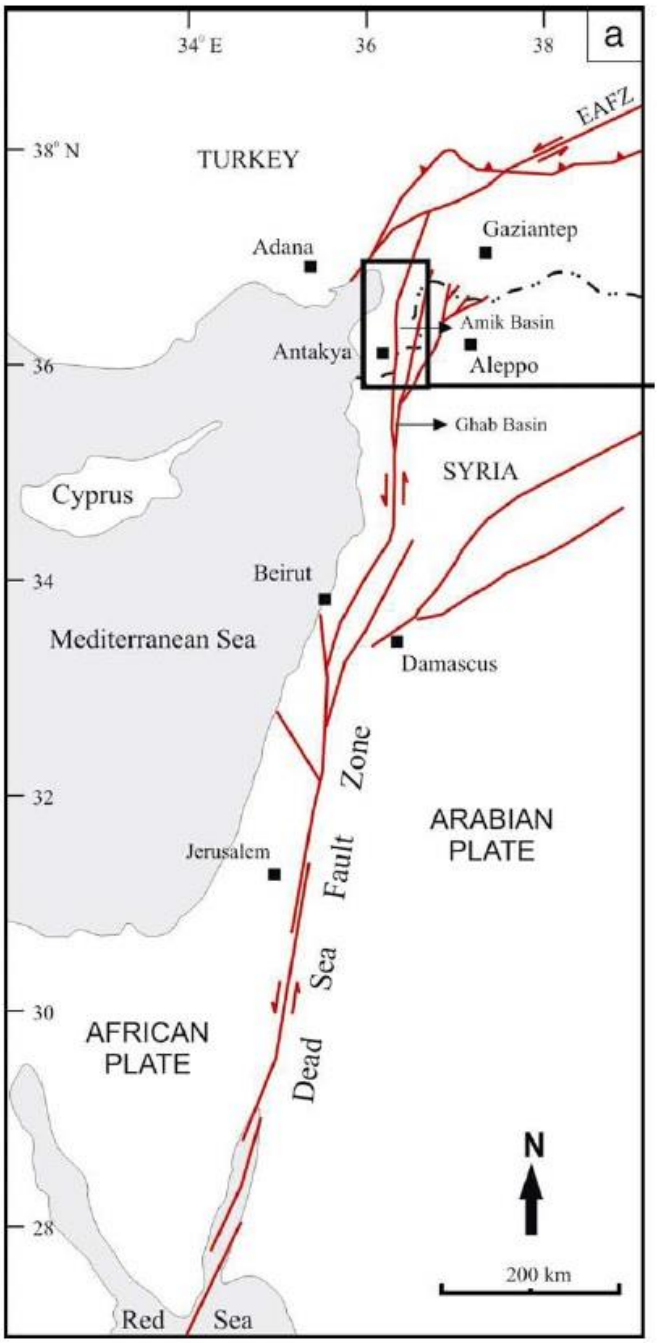

Figure 2.1 Antakya in the intersection of Dead Sea Fault Zone and East Anatolian Fault Zone (Akyüz *et* al, 2006)

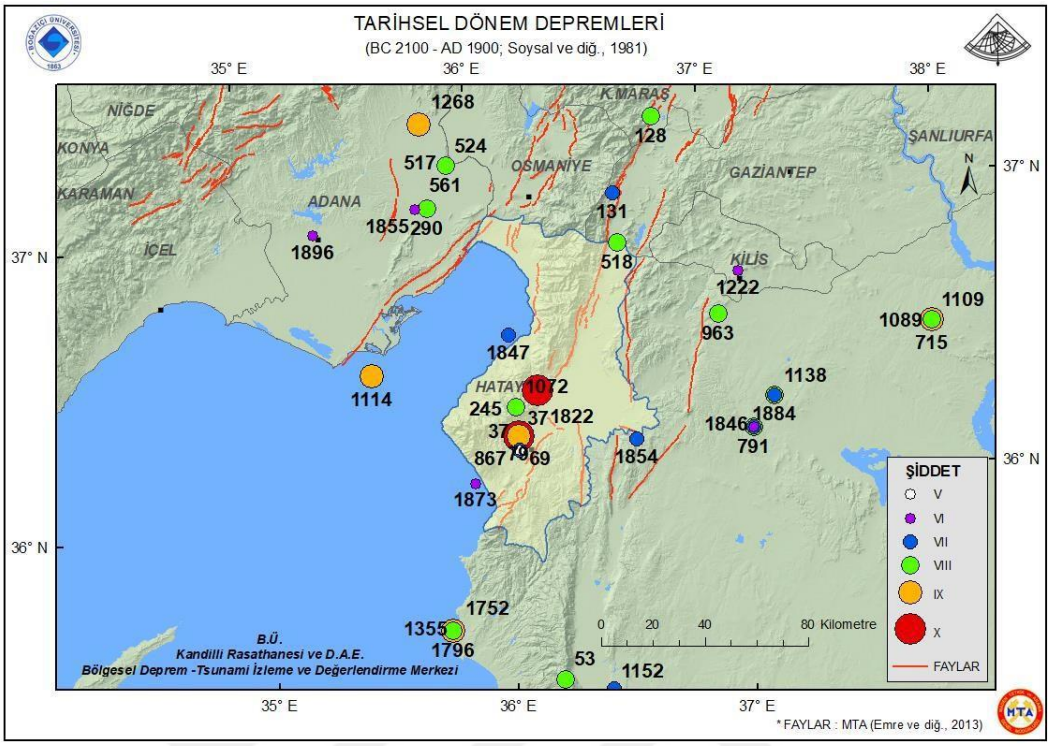

Figure 2.2 Historical earthquakes around Hatay between BC2100-AD1900 (KOERI, 2023)

Figure 2.3 shows the earthquakes took place as sequences in certain time periods in the history of Hatay (Ersoy, 2009). Among these sequential events, 19th century earthquakes that occurred in years 1822 and 1872 had been reported to cause major impacts to the built environment in Antakya (Ambraseys, 2009) and possibly Beştek House (METU CONS, 2019). Ambraseys (2009) stated that:

> 1822 earthquake was the largest to occur at the junction of the Dead Sea fault zone with the East Anatolian fault during the last five centuries. The earthquake was felt from the coast of the Black Sea to Gaza and it was followed by a long aftershock sequence. The shock almost entirely destroyed the region between Gaziantep and Antakya in Turkey and Aleppo and Han Sheikhun in northwestern Syria, killing a very large number of people.

1900	1872 - 1822	13. DEPREM KÜMESİ
1800		SUSKUNLUK 117 YIL
1700	1615	12. DEPREM KÜMESİ
1600		SUSKUNLUK 207 YIL
1500	1408	11. DEPREM KÜMESİ
1400		SUSKUNLUK 121 YIL
1300	1278	10. DEPREM KÜMESİ
1200		SUSKUNLUK 117 YIL
1100	1170 - 1169 - 1157 - 1114 - 1097 1091 - 1072 - 1068 - 1063 - 1053	9. DEPREM KÜMESİ 117 YIL
1000		SUSKUNLUK 81 YIL
	972 - 963	8. DEPREM KÜMESİ 9 YIL
900		SUSKUNLUK 98 YIL
	865 - 859 - 847 - 835	7. DEPREM KÜMESİ 30 YIL
800		SUSKUNLUK 122 YIL
	713	6. DEPREM KÜMESİ
700		SUSKUNLUK 125 YIL
600	588 - 577 - 561 - 557 - 528 526 - 506	5. DEPREM KÜMESİ 62 YIL
500		SUSKUNLUK 66 YIL
	458	4. DEPREM KÜMESİ
400		SUSKUNLUK 62 YIL
300	396 - 394 - 340 - 334 - 272 - 245	3. DEPREM KÜMESİ 151 YIL
200		SUSKUNLUK 130 YIL
	115 - 110 - 94	2. DEPREM KÜMESİ 21 YIL
100		SUSKUNLUK 131 YIL
MİLAT	37 - 64/69 - 148	1. DEPREM KÜMESİ 111 YIL
100		
200		

Figure 2.3 Earthquake periods in Hatay between 148 B.C. – 1900 A.C. (in Turkish) (Ersoy, 2009)

Figure 2.4 illustrates isoseismal map of the 1822 earthquake according to the Mercalli Scale (Ambraseys, 1989 cited in Sbeinati, 2005). It is clear from the map that the earthquake had been felt in a very wide area and Antakya seems to have been affected from this disaster with an intensity between VII and VIII.

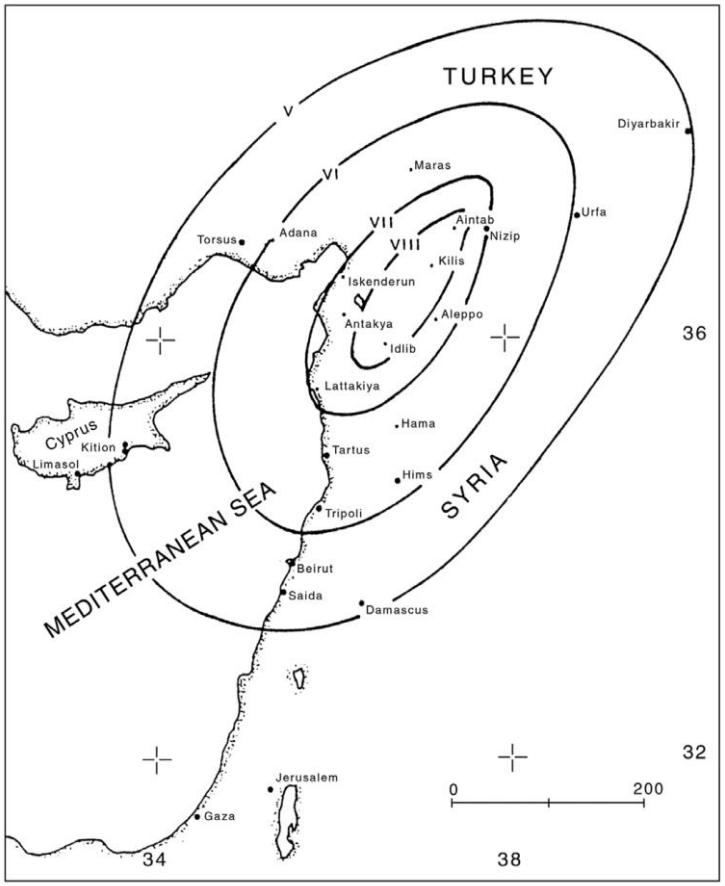

Figure 2.4 Map of intensity distribution for 1822 earthquake (Ambraseys, 1989 cited in Sbeinati, 2005).

After fifty years from this major earthquake, another devastating seismic event affected Antakya in 1872. With a reference to a consulate report about 1872 earthquake in Antakya the following information can be obtained as follows:

Antioch (Antakya), which had a population of 17600, the shocks lasted for 50 seconds. Of the 3000 houses in the town, 1960 were totally destroyed and 894 so damaged as to become uninhabitable, leaving only 149 in good condition (Ambraseys, 2009).

The earthquake intensity at some settlement locations during the 1872 earthquake is presented in Figure 2.5. Similar to the 1822 earthquake, Antakya seems to have felt this earthquake with a Mercalli Intensity between VII and VIII (Ambraseys, 1989 cited in Sbeinati, 2005).

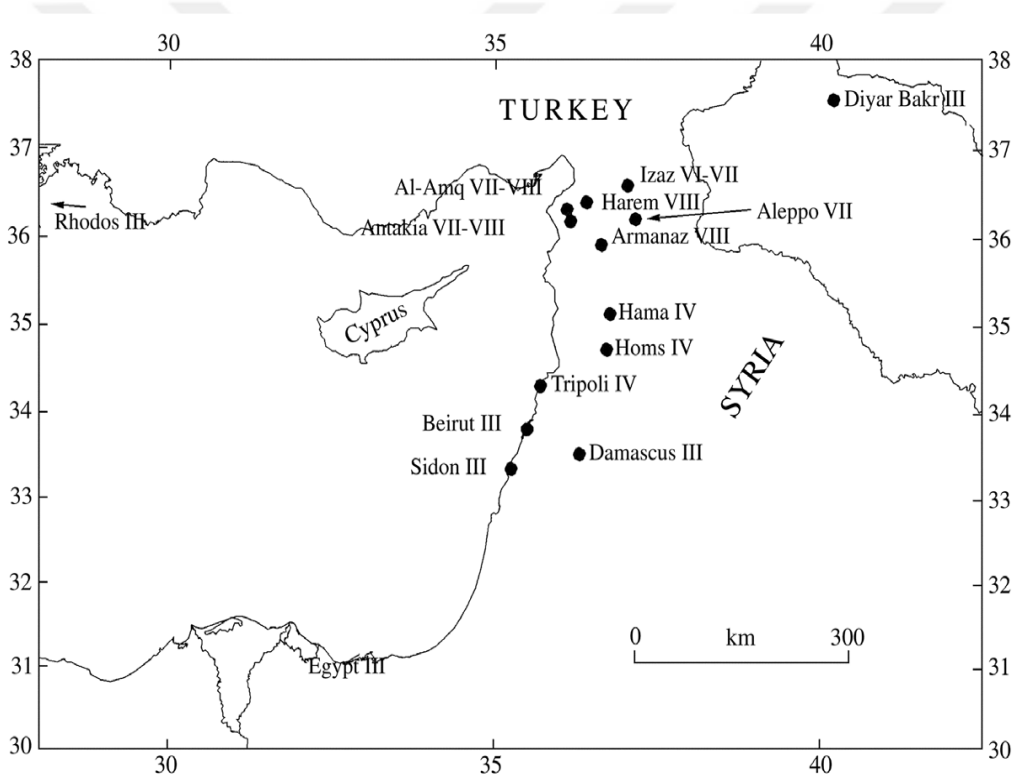

Figure 2.5 Map of intensity distribution for 1872 earthquake (Ambraseys, 1989 cited in Sbeinati, 2005).

From the start of the 20th century, numerous earthquakes with magnitudes M≥4.0 have occurred in the close vicinity of Antakya, that verifies the high seismicity in the region (Figure 2.6) (KOERI, 2023).

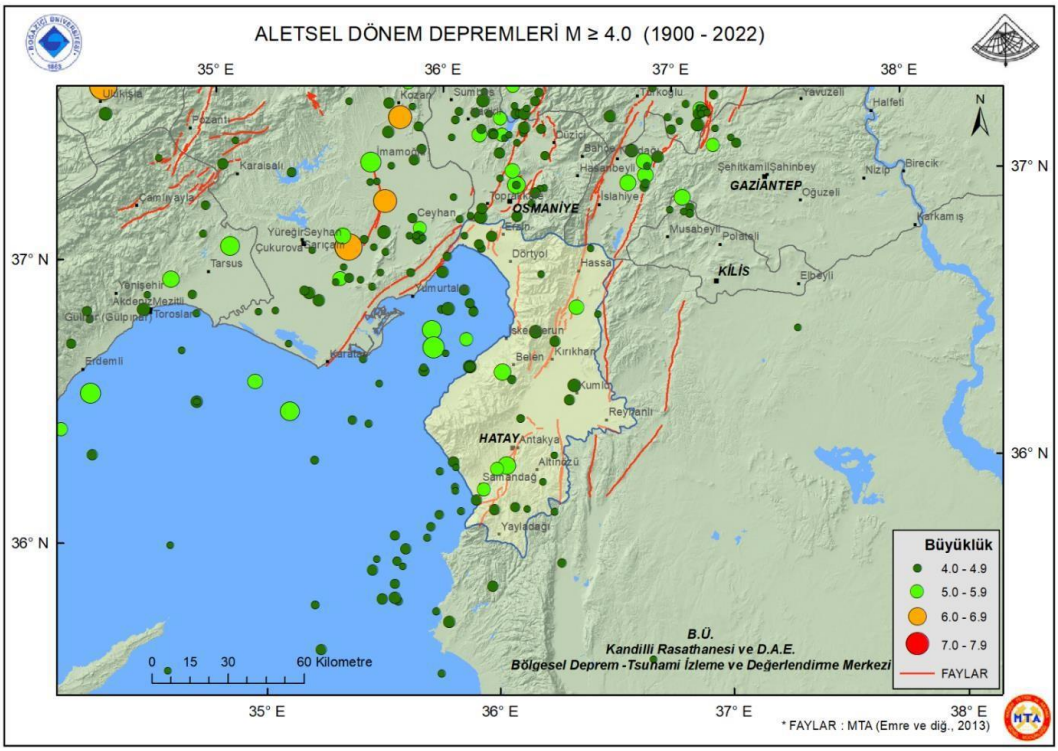

Figure 2.6 Earthquakes with a magnitude of M ≥ 4.0 between 1900-2022, falling in a 300 km radius area with Hatay at the center (KOERI, 2023)

2.2 2023 Türkiye Earthquake Sequence

On February 6, 2023, at 04:17 local time (01:17 GMT), an earthquake with a moment magnitude of Mw=7.7 occurred in south-eastern Türkiye (KOERI, 2023). According to the AFAD, the epicenter of this event, named as the Pazarcık-Kahramanmaraş-Türkiye earthquake, is located at N37.288°, E37.043° and approximately 40 km

north-west of Gaziantep, and 33 km south-east of Kahramanmaraş, with a focal depth of 8.6 km (EERC, 2023).

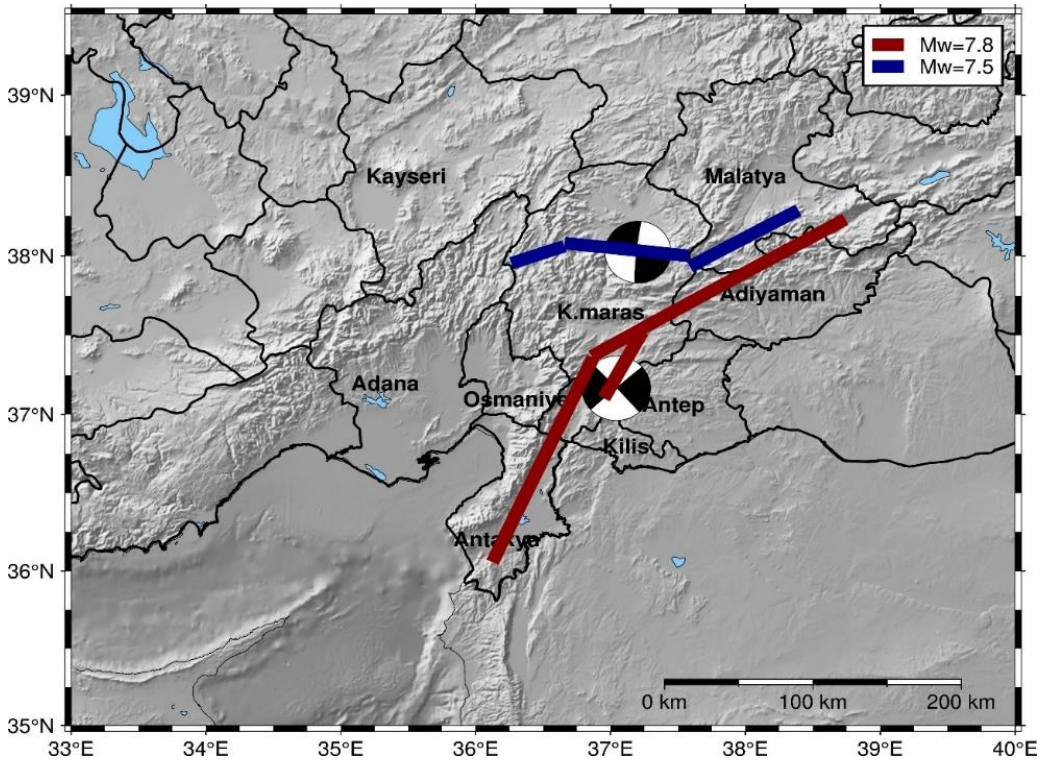

Figure 2.7 Seismological aspects of the Kahramanmaras earthquakes on Feb 6, 2023 (Askan *et* al 2024). Magnitudes in the legend are as assigned by the USGS.

On the same day, at 13:24 local time (10:24 GMT), another earthquake occurred with a magnitude of Mw.7.6 (AFAD) and a depth of 7.4 km, centered in Elbistan (38.011°N 37.196°E) according to United States Geological Survey (USGS). This earthquake has been named the Elbistan-Kahramanmaraş earthquake. These sequential earthquakes have been among the most destructive events in the history of Turkish Republic after the 1939 Erzincan event and the 1999 Marmara earthquake sequence. It affected 11 populated cities due to a fault rupture of approximately 400 km causing an incomprehensible damage and loss in the affected area (Figure 2.7) (Askan *et* al 2024).

The closest stations to Beştek House are the ones coded as 3131 in Bağrıyanık Neighborhood and as 3132 in Orhanlı Neighborhood (Figure 2.8). These stations are about 1km away from the house. Station with ID 3132 is located on softer soil conditions than the station with ID 3131. The characteristics of the earthquake records belonging to the Pazarcık (M=7.7) earthquake obtained from these stations are presented in Table 2.1.

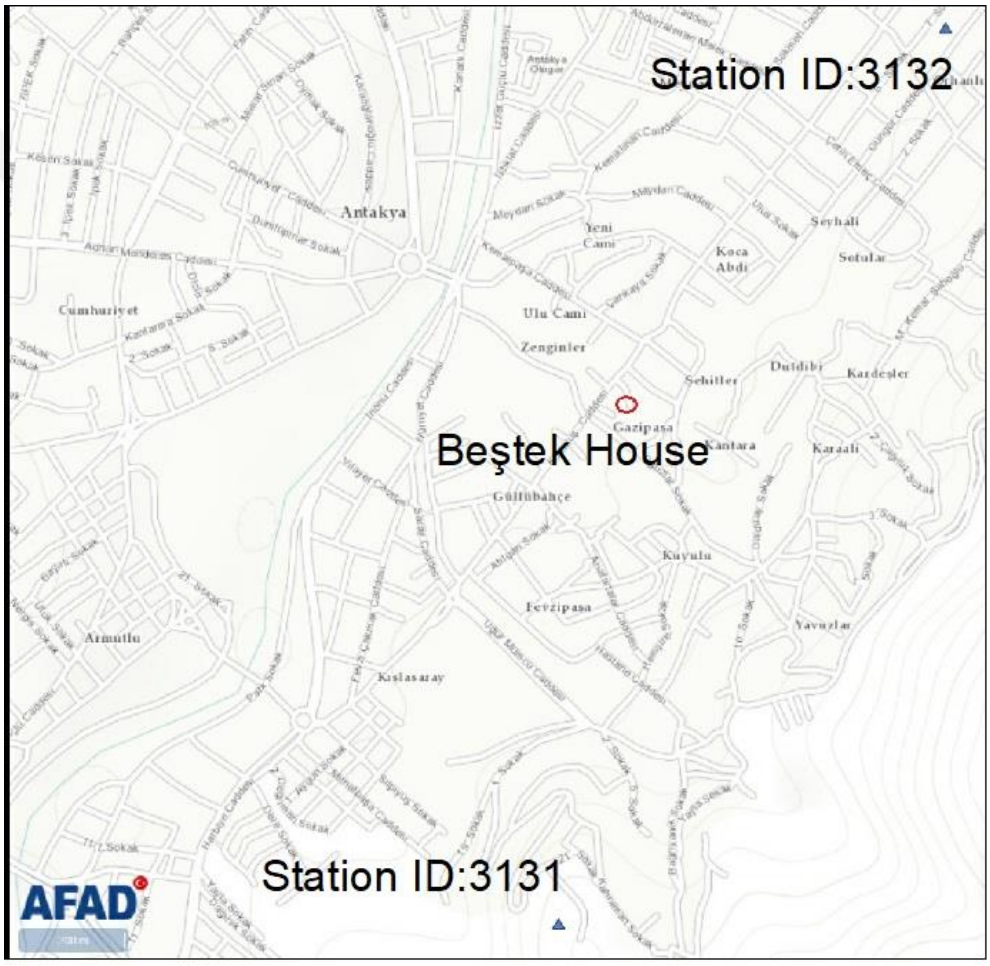

Figure 2.8 Locations of the closest stations to Beştek House in Antakya with the IDs 3131 and 3132

Table 2.1 Ground motion characteristics obtained from the considered stations in Antakya with IDs 3131 and 3132 during the Pazarcık earthquake (KOERI, 2023)

Station ID	Lat.	Lon.	Vs30 (m/s)	Repi (km)	Rjb (km)	Rrup (km)	Comp	PGA (cm/s2)	PGV (cm/s)	PGD (cm)
3131	36.191	36.163	567	144.98	14.87	14.87	E	358.31	44.10	12.49
							N	359.43	39.50	6.60
							U	146.34	18.20	5.38
3132	36.207	36.172	377	143.12	12.99	12.99	E	515.10	49.47	10.06
							N	516.03	67.19	15.40
							U	337.70	35.96	8.26

Considering the peak values of ground acceleration, velocity and displacement in Table 2.1, it is observed that the records have extremely high demands, which explains the extensive destruction of the building stock in the region. Due to relatively softer soil conditions, the seismic intensity values obtained from station with ID 3132 seem to be more amplified and demanding for structures. In addition, ground motion time series and spectral variations obtained from the recordings at stations with IDs 3131 and 3132 are presented in Figure 2.9 and Figure 2.10. Although the epicentral distances to the stations are long, the time series seem to contain significant pulses of acceleration, velocity and displacement, even in the vertical direction. Also, the acceleration response spectra of the records are compared with the design spectra from the current Turkish Building Seismic Code (TBSC-2018) for design basis (DD2) and maximum credible (DD1) seismic hazard levels. The comparison reveals that spectral values obtained in station 3131 exceed the design spectrum in the period range between 0.5 s to 3.0 s. This is the range in which most of the mid-rise and flexible structures reside. In the case of station 3132, the situation is even more critical, in which not only the DD2-level but also the DD1-level design spectrum is exceeded in similar period ranges. Noting that DD1-level corresponds to a return period of 2475 years, the extraordinary high level of seismic demand can be more easily anticipated. Of course, the exceedance of the design level does not necessarily mean the collapse of the structure since seismic design philosophy provides other fuses to the structure in order to ensure seismic safety like the capacity design rules. In other words, the structure is expected to conceive

damage beyond repair but, sudden collapse should be prevented by the additional rules in seismic design.

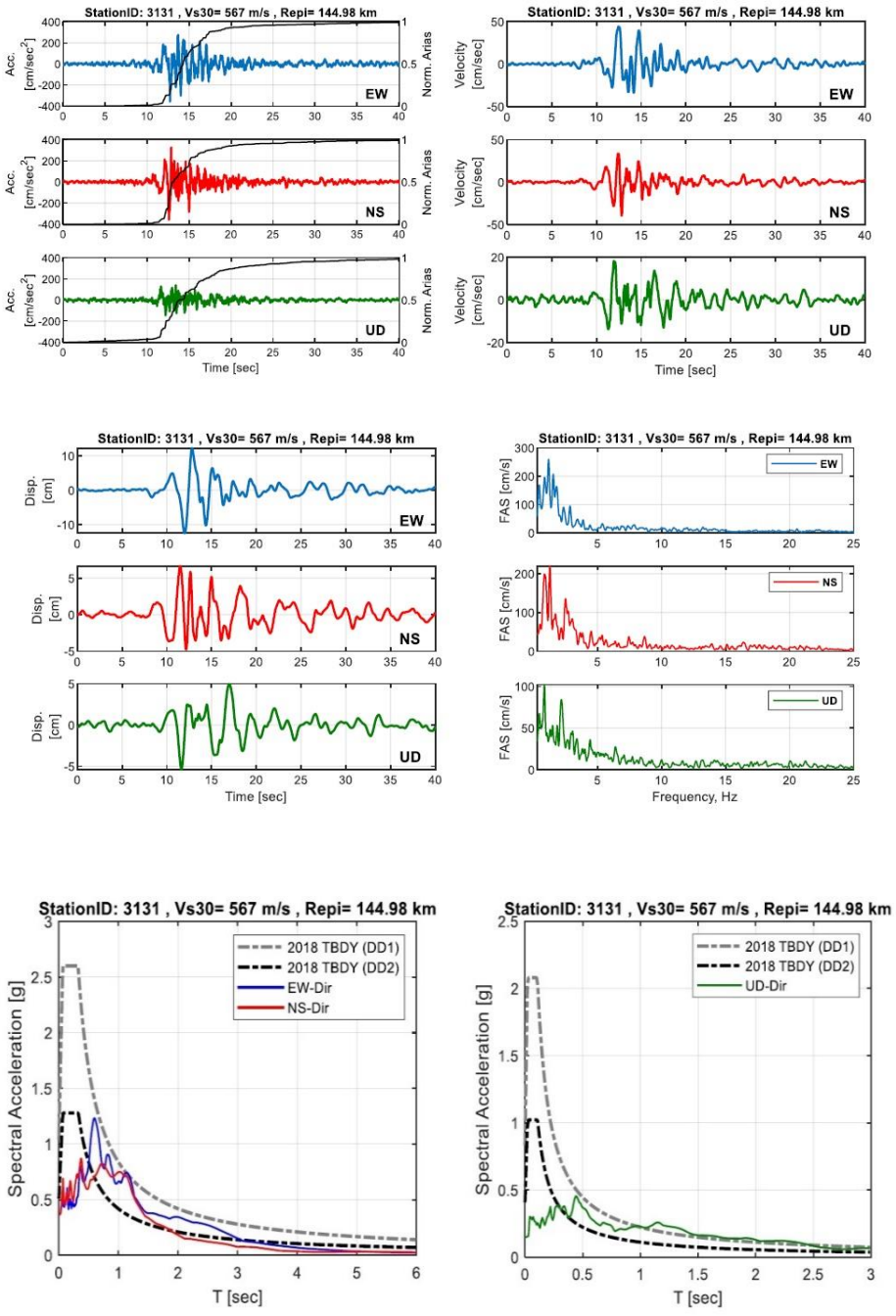

Figure 2.9 Ground motion time series and spectral variations obtained from the records at Station 3131 after Pazarcık (Mw=7.7) earthquake (ITU, 2023)

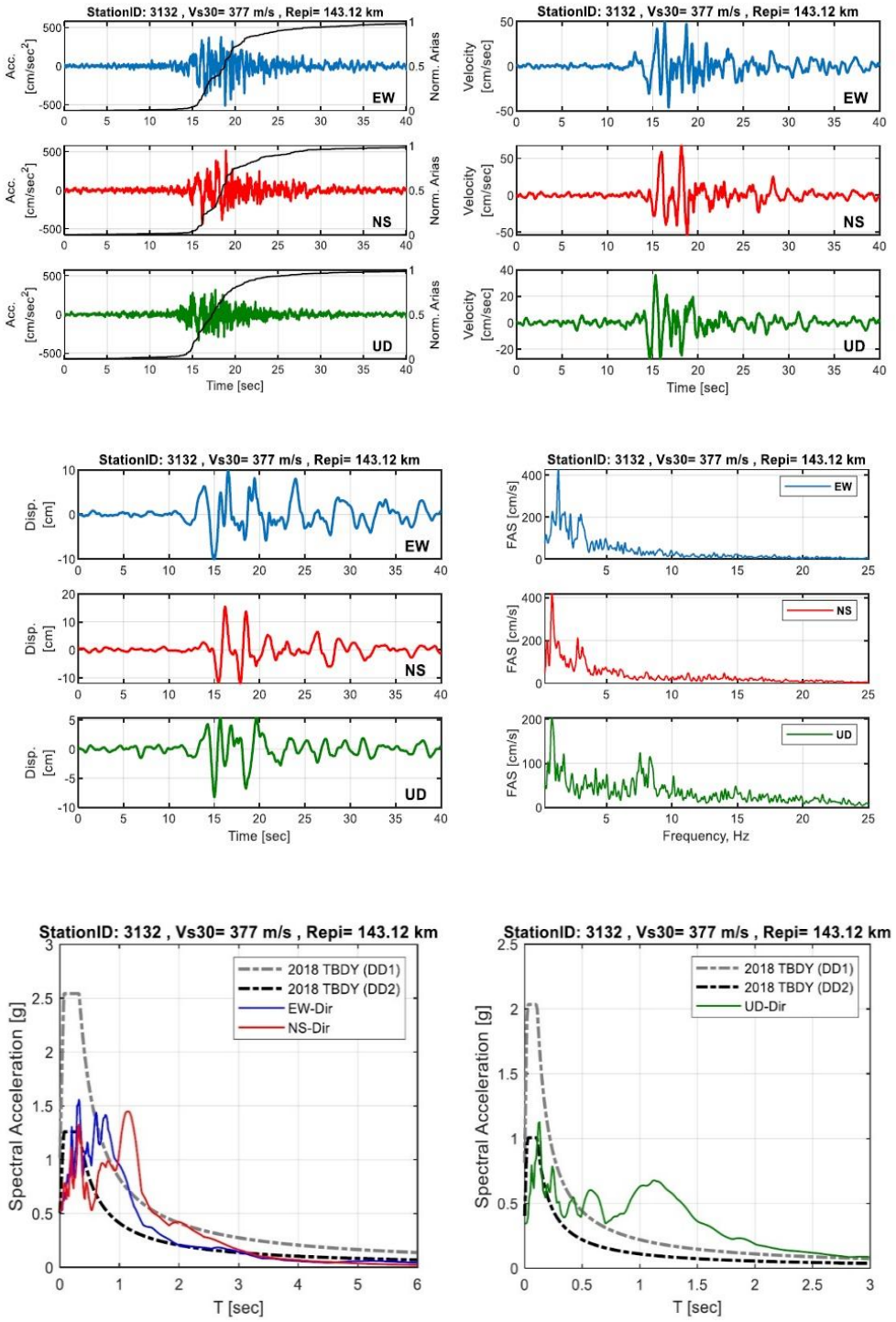

Figure 2.10 Ground motion time series and spectral variations obtained from the records at Station 3132 after Pazarcık (Mw=7.7) earthquake (ITU, 2023)

Another major earthquake affecting Antakya occurred in Defne on February 20, 2023 with magnitude Mw: 6.4 occurred at a depth of 8 km (KOERI, 2023). As displayed in the Table 2.2 the largest PGA values for the Defne Antakya earthquake was measured at station with ID 3124 located 5 km away from Beştek House as shown in Figure 2.11 (AFAD, 2023).

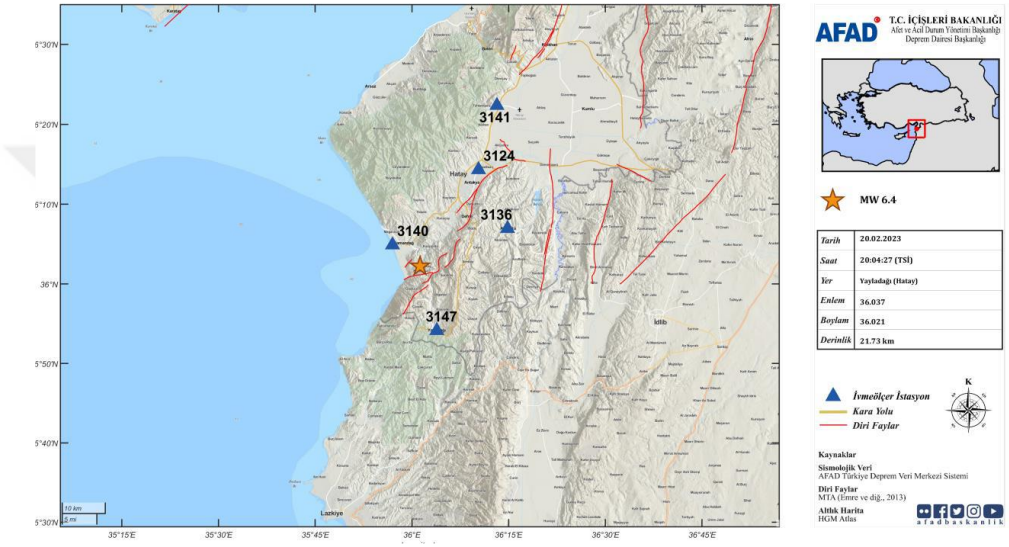

Figure 2.11 Distribution of the 5 nearest accelerometer stations that recorded the earthquake (AFAD, 2023)

Table 2.2 PGA values recorded at stations in the region during the Defne earthquake (AFAD, 2023)

Station					Measured Acceleration Values (gal)			Distance R_{epi}
ID	**City**	**District**	**Latitude**	**Longitude**	**N-S**	**E-W**	**Vertical**	**(km)**
3140	Hatay	Samandağ	36.0816	35.9498	181.4111	167.5423	149.6638	11.99
3126	Hatay	Altınözü	36.1159	36.2472	307.3794	217.9893	135.3987	15.57
3124	Hatay	Antakya	36.2387	36.1722	405.3000	445.3769	219.6553	15.78
3147	Hatay	Yayladağı	35.9024	36.0644	20.0514	22.2215	14.5429	24.33
3141	Hatay	Antakya	36.3726	36.2197	387.3669	237.449	215.8226	30.88

2.3 Architectural Characteristics and Structural Features of the Beştek House

Beştek House is located in the Gazi Paşa Neighborhood, District 3, and building lot 587 in the historical city center of Antakya (Figure 2.12). It is known that there has been settlement in this region since the Hellenistic period. The city developed on a grid-type plan in the Hellenistic period and this process continued in the Roman period (Pamir, 2009; Pinon, 2004). The urban fabric has started to evolve into an organic texture from the Mamluk period onwards. Despite this, while the Hellenistic grid plan can be observed on the surface in some parts of the city (Sauvaget, 1935; Downey, 1961; Pinon, 2004 cited in Rifaioğlu, 2012). It is seen that the current settlement of the historic area is on this grid plan with a small angle difference in certain areas (Figure 2.13) (METU CONS, 2019).

Figure 2.12 Building lot of the Beştek House

According to the 2019 study of the METU Conservation of Cultural Heritage Program, it is asserted hypothetically that Beştek House can be placed on the antique period housing texture. In addition, a vault remains on the wall in the basement of the building were interpreted as traces of the Mamluk period. Although the structure

underwent changes after the earthquakes in 1822 and 1872, it is thought that its layout and plan features on the parcel continued (METU CONS, 2019).

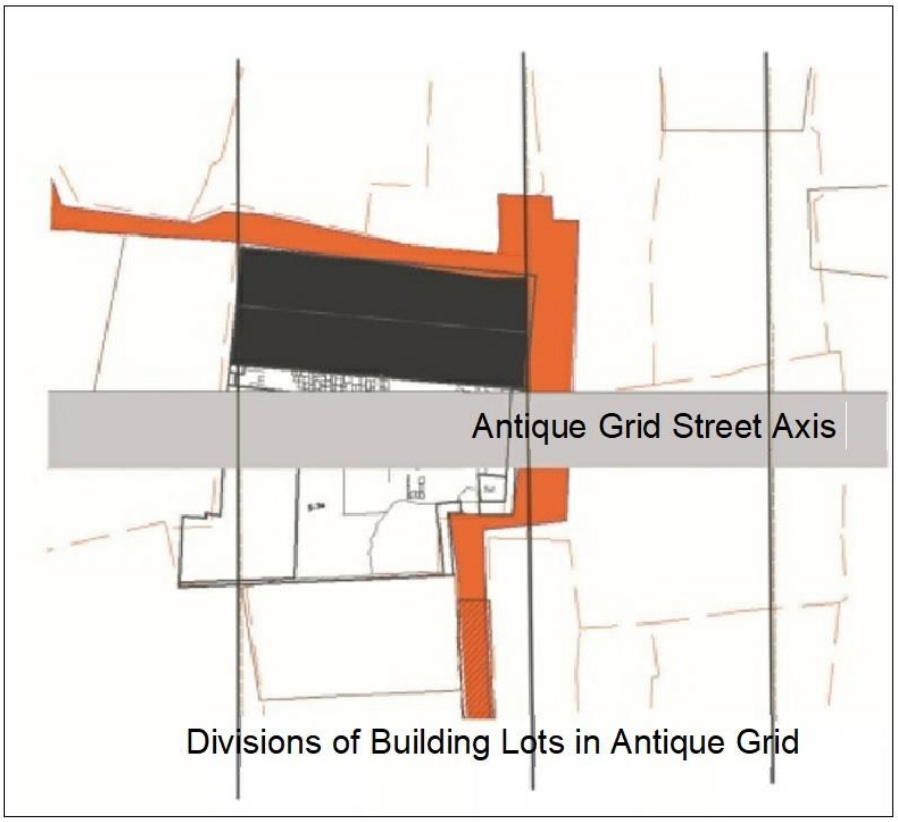

Figure 2.13 The relation of the Beştek House with the hypothetical antique urban form (METU CONS, 2019)

The relation of the building with the street is limited as many of the traditional Antakya Houses. Access from the street to the parcel and the courtyard is usually provided through narrow dead-ends. As seen in Figure 2.14, parcel is accessed from two different points. However, the access provided from the cul-de-sac on the north side of the building was closed by filling the door in the basement.

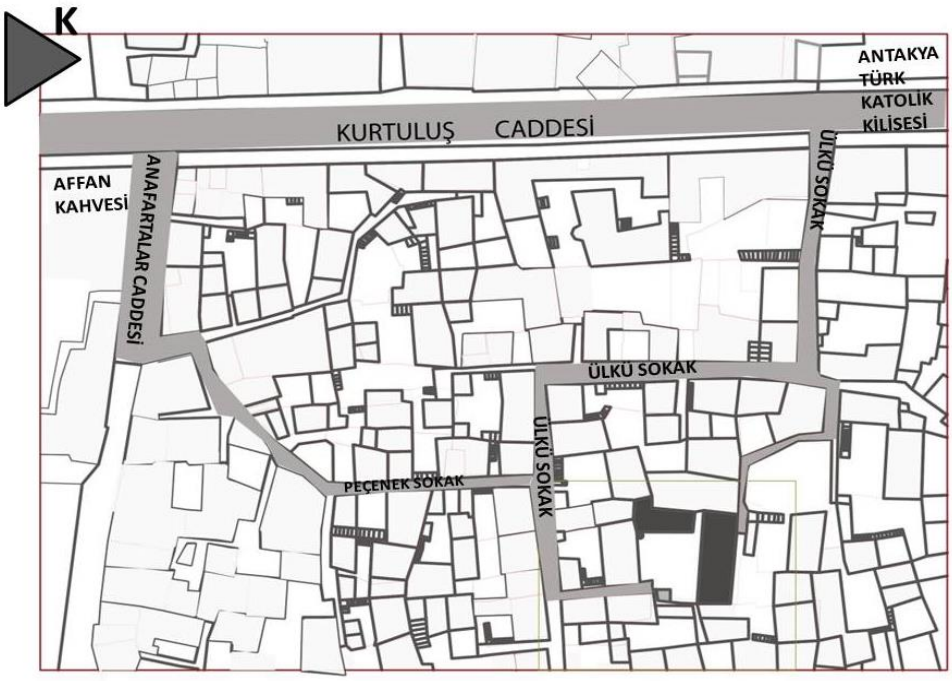

Figure 2.14 Beştek House site plan and surroundings - District 3, Building lot 587 (METU CONS, 2019)

Entrance to the parcel from two different places is a very rare feature in the region. The elevation difference has also caused the formation of the basement floor, which is not a common construction feature in the region. The main structure is located on the northern edge of the courtyard. The original service structure has been demolished and the mass containing the kitchen and toilet, which are single storey reinforced concrete service structures with period additions, is located in the west, and the toilet unit is located in the east, right next to the existing courtyard entrance (METU CONS, 2019).

The entrance to the building is from the courtyard. The light of the spaces comes from the courtyard. The courtyard of the Beştek House is located in the south of the building.

2.3.1 Architectural Characteristics of the Beştek House

Beştek House has a rectangular plan. The building sits on an area of approximately 15 meters long and 5 meters wide on the east-west axis. It consists of a basement floor, ground floor and an unfinished first floor.

It is adjacent to another building both in the west and in the east sides. On the west side, the neighboring building has similar mass characteristics with Beştek, whereas the one in the east side is relatively smaller in size and mass (Figure 2.15).

Figure 2.15 Beştek House site plan (METU CONS, 2019)

Due to the elevation difference in the land, the building has a basement floor. While the basement of the building is at the street level from the north facade, it is below the ground in the courtyard facade.

The building was built with unreinforced masonry (URM) construction technique (Figure 2.16). The first floor was added later but has never been completed. The walls of the first floor are made of stone masonry, the interior and front facade are made of timber frame. The slab system is made of timber beams and steel I-profile beams. Steel elements started to be used in the region with the railways coming to the nearby region in the second half of the 19th century and the beginning of the 20th century (Sandalcı, 2005). It is probable that these steel beams were constructed after the 1872 earthquake when the house was built again (METU CONS, 2019). Steel I-profile beams are original elements in the building where the socio-cultural transition periods of the region can be red. The roof is gabled roof. Its frame and covering has been completed but there is no ceiling constructed in the first floor. Ground floor and basement floor plans are presented in Figure 2.16 and Figure 2.17.

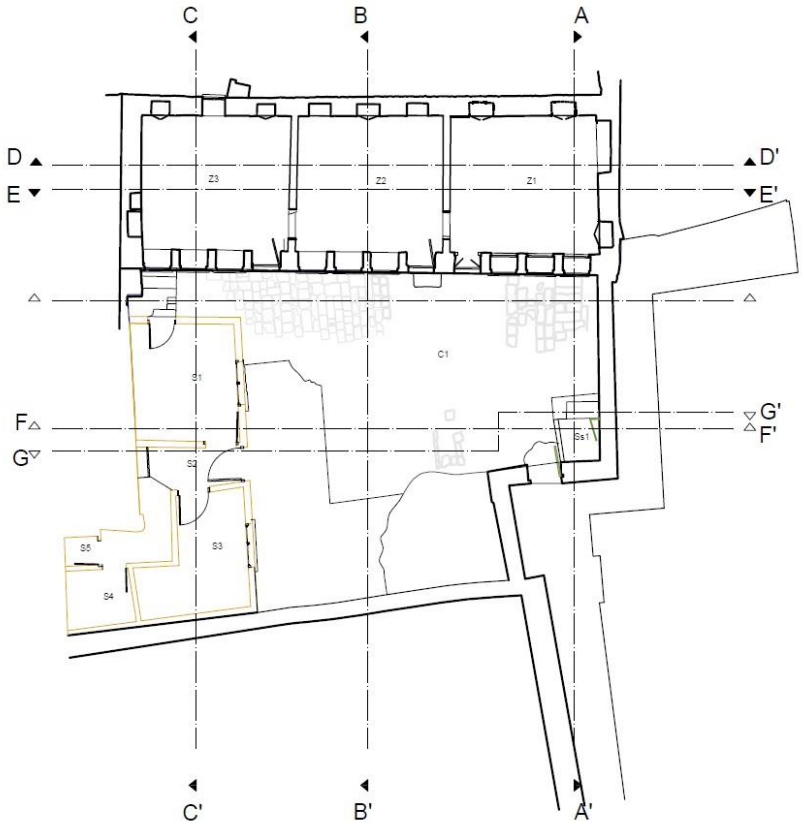

Figure 2.16 Section lines (METU CONS, 2019)

The stairs opening from the courtyard to the B01 and B03 rooms of the building provides the entrance to the basement (Figure 2.18). The basement is divided into three spaces with almost equal dimensions. There were doors in rooms B01 and B03 one each, which used to provide entrance and exit to the building, which is at street level from the north (Figure 2.20).

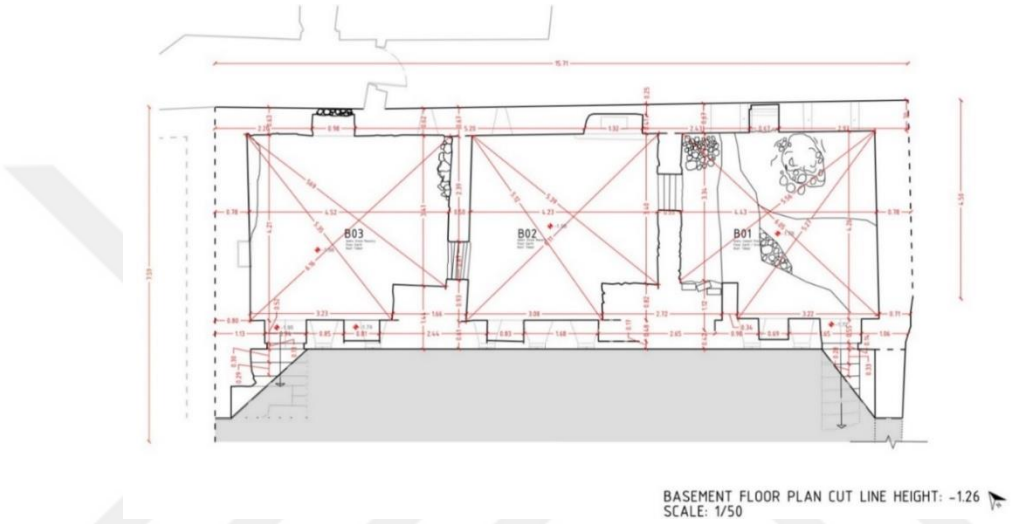

Figure 2.17 Basement floor plan - cut line height: -1,26m (METU CONS, 2019)

Figure 2.18 Stairs form courtyard to B01 & B03 (Şahin Güçhan, 2019)

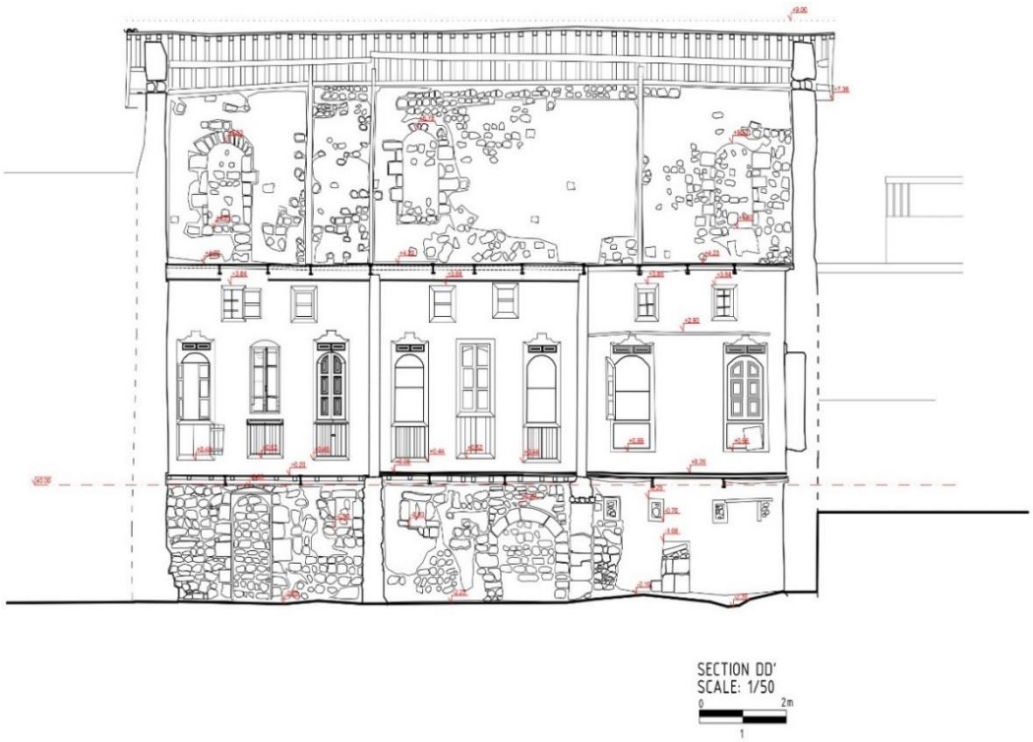

Figure 2.19 Section DD' (METU CONS, 2019)

Figure 2.20 Filled door openings in B01 and B03 (Şahin Güçhan, 2019)

The north wall of the basement floor is at street level (Figure 2.21). The wall thickness is approximately 60 cm. However, in the sections where there are niches that were previously used as doors and later filled in, the wall thickness decreases to

5, 10 and 15 cm. The windows in room B01 have been filled in with stones and closed.

Figure 2.21 North wall (Şahin Güçhan, 2019)

The west wall of the basement floor is about 85 cm. longer than the front facade level (Figure 2.24). It is thought that the front facade was fixed to this level for some reason before it was rebuilt. This construction feature might have been due to possible damage during the 1872 earthquake that the front facade might have been rebuilt later from inside (METU CONS, 2019). The masonry wall type on the front facade was rubble masonry while rough cut stone was used on the edges of the openings. The wall thickness is approximately 65 cm. The thickness decreases to 50cm where the niches are located on the wall.

Figure 2.22 Basement west wall (Şahin Güçhan, 2019)

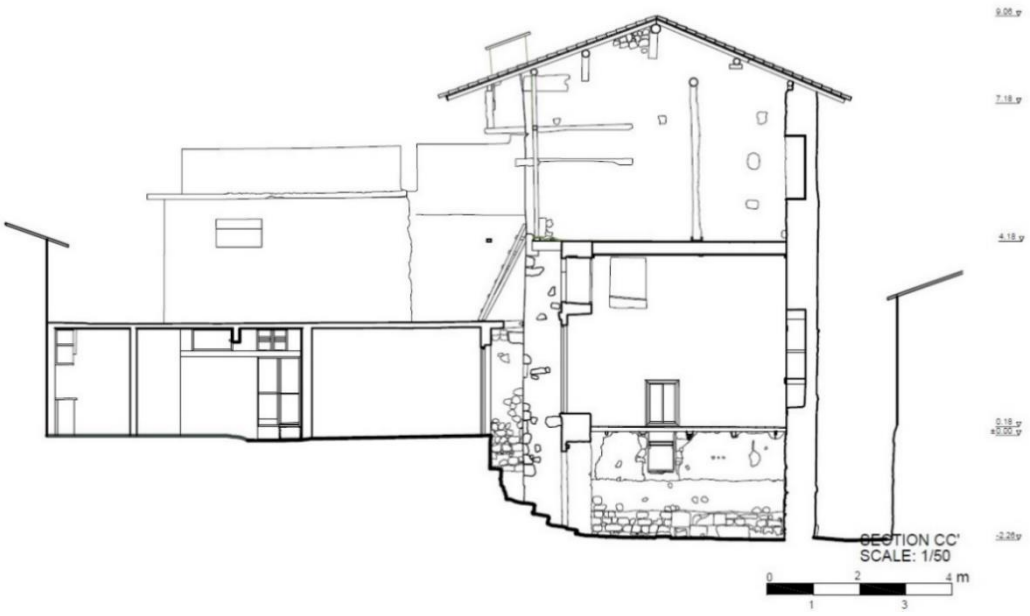

Figure 2.23 Section CC’ (METU CONS, 2019)

Figure 2.24 Trace of longer wall (Şahin Güçhan, 2019)

The south facade of the building has always been the main facade. There are many openings on this wall compared to the other walls (Figure 2.25). Rooms B01 and B03 each have a door providing entrance and exit to the courtyard. There are arch-shaped elements on the south wall that indicate different uses in the previous periods of the building than today (METU CONS, 2019). The wall thickness in this region is around 20 cm. In parts of the wall without openings, thickness is about 60 cm. The wall is constructed on the front facade with rubble stone and fine cut stone facing. There are windows allowing light to enter the spaces from the courtyard. Their relationship with the ceiling shows that the dimensions of the space have been changed (Figure 2.26) (METU CONS, 2019).

Figure 2.25 Section EE' (METU CONS, 2019)

Figure 2.26 South wall in the basement floor (Şahin Güçhan, 2019)

The east wall of the basement floor extends beyond the front facade level and is followed by courtyard wall (Figure 2.27-Figure 2.28). The wall thickness is approximately 75 cm. There is no opening in this wall in the basement.

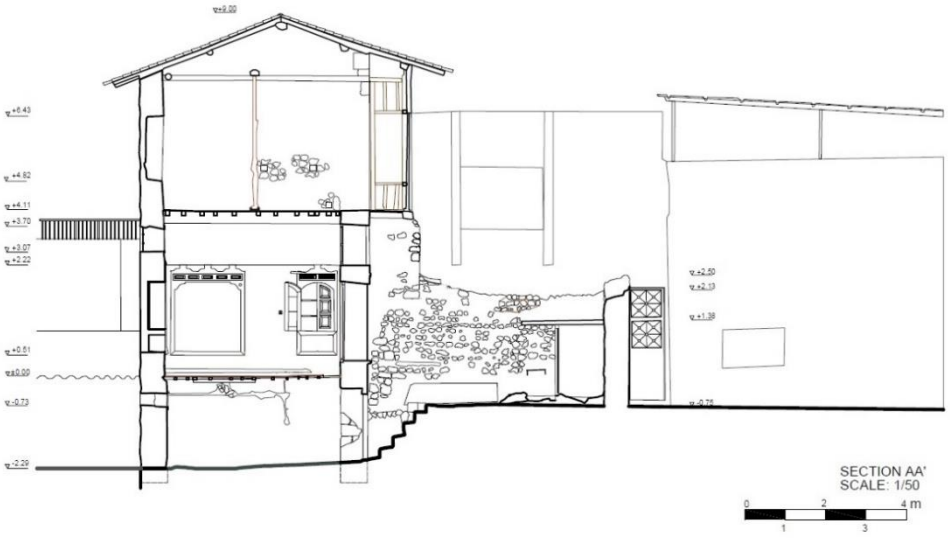

Figure 2.27 Section AA’ (METU CONS, 2019)

Figure 2.28 East wall and courtyard wall (Şahin Güçhan, 2019)

2.3.1.1 Basement Floor

This section gives detailed information regarding the rooms on the basement floor. The floor plan is provided in Figure 2.29.

Room B01: This is the place located to the east of the basement floor. A staircase opening from the courtyard provides the entrance to B01. The space is approximately 4.40 m x 4.30 m in size and 2.20 m in height. It is separated from B02 to its west by a masonry wall added later. The passage to B02 is provided by an opening in this wall. Although the western and northern walls are plastered, masonry wall mesh is visible. All walls are rubble masonry with mortar. Lime and mud mortar were used. There are horizontal and vertical traces of intervention on the wall in room B01 due to a possibly a filled niche (Figure 2.32) (METU CONS, 2019). There is a door with a 1 m height on the northern wall that previously opened to the street and was filled in later. Similarly, four windows with timber frames were closed later. The B01 eastern wall mesh is different from the surrounding walls. This suggests that the partition wall was an addition. The opening through which the passage to B02 is provided is constructed by relatively larger size and rough-cut stones. There is a door opening to the courtyard, two windows and an arched niche approximately 1 m height on the B01 southern wall. There is also a masonry mass at the corner of the southern wall and eastern wall. This mass might have been built to support the construction that was demolished after the earthquake occurred in 1872 (METU CONS, 2019). Steel profiles were possibly used during the rebuilding period, as well.

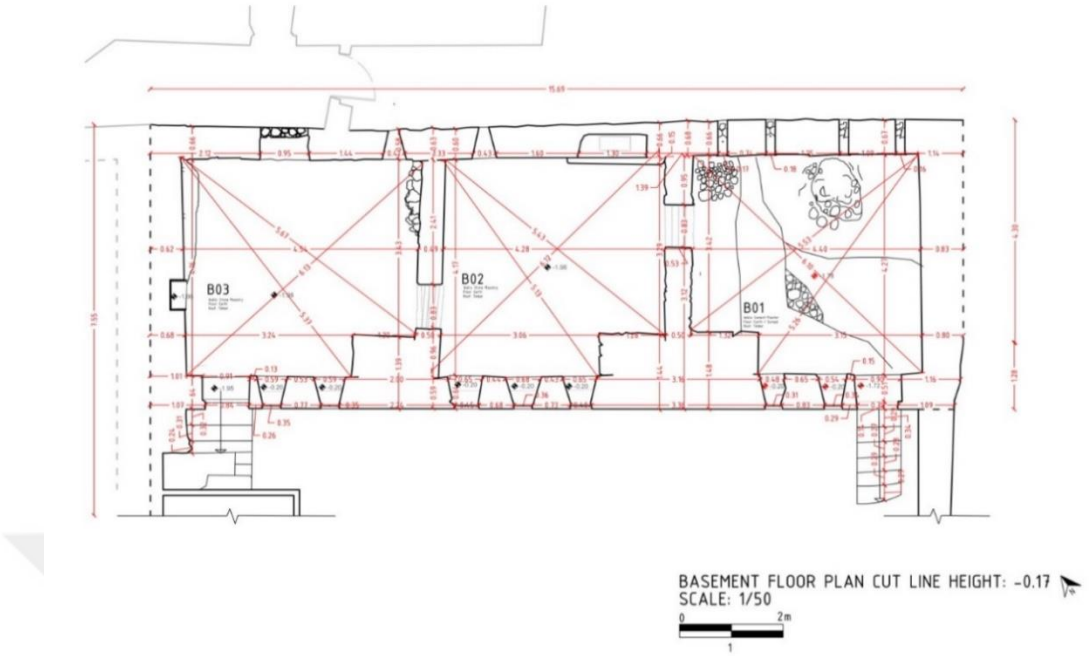

Figure 2.29 Basement floor plan - cut line height: -0,17m. (METU CONS, 2019)

The basement partition walls are made of stone masonry with mud mortar. Cut stones are used on the edges of openings such as doors, windows, and niches. Partition walls are addition walls having different type of mesh and different sizes of stones from the main walls and without a proper connection (Figure 2.30). There are also masonry masses on the southern facade of the basement (Figure 2.31).s

Figure 2.30 Partition walls in the basement (Şahin Güçhan, 2019)

Figure 2.31 Basement floor masses (Şahin Güçhan, 2019)

Figure 2.32 Traces of intervention in the east wall of the B01 Room (Şahin Güçhan, 2019)

Figure 2.33 Masonry mass and steel I-frame beam (Şahin Güçhan, 2019)

The floor is a partially screeded earth floor (Figure 2.34). Traces of stone slab are also seen on the floor. On the corner of the floor there is a collapsed region. On the ceiling, the floor construction is visible as it is without coating. The floor system is formed by steel I-profiles and timber beams stuck to these profiles or placed on them. Steel I-profile beams are original elements used in some Antakya houses after the railway came to the nearby region. Steel beams were placed on the walls by opening holes in the walls. The north wall was filled with plaster, and on the south, it was placed on the wall without any other connection. The timber elements in the slab are hand-cut or re-used elements. Some of the elements might have been re-used from the *mabeyn* in traditional Antakya Houses (Demir, 2004). There is also a gap in the slab near the south facade

Figure 2.34 Basement floor plan material use (METU CONS, 2019)

Room B02: This is the room in the middle of the basement. The space is approximately 4.30 m x 4.20m in size and 2.20m in height. Entry and exit are provided through an opening in the walls added later, B01 to the east and B03 to the west. All the walls are rubble masonry with mortar. On the north wall, there is an arched niche that is assumed to be a fireplace and a window that was closed later. The edges of the openings are constructed with rough cut stone. The partition wall to the west of B02 has a similar wall mesh to the partition wall to the east. These two walls were probably built later and at the same period. The partition wall to the west has a door opening of 2 m in height. There are timber lintels over the opening (Figure 2.35).

Figure 2.35 Partition wall with timber lintels over opening (Şahin Güçhan, 2019)

On the south wall of B02, there is an arched niche of approximately 1.20 m in height and 3 window openings. This niche is covered by the mass added later. There is a masonry mass in the southeast corner of the space. There is a passage to B01 with

an opening of 85 cm in the east. The floor is made of earthen material. The ceiling contains hand-cut, machine-cut and re-used timber elements along with steel profiles.

Room B03: There is an entrance to B03 from the courtyard and B02. It is a space measuring approximately 4.6 m by 4.2 m and 2.2 m high. There is a window on the north wall that was closed later and an arched door that was previously in service and opened to the street but was later filled and closed, approximately 2 m high. There are two separate plaster traces on two different levels on the west wall. Below, masonry texture can be seen. Also, there are projecting stones into the room, which could be a trace of a vault (METU CONS, 2019). A cupboard is also embedded in this wall. On the south wall, there is an arched niche, two windows with irregular relations to the floor level, a door opening to the courtyard and a masonry mass at the corner of the partition wall. The floor is made of earthen material. The timber elements on the ceiling are machine-cut.

2.3.1.2 Ground Floor

The ground floor consists of three spaces with similar dimensions as the basement floor in plan (Figure 2.36). The storey height is about 3.90 m. Partition walls are additions that were made of briquette with cement mortar. All three rooms are open to the courtyard and there are doors between the rooms. Main facade is the ornamented south facade with fine cut stones. All rooms are plastered inside.

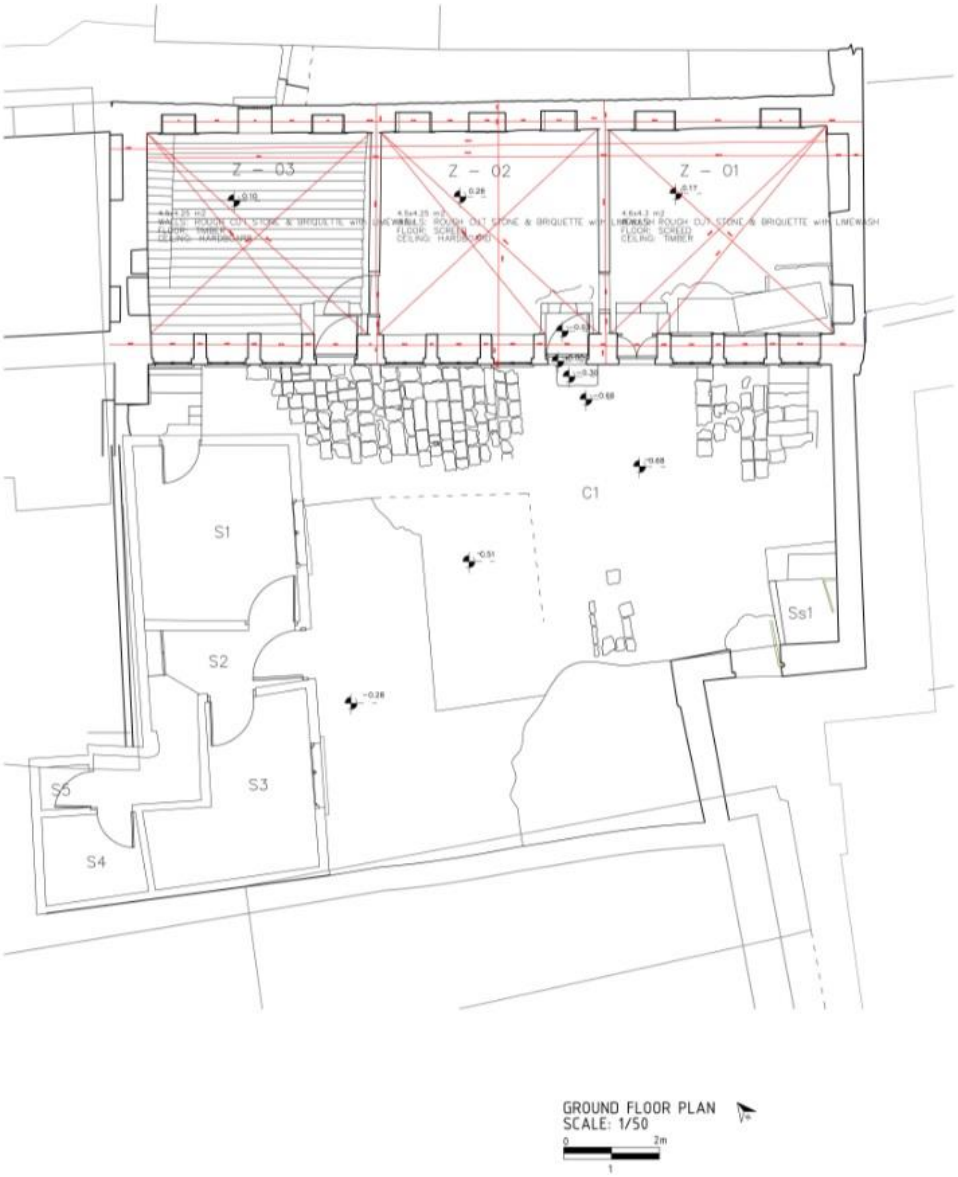

Figure 2.36 Ground floor plan (METU CONS, 2019)

G01 Room: It is located on the east of the floor having direct access from the courtyard. The entrance of the space has a step approximately 25 cm high from the threshold. The space is 4.6 m long, 4.3 m wide and 3.90 m high. The walls are rubble stone masonry with mortar. There are two niches and two windows on the north wall. It is separated from B02 on the west by a briquette wall added later. A door on this wall provides access to the spaces. There is a door opening to the courtyard on the south wall and three windows approximately 2.25 m high. There are additional four windows in the upper-middle section of each of these four openings. There is a niche on the east wall, one 80 cm wide, the other 160 cm wide, both approximately 2.25 m high. The floor is covered with screed and the ceiling is uncoated. The slab is constructed with steel beams, timber beams stuck to them and timber planks, as in the basement.

Figure 2.37 G01 room (Şahin Güçhan, 2019)

G02 Room: It is in the middle having access from both courtyard and G01 and G03. Dimensions are 4.6 m and 4.3 m with a height of approximately 3.7 m. On the north wall, there are three niches and two windows. On the west, there is a plastered briquette wall added later. On the south wall, in lower level, there is a door opening to courtyard and three windows. In the upper level, there are four more windows. In the east, a wall, which was added later, exists. The floor is covered with screed and the ceiling is covered with hardboard (Figure 2.38).

Figure 2.38 G02 room (Şahin Güçhan, 2019)

G03 Room: It has access to both the courtyard and room G02. Dimensions are 4.5 m and 4.2 m with a height of approximately 3.7 m. On the north wall, there are three niches and two windows. On the west, there are two niches: one close to the ground and one to the ceiling. On the south wall, there is a similar opening pattern to G02. In the east, an addition wall exists. The floor is covered with timber planks whereas the ceiling is covered with hardboard (Figure 2.39).

Figure 2.39 G03 room (Şahin Güçhan, 2019)

2.3.1.3 First Floor

This floor is a later addition, but it has never been completed. The plan of the first floor is given in Figure 2.40. The three perimeter masonry walls of the floor do not connect in the south which was designed as timber facade. There are no partition walls, either. In the east and west walls two partially timber lintels exist. The I-Beams of the slab project through the south facade. There is an incomplete timber frame structure and tin elements in the facade (Figure 2.41). On the first floor, there is a C-profile steel frame on which the timber posts are reside.

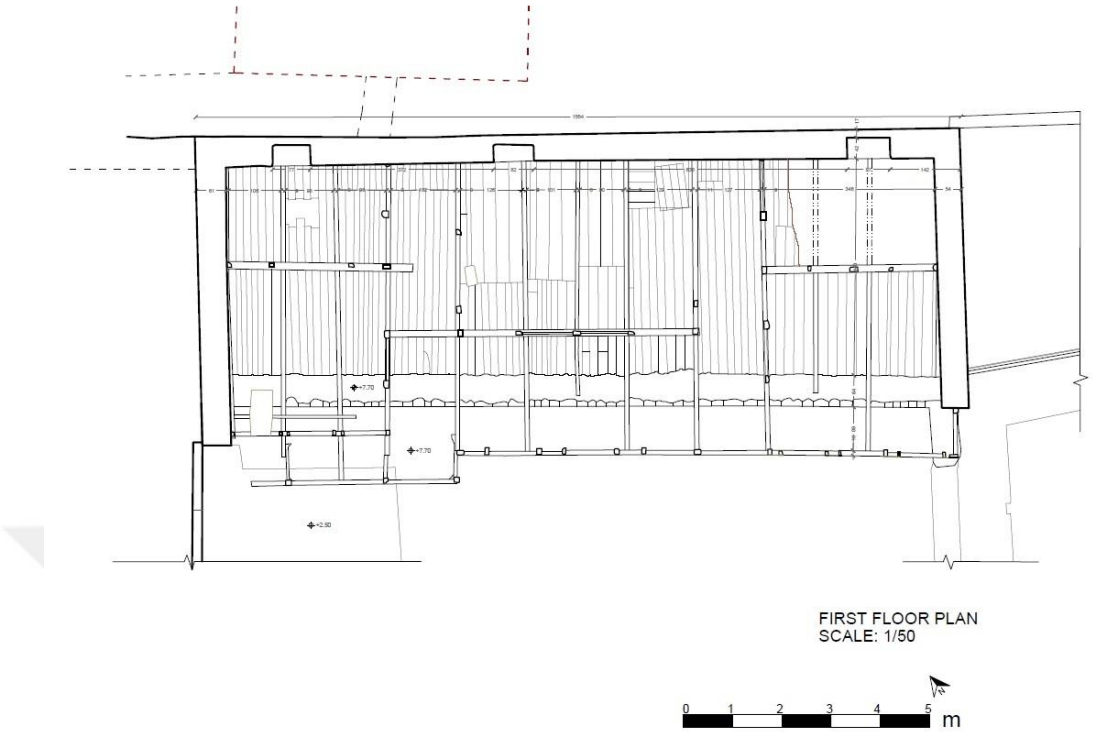

Figure 2.40 First floor plan (METU CONS, 2019)

Figure 2.41 First floor timber frame (METU CONS, 2019)

In the first floor the thickness of the north wall is 58cm. Within the wall, there are three arched niches where the thickness of the wall is reduced to 17cm. West wall has a thickness of 54cm, whereas east wall is 61 cm thick without niches. All the walls were made of rubble stone with mortar.

2.3.1.4 Construction Technique

As explained in the previous section, Beştek House has been constructed with URM technique and steel I beam-timber composed slab system. Masonry wall texture is composed of rubble stone with mortar. The ground floor south facade wall was finished with fine cut stone over rubble stone mesh. The unfinished first floor and front facade of the first floor were constructed with timber elements. Construction technique of the Beştek House can be understood better with the assistance of illustrations in Figures Figure 2.42 and Figure 2.43 together with the photo in Figure 2.44.

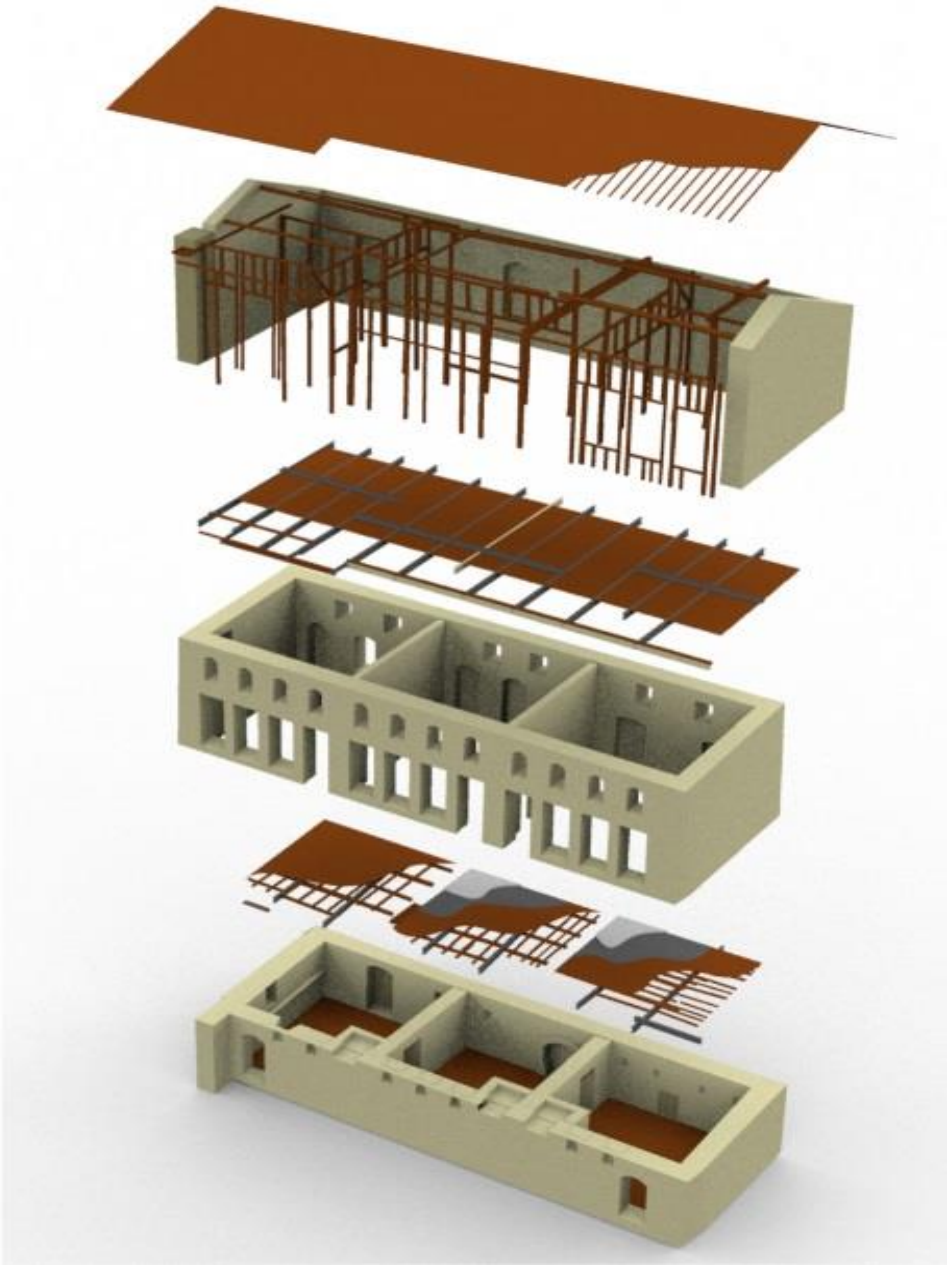

Figure 2.42 Construction technique (METU CONS, 2019)

Figure 2.43 Construction technique - Section (METU CONS, 2019)

Figure 2.44 Unfinished facade of the first floor (METU CONS, 2019)

2.3.1.5 Slab System

The details of the basement floor slab are unknown. It ends with screed-soil. There is a collapse in the corner of room B01. This reveals that the floor system might have been hollow underneath. There are projecting stones in room B03, which might be elements of a vault (METU CONS, 2019).

The ground floor slab system is composed of timber and steel. The slab system is formed by 20 cm wide timber planks placed on timber beams placed at approximately 1 m intervals. These timber beams are carried by steel I-profile beams placed along the short axis of the building. Timber beams are stuck to the bodies of I-profile beams. The connection of steel I-profiles to the wall had been carried out with different construction techniques. In the first one, the wall section was cut as much as the area where the profile will sit on the wall and the beam was placed on

the wall without any other connection. In another connection type, the placed beam was filled with mortar and the beam was embedded into the wall.

The details of the slab system vary also in the rooms. While rooms G01 and G02 have been finished with screed, Z3 was finished with timber planks. Tin was used in G02, whereas nylon is used in Z1 (Figure 2.45). There is probably a gap in the floor for the stairwell in the northern corner of G02.

Figure 2.45 Slab system of the rooms G03 and G02 (METU CONS, 2019)

The slab system of the first floor is similar to the ground floor. The slab was finished with timber planks on timber beams stuck to steel I-profiles. The steel profiles were finished with timber planks. On the first floor, the steel profiles were extended as cantilevers on the south face of the building.

The slab thickness is measured approximately as 25-28 cm in B01, 30 cm in B02 and 26 cm in B03.The slab thickness is approximately 17 cm in G01, 25 cm in G02 and G03.

In the first-floor slab, C-profile steel elements, on which the timber elements reside, were placed on the slab.

There exist machine-cut and hand-cut timber elements. There are re-used elements, as well. These notched elements might have been the *mabeyn* stairs used in Antakya Houses (Demir, 2004).

2.3.2 Structural Features of the Beştek House

The structural features of Beştek House can be examined by considering the soil-foundation properties, the presence of adjacent buildings, vertical and horizontal irregularities, the presence of a basement, box effect, rigid floor diaphragm, connections, material properties and geometric conditions.

The first and a very important parameter of these, soil properties, are not sufficiently known. As explained in Section 2.3, both the literature and the traces observed in the basement of the house and explained by the study of METU CONS, 2019 suggest that the area of the building has been inhabited since the Hellenistic period. The building was probably demolished for various reasons throughout history and rebuilt in its place with some changes in its features (METU CONS, 2019). The traces of the arch in the basement and the collapse of the floor in B01 indicate that the building does not have a proper mat foundation. It is highly probable that the walls were placed on the remains of the previous construction. Therefore, it can be assumed that there are spread footings under the walls.

In historical centers, it is quite common for buildings to be constructed in adjacent order. The existence of adjacent order buildings may have advantages and disadvantages. Buildings with similar mass properties and similar dynamic properties may help each other to stand during an earthquake by limiting the level of

lateral drift of the structure. On the other hand, it is known that adjacent buildings with different mass and rigidity properties, different number of floors, and different elevation of floor slabs transfer extra sudden loads to each other due to the hammering effect in an earthquake. Beştek House is adjacent to the neighboring building to its west with similar mass properties. There is another adjacent structure to its east but does not have similar mass properties. The east-west axis is also the axis where Beştek House is long and strong. There are no adjacent structures in the north-south direction which is the short axis of the building. South facade is critical due to the ground floor front facade with many openings and the first-floor facade without a masonry wall connecting the other walls, so that a box-like behavior can occur.

Regularity is an important criterion for masonry buildings where horizontal and vertical loads are carried by walls. Irregularity, asymmetric distribution of structural members, large projections, non-overlapping walls in the plan, the difference between the building's center of rigidity and center of mass, especially in horizontal loading situations such as earthquakes, can cause extra forces in the building, stress concentrations, consequently in-plane and out-of-plane cracks. Beştek House is a regular building with a rectangular form. In addition, the partition walls overlap in the plan. On the other hand, there is no masonry wall on the front facade of the first floor. In this sense, vertical continuity cannot be ensured.

Beştek House is one of the rare buildings in the historical city of Antakya with a basement floor. It is known that buildings with basements contribute to the general behavior of the building in areas with different ground properties and are effective in preventing ground failure.

Wall distribution is another important criterion in masonry structures to carry lateral forces in both directions (Hendry *et* al., 2006). Beştek House is strong in its longitudinal axes. On the other hand, walls in the short direction are thicker. East and west walls have thicknesses of 75 cm and 65 cm in the basement whereas north and south walls are approximately 60 cm. In the ground floor, wall thicknesses are

63 cm in the west, 65 cm in the east, 60 cm in the north and 64 cm in the fine-cut finished south. Also, partition walls are also in the short direction of the building. The thickness of the basement walls and thick additional masonry walls and the masses in the basement increase the rigidity of this floor. As such, wall distribution can be regarded as regular.

Connections in masonry buildings are a very important issue in terms of ensuring load transfer and also box-like behavior. The connections between the walls, the wall-floor connections, the connections between the floor elements, the connections between the elements made of different materials affect the load transfer mechanism of the building and the dynamic properties of the building.

It can be stated that the original masonry walls in the basement and ground floor have relatively proper connections on their own floor level. Although the thick masonry partition walls added to the basement floor are not connected properly to the existing walls, they are very important load-bearing elements due to their thickness. On the ground floor, the connection of the briquette partition walls added later with the existing walls is not proper, as well. On the first floor, there is no masonry wall on the front facade. This means that the box effect, which means that the masonry walls can work together like a box, cannot be provided on this floor. Therefore, it can be said that the in-plane wall displacement and out-of-plane behavior of the walls on the first floor are critical during seismic action.

The slabs were constructed with steel and timber together. Steel beams were placed on the masonry walls by opening a hole in the walls without any other connection. It has been observed that the gaps opened in some connections are filled with mortar. Timber beams were also placed on steel beams or stuck into their bodies. With these connections, it does not seem possible to transfer loads between floors and walls. In such cases, the presence of the rigid floor diaphragm effect, which is very important in masonry buildings, is of concern. Rather than a one-way load transfer mechanism though in the slab, it can be mentioned one-way frame behavior due to steel beams having higher load-bearing capacity than timber elements.

The use of joists in masonry buildings is also an important feature for the provision of load transfer mechanism. In Beştek House, it is not possible to mention the use of regular, continuous horizontal or vertical joists.

The building under consideration consists of elements with different mechanical properties, such as stone, steel, timber, briquette and screed. Elements with different rigidity properties enforce peculiar load transfer paths and unexpectedly localized stress concentrations during seismic action.

The main load-bearing elements in masonry structures are walls. The importance of the effect of mortar on the mechanical properties of walls is well-studied. Although the properties of the mortars used in Beştek House have not been examined in detail, it can be stated that mud and lime mortars had been utilized. The strength of the mortars used in the region and therefore the mechanical properties affecting the wall strength have been reported as quite low (Bozyigit *et* al., 2024). It is very probable that mortar with similar properties had been employed in Beştek House.

2.3.2.1 Geometric Conditions of the Masonry Walls of the Beştek House

In literature and codes, geometric conditions are given for load-bearing masonry elements. First of these is the height over thickness ratio given in Table 11.4 in TBSC-2018. For the walls under shear effect, load-bearing walls should provide the conditions of $t_{ef} \geq 350$mm and $h_{ef} / t_{ef} \leq 9$. Below in Table 2.3, results are presented.

Table 2.3 Minimum wall thickness & slenderness check

	Wall Properties					CHECK (tef ≥ 350mm)		CHECK (hef / tef ≤ 9)		
	Floor	Wall	Height (m)	Wall Thickness (cm)	Minimum Wall Thickness (Niches) (cm)	Minimum Wall Thickness (cm)	Minimum Wall Thickness - Niches(cm)	hef / tef	Minimum Wall Thickness (cm)	Minimum Wall Thickness - Niches(cm)
1	Basement Floor	North	2,4	60	15-20	CHECK	FAIL	4,0	CHECK	FAIL
2	Basement Floor	West	2,4	65	50	CHECK	CHECK	3,7	CHECK	CHECK
3	Basement Floor	South	2,4	59	20	CHECK	FAIL	4,1	CHECK	FAIL
4	Basement Floor	East	2,4	75	-	CHECK	-	3,2	CHECK	-
5	Basement Floor	South	2,4	59	20	CHECK	FAIL	4,1	CHECK	FAIL
6	Basement Floor	Partition West	2,4	49	-	CHECK	-	4,9	CHECK	-
7	Basement Floor	Partition East	2,4	50	-	CHECK	-	4,8	CHECK	-
8	Ground Floor	North	4,2	60	20	CHECK	FAIL	7,0	CHECK	FAIL
9	Ground Floor	West	4,2	63	20-30	CHECK	FAIL	6,7	CHECK	FAIL
10	Ground Floor	South	4,2	64		CHECK	-	6,6	CHECK	-
11	Ground Floor	East	4,2	65	20-29	CHECK	FAIL	6,5	CHECK	FAIL
12	Ground Floor	South	4,2	64		CHECK	-	6,6	CHECK	-
13	First Floor	North	3,2	58	17	CHECK	FAIL	5,5	CHECK	FAIL
14	First Floor	West	5,2	54	-	CHECK	-	9,6	FAIL	-
15	First Floor	South	3,2	-	-	CHECK	-		CHECK	-
16	First Floor	East	5,2	61	-	CHECK	-	8,5	CHECK	-

Second is the unsupported wall length criteria described in 11.5.2 in TBSC-2018. In ground floor, there are partition walls made of briquette. Even though these walls are not accepted as load-bearing elements, due to their rigidity, ground floor wall lengths are limited with these partition wall. North wall of the first floor does not meet this condition. Below in Table 2.4 conditions are presented.

Table 2.4 Unsupported wall length check

Wall Properties (Unsupported Wall Length)				
	Floor	Maximum Unsupported Wall Length (m)	limit (m)	Check
1	Basement	5,25	5,50	✓
2	Ground	5,08	5,50	✓
3	First	15,08	5,50	X

In Turkish Building Seismic Code-2007 (TBSC-2007) there were other geometric conditions which do not exist in 2018. The total length of perpendicular walls on a floor should not be less than 20% of the floor area. (TBSC, 2007). Only, basement floor walls meet this condition, presented in Table 2.5.

Table 2.5 Wall length / area check

Wall Properties (l_d / A)						
	Floor	**Facade**	**Wall Length (without void) (l_d) (m)**	**A (m2)**	**ld/A**	**Check (ld / A ≥ 0.2 l m/m2)**
1	Basement Floor	North	11,41	75		-
2	Basement Floor	West	5,48			-
3	Basement Floor	South	8,67			-
4	Basement Floor	East	5,58			-
5	Basement Floor	Partition West	3,30			-
6	Basement Floor	Partition East	3,37			-
	Basement Floor	**Sum (X)**	**20,08**		**0,27**	✓
	Basement Floor	**Sum (Y)**	**17,73**		**0,24**	✓
1	Ground Floor	North	9,53	75		-
2	Ground Floor	West	4,09			-
3	Ground Floor	South	5,01			-
4	Ground Floor	East	3,20			-
	Ground Floor	**Sum (X)**	**14,54**		**0,19**	**X**
	Ground Floor	**Sum (Y)**	**7,29**		**0,10**	**X**
1	First Floor	North	13,05	75		-
2	First Floor	West	6,27			-
3	First Floor	South	0			-
4	First Floor	East	5,67		-	-
5	**First Floor**	**Sum (X)**	13,05		**0,17**	**X**
6	**First Floor**	**Sum (Y)**	11,94		**0,16**	**X**

The ratio of wall lengths to wall thickness is used for robustness of elements. According to the study of Arya *et* al (2010), this ratio should be a / t ≤ 40. Below, in Table 2.6 , this condition is checked.

Table 2.6 Robustness of masonry walls

Wall Section Properties (a/t)						
	Floor	**Facade**	**Wall Thickness (t) (cm)**	**Wall Length (a) (cm)**	**a / t**	**Check (a/t <40)**
1	Basement Floor	West	65	548	8,4	✓
2	Basement Floor	North	60	1569	26,2	✓
3	Basement Floor	East	75	558	7,4	✓
4	Basement Floor	South	59	1569	26,6	✓
5	Basement Floor	Partition West	49	440	9,0	✓
6	Basement Floor	Partition East	50	440	8,8	✓
7	Ground Floor	West	63	552	8,8	✓
8	Ground Floor	North	60	1560	26,0	✓
9	Ground Floor	East	65	566	8,7	✓
10	Ground Floor	South	64	1560	24,4	✓
11	Ground Floor	Partition West	21	-	-	-
12	Ground Floor	Partition East	20	-	-	-
13	First Floor	West	54	564	10,4	✓
14	First Floor	North	58	1554	26,8	✓
15	First Floor	East	61	569	9,3	✓
16	First Floor	South	-	-	-	-

2.4 Structural Condition of the Building after 2023 Türkiye Earthquake Sequence

Detailed information regarding the 2023 Kahramanmaraş Türkiye earthquake sequence has been explained in Section 2.1. The strong shaking caused extensive and heavy destruction in many populated cities in the south-east region of Türkiye. But among these cities, the most affected one was Antakya in Hatay, especially the historical city center (Figure 2.46) (KOERI, 2023). Later, on February 20, 2023, another earthquake with a magnitude of Mw=6.3 centered in Defne occurred, causing additional stresses to the already damaged buildings in the region.

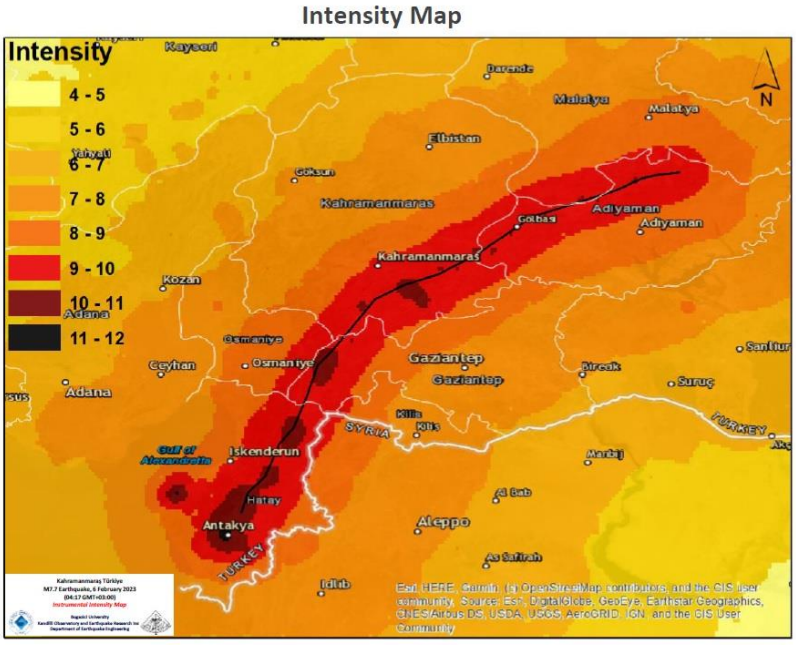

Figure 2.46 Intensity map of the 6 February 2023 Pazarcık earthquake (KOERI, 2023)

After the earthquake sequence, field visits were carried out by METU TAÇDAM to Antakya in March 2023 and June 2023. According to field observations, the roof of the building, the timber-frame construction of the first floor, and the walls of the first floor collapsed (Figure 2.47-Figure 2.48). The first floor and ground floor slabs partially collapsed (Figure 2.49- Figure 2.50). The ground floor walls remained standing with various cracks due to in-plane and out-of-plane movements within the walls (Figure 2.49-Figure 2.52). Basement floor damage could not be observed and detected in detail due to safety concerns (Figure 2.50). According to the EMS-98 Damage classification, the building can be classified as Grade-4 which stands for "very heavy damage" by definition (Figure 2.53).

Figure 2.47 Point cloud created by 3D laser scanning (METU TAÇDAM, 2023)

Figure 2.48 South and north wall (METU TAÇDAM, 2023)

Figure 2.49 First and ground floor slabs (METU TAÇDAM, 2023)

Figure 2.50 Damage in the B01 room (METU TAÇDAM, 2023)

Figure 2.51 First floor failure (METU TAÇDAM, 2023)

Figure 2.52 Wall coursing with weak mortar (left) and wall intersections (right) (METU TAÇDAM, 2023)

Classification of damage

Note: the way in which a building deforms under earthquake loading depends on the building type. As a broad categorisation one can group together types of masonry buildings as well as buildings of reinforced concrete.

Classification of damage to masonry buildings	
	**Grade 1: Negligible to slight damage** **(no structural damage,** **slight non-structural damage)** Hair-line cracks in very few walls. Fall of small pieces of plaster only. Fall of loose stones from upper parts of buildings in very few cases.
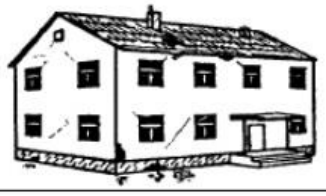	**Grade 2: Moderate damage** **(slight structural damage, moderate non-structural damage)** Cracks in many walls. Fall of fairly large pieces of plaster. Partial collapse of chimneys.
	**Grade 3: Substantial to heavy damage** **(moderate structural damage,** **heavy non-structural damage)** Large and extensive cracks in most walls. Roof tiles detach. Chimneys fracture at the roof line; failure of individual non-structural elements (partitions, gable walls).
	**Grade 4: Very heavy damage** **(heavy structural damage,** **very heavy non-structural damage)** Serious failure of walls; partial structural failure of roofs and floors.
	**Grade 5: Destruction** **(very heavy structural damage)** Total or near total collapse.

Figure 2.53 EMS-98 damage scale (EMS, 1998)

As explained through Section 2, Beştek House is a unique traditional house with architectural and structural features located in the historical center of Antakya. There are adjacent buildings on its east and west. Despite having a regular geometry, its structural features have changed over time with various interventions. The addition first floor, addition briquette partition walls of the ground floor, the steel I-profile frames in its slabs, and the change in the load transfer mechanism due to elements with different mechanical properties have made the buildings behavior quite irregular and complex in the case of seismic effects.

2023 Turkey Earthquake Sequence is a major earthquake that caused a very large destructive effect in a large area and Antakya in particular. This earthquake also caused the Beştek House to suffer Grade 4: Very Heavy Damage according to the EMS-98 scale.

CHAPTER 3

MODELLING AND STRUCTURAL ANALYSIS OF THE BEŞTEK HOUSE

In this chapter, modelling and structural analysis of the Beştek House is explained in detail. First, structural modelling approaches for masonry structures are introduced briefly. Next, the structural model of the Beştek House is explained together with the analysis method employed. The seismic response obtained from analysis is discussed in terms. In last part of the chapter, the actual damage observed after the earthquake is compared with the numerical analysis output and the results are discussed in detail.

3.1 Modelling Approaches for Masonry Structures

Historical masonry structures are complex structures due to the differences in construction techniques, materials used, and elements added and removed from the structure over time. Various assumptions and simplifications are employed to model this complex behavior as accurate as possible. Simplifications can be considered as trade-offs between computational cost and accuracy. A historical masonry structure can be modelled by using simplified or detailed approaches. According to the Guideline for Earthquake Risk Management of Historical Structures (GERMHS, 2017), since more parameters related to materials and structures are required in detailed models, it can be assumed that more realistic results are obtained. However, the results may not have the expected precision, especially due to the uncertainty in the numerical values of material parameters. For this reason, models as simple as can be preferred in cases where there is a lack of structural input data. Therefore, even if a detailed model is developed, it may be useful to work on a simple model to make order of magnitude comparisons to see how meaningful the results are.

Modelling approaches can be considered at loading level, material level, or structural level (GERMHS, 2017, Lourenço 2008). In accordance with the modelling approach

for loading level, it has been stated in GERMHS (2017) that self-weight of the members should be modelled accurately since they are significant due to large sections and dimensions of load-bearing walls. When compared to dead loads, live loads are generally much lower, except in the case of timber structures. Modelling of mass distribution throughout the structure becomes important in the case of lateral earthquake effects, which impose inertial forces to the structural members.

Definitions at the material level are determined by the relationship between masonry units, mortar and the interface between the two. Modelling techniques can be examined under three approaches according to the distinction at the material level (GERMHS, 2017, Lourenço, 2008). These are, respectively, detailed micro modelling, simplified micro modelling and macro modelling (Figure 3.1).

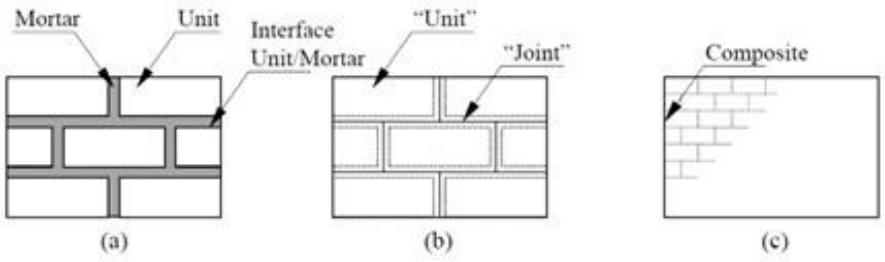

Figure 3.1 Modelling strategies for masonry structures a) detailed micro modelling b) simplified micro modelling c) macro modelling (Lourenço, 1996)

First of these approaches is called detailed micro-modelling. In this approach, the models are prepared for unit and mortar, independently. Then, these are combined using interface elements. The role of interface elements are to act as a failure plane with pseudo-stiffness in the beginning. Modulus of elasticity, Poisson's ratio and nonlinear properties of mortar and masonry unit are considered. As such, unit, mortar and interface elements can be examined in detail. (Lourenço, 1996). In this approach, additional assumptions and numerical values of defined parameters are required for the realistic behavior of units, mortar and intermediate joints under load. This method

is generally used to determine the individual behavior of a structural element in detail (GERMHS, 2017).

The second is called simplified micro-modelling. Differing from the first approach, units are taken extended in this approach. The interface between unit and mortar and joints in between are aggregated into elements with discontinuity. The Poisson effect of mortar is not taken into consideration, so a failure line is described at the joints. Masonry is considered as elastic pieces linked with this lines. (Lourenço, 1996, Lourenço, 2008)

The third approach is the macro modelling technique where the walls are defined as a composite medium. In this technique, units, mortar and interfaces are not considered as individual elements. It is assumed that a wall exhibits homogeneous properties and acts as a macro-unit. This model is more suitable for large masonry wall structures with evenly distributed members (GERMHS, 2017, Lourenço, 2008).

Definitions at the structural level are defined in the (GERMHS, 2017) as Simple Wall Model, Equivalent Frame Model (EFM) and Finite Element Model (FEM). According to Lourenço (2008), FEM seems to be the best model in order to simulate the structural behavior of masonry elements in detail together with the observed local failure modes.

Micro-modelling techniques are often used to examine specific elements. The cost of using these detailed techniques is the time spent on calculations. In order to use such detailed modeling techniques, detailed laboratory studies must be carried out. When examining real buildings, such studies are usually not available, so more general assumptions representing these features are made. However, assumptions that are far from reality can also reverse the advantages provided by detailed studies. (Roca, 2010).

3.2 Structural Modelling of the Beştek House

The Beştek House is modelled using the FEM with a macro modelling approach by using SAP2000 Software V.21.1.0. The building has a plan area of approximately 15 m by 5 m. The basement floor height is taken 2.4 m whereas the ground floor height is 4.2 m. The upper level of the first-floor walls is 7.4 m. The upper level of the gable walls is 9.4 m. The load-bearing system is composed of masonry walls as the vertical element and floors as the horizontal element. Wall thicknesses considered in the structural model are given in Table 3.1.

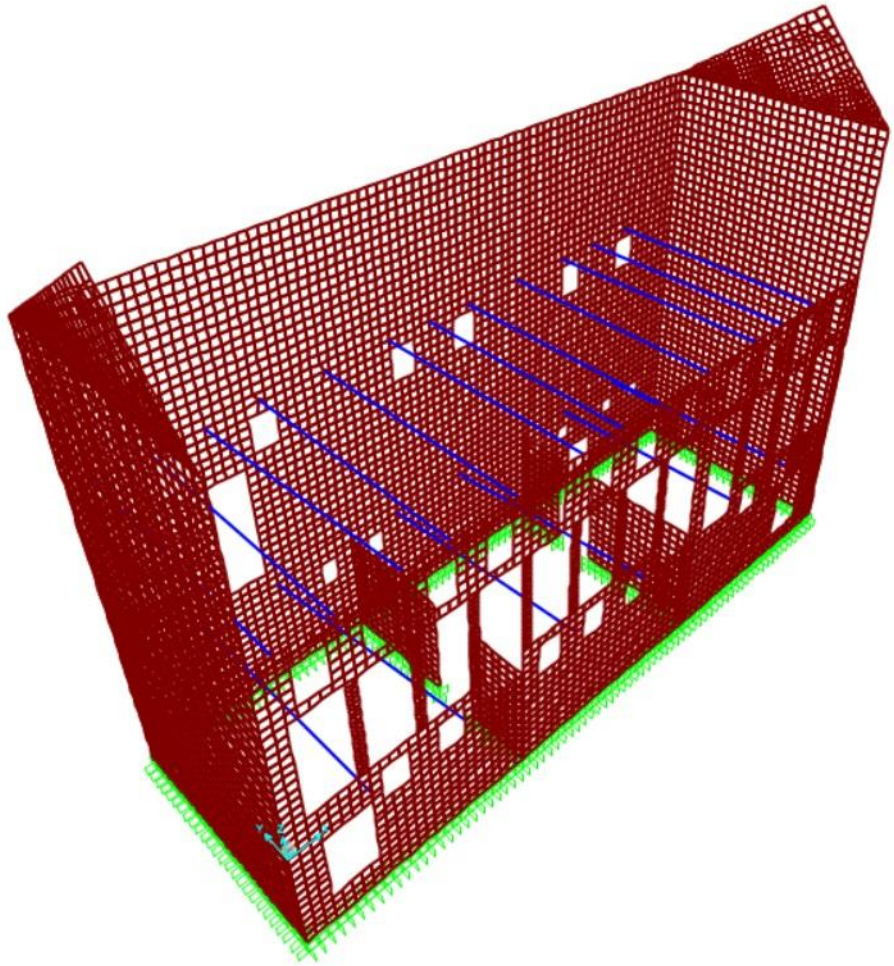

Figure 3.2 Finite element model of the Beştek House

As the walls had been constructed with rubble masonry and mortar, they are modelled with shell elements with a maximum mesh spacing of 0.20 m. The section where the masonry piers are located on the ground floor and the front facade is divided into at least two elements and 0.10 m elements are used. The sections where niches are located on the basement floor and ground floor and where wall sections are reduced are modelled with elements with smaller wall thickness. The partition walls in the basement are considered as load-bearing walls and they are considered in the model. The contribution of the ground floor partition walls constructed from briquettes is not taken into account and is assumed as an additional weight only.

Since the floors are constructed with steel I-profiles and relatively weaker timber elements, the floors do not seem to work as rigid diaphragms. For this reason, only the steel elements in the floors are modelled as frame elements. The self-weights of the floors are calculated and applied to the frame elements as a distributed load. Since the steel beam-wall connections are not proper and they are not supported to the wall using other elements, their connections to the walls are considered as elements that do not transfer moment and are modelled as joints. Wall-foundation connections are modelled as fixed connections.

The timber construction of the first floor and the roof construction are not considered as load-bearing elements and are applied to the model as additional weight.

Table 3.1 Wall thicknesses used in the structural model

Wall Section Properties				
	Floor	**Facade**	**Wall Thickness (cm)**	**Minimum Wall Thickness (cm)**
1	Basement Floor	West	65	50
2	Basement Floor	North	60	5-15-20
3	Basement Floor	East	75	-
4	Basement Floor	South	59	20
5	Basement Floor	Partition West	49	-
6	Basement Floor	Partition East	50	-
1	Ground Floor	West	63	20-30
2	Ground Floor	North	60	20
3	Ground Floor	East	65	20-29
4	Ground Floor	South	64	
5	Ground Floor	Partition West	21	
6	Ground Floor	Partition East	20	
1	First Floor	West	54	-
2	First Floor	North	58	17
3	First Floor	East	61	-
4	First Floor	South	-	-

3.2.1 Material Properties in the Structural Model

In the Beştek House, different construction materials such as stone, mortar, steel, timber, screed, and tile were used together. Among these, the walls, which are load-bearing elements, are modelled by using macro elements with 2-D shell elements and steel beams as 1-D frame elements. The weights of non-structural elements have been calculated and applied to the model as additional weight. Other material properties that are required during analysis are the modulus of elasticity and the Poisson ratio. These mechanical properties of the walls are provided in Table 3.2.

Table 3.2 Mechanical properties of the walls used in the model

Wall Mechanical Properties						
Floor	**Wall**	**Stone / Wall Mesh**	**Mortar**	**Weight per Unit Volume kN / m3 [ρ_{wall}]**	**Modulus of Elasticity [E] (Mpa)**	**Poisson (U)**
Basement	South	Rubble Masonry	General Purpose / Lightweight Mortar	19	2585	0,25
	East	Rubble Masonry	General Purpose / Lightweight Mortar	19	2585	0,25
	North	Rubble Masonry	General Purpose / Lightweight Mortar	19	2585	0,25
	West	Rubble Masonry	General Purpose / Lightweight Mortar	19	2585	0,25
	PartitionW	Rubble Masonry	General Purpose / Lightweight Mortar	19	2585	0,25
	PartitionE	Rubble Masonry	General Purpose / Lightweight Mortar	19	2585	0,25
Ground	South	Drywall & Fine Cut Stone	-	21	2585	0,25
	East	Rubble Masonry	General Purpose / Lightweight Mortar	19	2585	0,25
	North	Rubble Masonry	General Purpose / Lightweight Mortar	19	2585	0,25
	West	Rubble Masonry	General Purpose / Lightweight Mortar	19	2585	0,25
	PartitionW	Briquette Masonry	Cement	-	-	-
	PartitionE	Briquette Masonry	Cement	-	-	-
First	South	-	-			
	East	Rubble Masonry	General Purpose / Lightweight Mortar	19	2585	0,25
	North	Rubble Masonry	General Purpose / Lightweight Mortar	19	2585	0,25
	West	Rubble Masonry	General Purpose / Lightweight Mortar	19	2585	0,25

The elasticity modulus of the walls was taken as 2585 MPa, which is the minimum value calculated according to TBSC (2018) for different samples from the study by Bozyigit *et* al. (2024) as shown in Figure 3.3. The Poisson ratio is assumed as 0.25. The values in Table 6.1 in GERMHS (2017) have been used for wall weights. The unit weight per volume is taken as 19 kN/m^3 for all walls except the front wall in the ground floor finished with cut stone over rubble masonry, which is considered as 21 kN/m^3 .

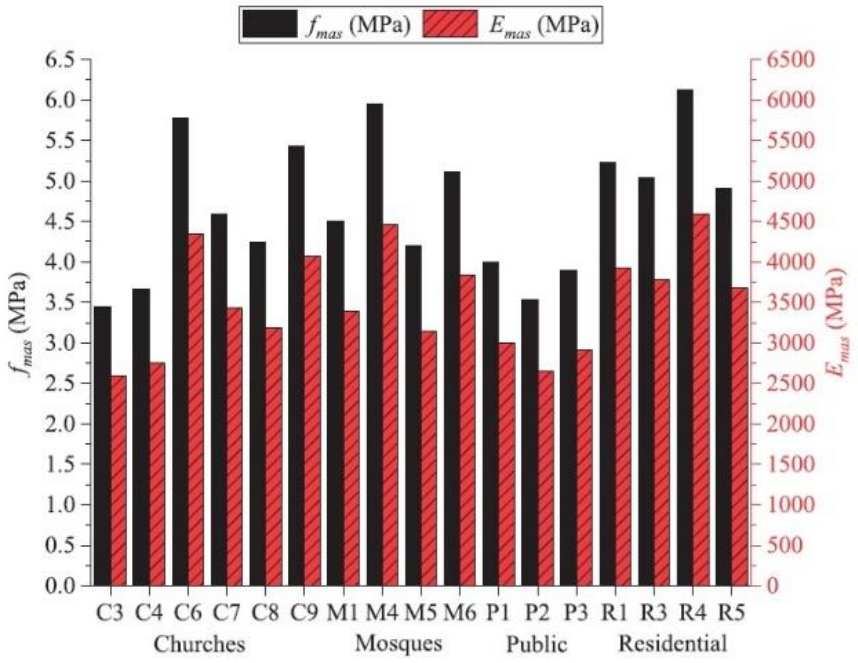

Figure 3.3 Compressive strength and elastic modulus values for masonry using the formulations in TBSC-2018 (Bozyigit *et* al. 2024).

3.3 Structural Analysis of the Beştek House

The Beştek House is analyzed by using the Response Spectrum Analysis (RSA). RSA is the multi-modal linear static analysis method that has commonly been used in seismic codes and standards as the main force-based seismic design and analysis tool.

The acceleration spectrum used in the calculation of the seismic force acting on the building is created by defining the building location by coordinates (Figure 3.4) and the soil class (Table 3.). This calculation can be achieved by accessing the Turkish Seismic Hazard Map web site (https://tdth.afad.gov.tr/) within the context of the current Turkish Building Seismic Code (TBSC 2018). Six soil classes have been defined in TBSC (2018). The average shear-wave velocity in the first 30 m depth

(V_s30) values at the stations close to Beştek House (Figure 2.9 and Figure 2.10) correspond to the ZC soil class as defined by the TBSC (2018). Therefore, the local soil class has been chosen as ZC. $R_a(T)$ is taken as 1.

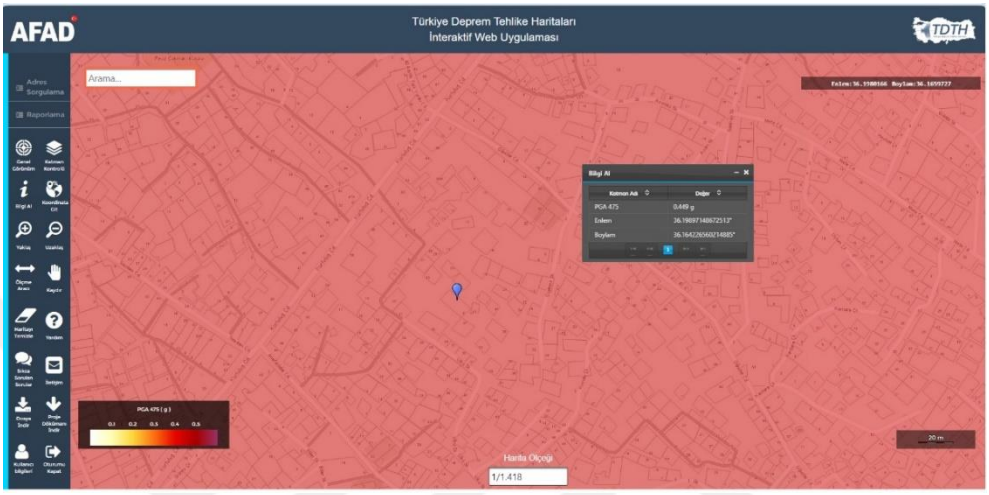

Figure 3.4 Location of the Beştek House by coordinate mapping

Table 3.4 Local soil classes in Turkish (TBSC, 2018)

Yerel Zemin Sınıfı	Zemin Cinsi	Üst 30 metrede ortalama		
		$(V_S)_{30}$ [m/s]	$(N_{60})_{30}$ [darbe /30 cm]	$(c_u)_{30}$ [kPa]
ZA	Sağlam, sert kayalar	> 1500	–	–
ZB	Az ayrışmış, orta sağlam kayalar	760 – 1500	–	–
ZC	Çok sıkı kum, çakıl ve sert kil tabakaları veya ayrışmış, çok çatlaklı zayıf kayalar	360 – 760	> 50	> 250
ZD	Orta sıkı – sıkı kum, çakıl veya çok katı kil tabakaları	180 – 360	15 – 50	70 – 250
ZE	Gevşek kum, çakıl veya yumuşak – katı kil tabakaları veya $PI > 20$ ve $w > \%\ 40$ koşullarını sağlayan toplamda 3 metreden daha kalın yumuşak kil tabakası $(c_u < 25\ \text{kPa})$ içeren profiller	< 180	< 15	< 70
ZF	Sahaya özel araştırma ve değerlendirme gerektiren zeminler: 1) Deprem etkisi altında çökme ve potansiyel göçme riskine sahip zeminler (sıvılaşabilir zeminler, yüksek derecede hassas killer, göçebilir zayıf çimentolu zeminler vb.), 2) Toplam kalınlığı 3 metreden fazla turba ve/veya organik içeriği yüksek killer, 3) Toplam kalınlığı 8 metreden fazla olan yüksek plastisiteli (PI >50) killer, 4) Çok kalın (> 35 m) yumuşak veya orta katı killer.			

Seismic Intensity Level according to the TBSC (2018) is chosen as DD2 (i.e. design-basis earthquake level). This intensity level has been taken by considering the earthquake records of two stations with IDs 3131 and 3132, which are approximately 1 km away from the case study building, as explained in Section 2 in detail. The acceleration spectrum developed at the location of the building, the selected soil class and the earthquake intensity level is shown in Figure 3.5.

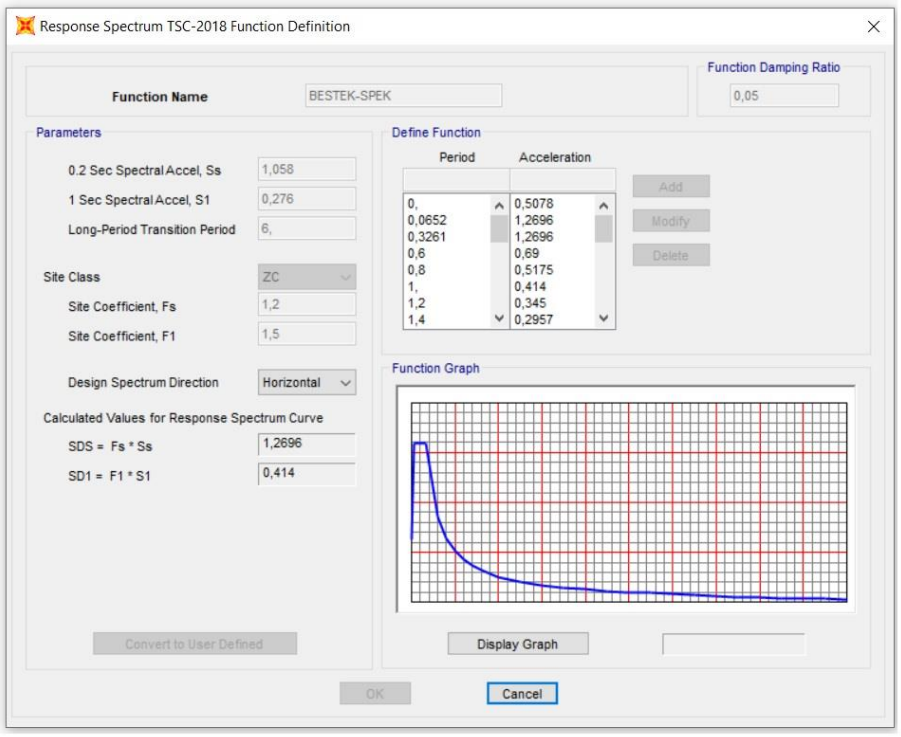

Figure 3.5 Acceleration spectrum developed for the Beştek House

In the first phase, the modal analysis of the developed structural model has been performed. Mass participation ratios, mode shapes and periods are examined. The total number of modes where the total mass participation values exceeded 90% in both directions is 150 (Table 3.5). The total mass participation is 2% in the last 50 modes. The contribution of too many modes to the total response is due to the inherent structural properties of the Beştek House, such as the load transfer between

members with different materials, irregularities in the load transfer paths and more importantly the absence of rigid floor diaphragm. Hence there exist many local modes in the structural model with small contributions to total response. That is why the calculations have been made according to the analysis results that takes 150 modes into account. The maximum values of mass participation in a single mode in either X or Y direction is around 30%. The vibration periods in the first two modes are observed to be 0.33 s (Y-direction) and 0.25 s (X-direction).

Table 3.5 Vibration periods and mass participation ratios of the structural model

Mod Number	**Period**	**MPR-X**	**MPR-Y**	**Sum_MPR-X**	**Sum_MPR-Y**
	s	**(%)**	**(%)**	**(%)**	**(%)**
1	0,335	0,00	29,93	0,00	29,93
2	0,250	23,22	0,00	23,22	29,93
3	0,167	0,00	0,61	23,22	30,55
4	0,160	5,57	0,15	28,79	30,69
5	0,131	0,74	0,09	29,54	30,78
6	0,119	0,02	21,71	29,56	52,49
7	0,108	0,04	9,06	29,60	61,55
8	0,102	2,68	0,00	32,28	61,55
9	0,080	32,14	0,02	64,42	61,57
10	0,076	0,36	0,84	64,78	62,41
11	0,073	0,04	0,00	64,82	62,41
12	0,070	0,18	0,06	65,00	62,47
13	0,055	0,02	1,01	65,01	63,48
14	0,053	0,01	10,58	65,02	74,06
15	0,052	0,26	0,78	65,28	74,84
50	0,026	0,37	0,18	78,73	83,18
100	0,017	0,09	0,08	87,97	87,53
150	0,012	0,01	0,48	90,04	90,13

The mode shapes of the 1st, 2nd and 9th modes of the structure are shown below in Figure 3.6. In the first mode, the buildings behavior is in the Y direction. In this mode, north wall of the first floor shows significant out of plane behavior. In the second mode, there is horizontal translation in the X direction, and in the 9th mode,

it is seen that torsional behavior is also effective in addition to translation in the X direction. In the 2nd and 9th modes, out-of-plane movement of the east and west walls of the first floor is observed.

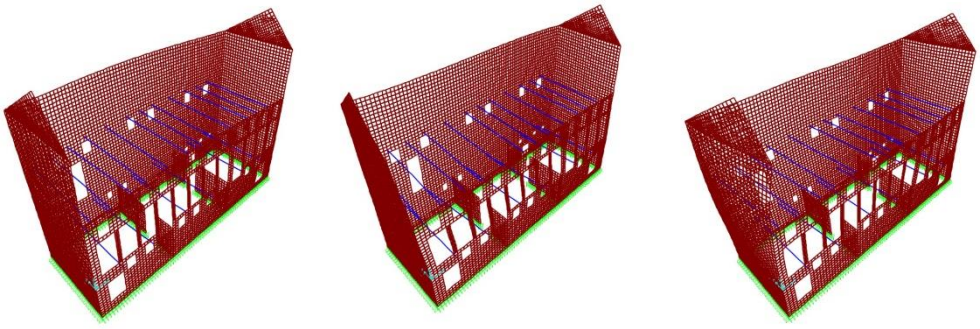

Figure 3.6 Mode shapes of the structural model (Mode 1 & Mode 2 & Mode 9)

The base shear forces occurring under earthquake loading in the X and Y directions are shown in Table 3. Accordingly, a horizontal earthquake force of approximately 55% of the building weight has been applied in both directions by using the derived acceleration spectrum

Table 3.6 Base shear forces under EQX and EQY loading

TABLE: Base Reactions

Loading code	Analysis Type	Value	kN	kN	kN
DEAD	LinStatic		3,8E-12	3,8E-11	3975.9
EQX	LinRespSpec	Max	2152.1	77.6	60.5
EQY	LinRespSpec	Max	77.5	2170.7	90.4

3.3.1 Drift Control for the Structural Model

Drift control has been performed by considering the locations of the walls on each floor that yields the maximum drift under the combined effect of vertical and

horizontal loads in its most critical direction. Table 3.3 presents performance levels and drift ratios for different analysis types in GERMHS (2017). Accordingly, the calculated deformation values and damage limit states corresponding to the three performance levels defined in the GERMHS are compared in Table 3.4 for each load-bearing masonry wall of the case study building. According to the color code, yellow, orange and red colors stand for the exceedance of drift ratio for Limited Damage, Controlled Damage and Collapse Prevention performance states, respectively. Hence, the drift checks reveal that the north wall in the first storey exceeds the collapse drift limit whereas exceed the limited damage state. On the ground floor, north and south walls exceed the controlled damage, and they seem to be the critical walls under seismic action. All the walls in the basement floor satisfy the drift criterion and they seem to be safe.

Table 3.3 Calculation methods regarding performance levels and drift ratios (GERMHS, 2017)

Performance Level	**Calculation Methods and Limitations**
Limitad Damage	Drift Ratio is not exceeding %0,3 under unreduced seismic effect
Controlled Damage	Drift Ratio is not exceeding %0,7 under unreduced seismic effect
Collapse Prevention	Drift Ratio is not exceeding %1 under unreduced seismic effect

Figure 3.7-Figure 3.9 demonstrate the performance state of the walls at each floor in plan view. In addition to previous colors used for the exceedance of specified limit states, green color stands for the safe walls which satisfy all drift limit. It should be noted that for both ground and first floor, walls in the long direction are critical for drift. The inferior performance of the north wall in the first storey is not an

unexpected outcome. Since the front facade of the first floor is incomplete and there is no floor diaphragm, the north wall acts like a long cantilever wall detached from the rest of the structure as the only contributor to the lateral stiffness in the east-west direction, which makes it very vulnerable for horizontal seismic actions.

Table 3.4 Drift control for the load-bearing walls

Wall	Height of the Wall (m)	Displacement (m)	Displacement Ratio (%)	Check (Before Collapse) (%1)	Check (Controlled Damage) (%0,7)	Check (Limited Damage) (%0,3)
Basement North	2,40	0,0051	0,21%	✓	✓	✓
Basement West	2,40	0,001	0,04%	✓	✓	✓
Basement South	2,40	0,005	0,21%	✓	✓	✓
Basement East	2,40	0,0009	0,04%	✓	✓	✓
Basement Partition West	2,40	0,002	0,08%	✓	✓	✓
Basement Partition East	2,40	0,0035	0,15%	✓	✓	✓
Ground North	6,60	0,0448	0,95%	✓	X	X
Ground West	6,60	0,0208	0,47%	✓	✓	X
Ground South	6,60	0,0447	0,95%	✓	X	X
Ground East	6,60	0,0211	0,48%	✓	✓	X
First North	9,80	0,0787	1,06%	X	X	X
First West (with Gable)	11,80	0,0407	0,38%	✓	✓	X
First East(with Gable)	11,80	0,0365	0,30%	✓	✓	X

Limited Damage
Controlled Damage
Collapse Prevention

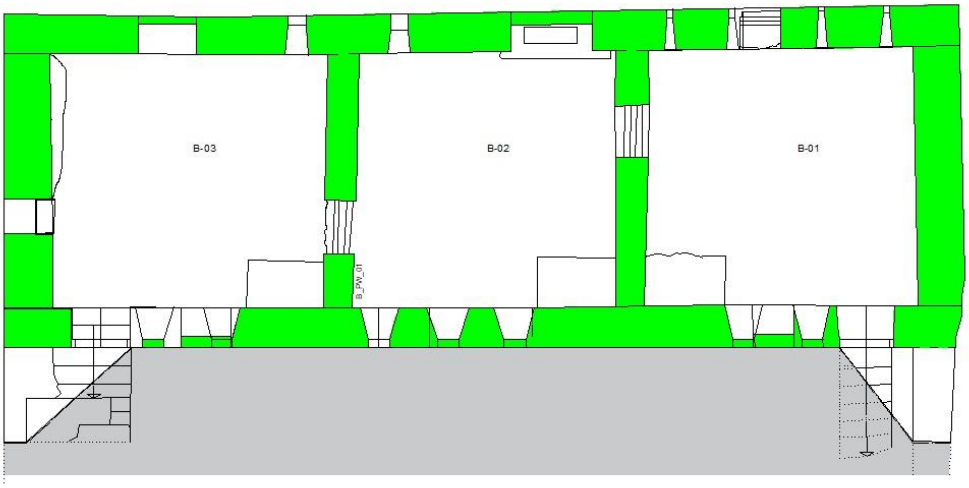

Figure 3.7 Drift control for basement walls

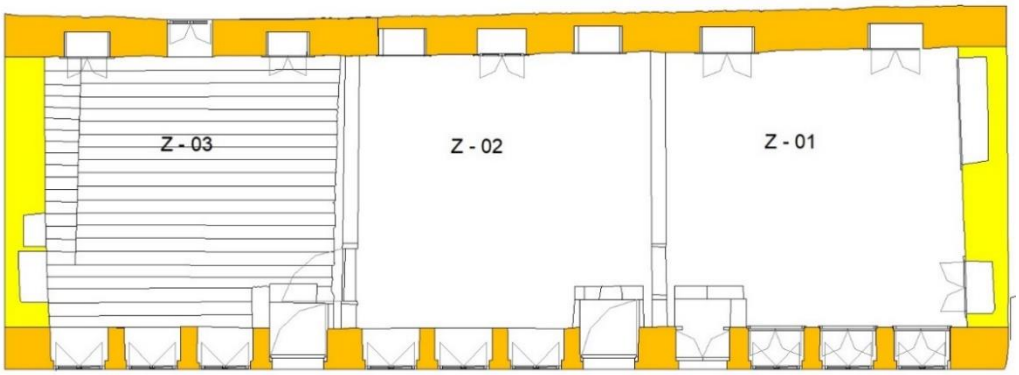

Figure 3.8 Drift control for ground floor walls

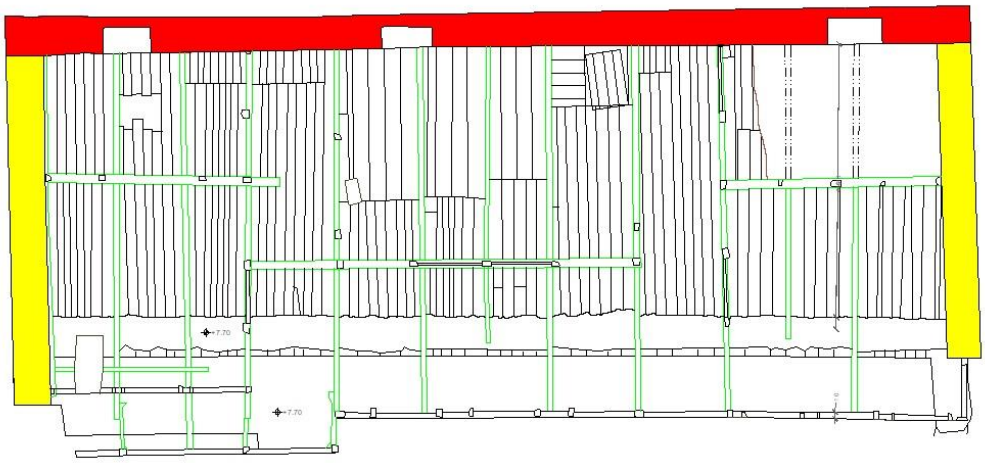

Figure 3.9 Drift control for first floor walls

3.3.2 Strength Control for the Structural Model

The seismic force demands acting on each load-bearing wall piece should be compared with the strength of each wall component. Vertical compressive and horizontal shear strength checks are carried out under the loading combination that causes the maximum forces on that wall section. These combinations are given in Table 3.

Table 3.9 Critical force combinations acting on the structural model

Critical Force Combinations				
	Floor	**Elevation**	**Failure Mode**	**Combination**
1	**Basement**	North Wall	Compression	G+Q+0,3EX+EY
			Shear	G+Q+EX+0,3EY
2		West Wall	Compression	G+Q+0,3EX+EY
			Shear	G+Q+0,3EX+EY
3		South Wall	Compression	G+Q+EX+0,3EY
			Shear	G+Q+EX+0,3EY
4		East Wall	Compression	G+Q+0,3EX+EY
			Shear	G+Q+0,3EX+EY
5		Partition West	Compression	G+Q+0,3EX+EY
			Shear	G+Q+0,3EX+EY
6		Partition East	Compression	G+Q+0,3EX+EY
			Shear	G+Q+0,3EX+EY
7	**Ground**	North Wall	Compression	G+Q+EX+0,3EY
			Shear	G+Q+EX+0,3EY
8		West Wall	Compression	G+Q+EX+0,3EY
			Shear	G+Q+EX+0,3EY
9		South Wall	Compression	0,9G+EX+0,3EY
			Shear	G+Q+EX+0,3EY
10		East Wall	Compression	G+Q+EX+0,3EY
			Shear	0,9G+EX+0,3EY
11	**First**	North Wall	Compression	G+Q+0,3EX+EY
			Shear	0,9G+0,3EX+EY
12		West Wall	Compression	G+Q+0,3EX+EY
			Shear	G+Q+0,3EX+EY
13		-		
14		East Wall	Compression	G+Q+0,3EX+EY
			Shear	G+Q+0,3EX+EY
15		Gable West	Compression	G+Q+EX+0,3EY
			Shear	G+Q+0,3EX+EY
16		Gable East	Compression	0,9G+EX+0,3EY
			Shear	G+Q+0,3EX+EY

3.3.2.1 Vertical Compressive Strength Control

TBSC (2018) provides the following equations for vertical design load of the wall (N_{Rd}).

$$N_{Rd} = \lambda \, A \, f_d \tag{3.1}$$

$$f_d = f_k / \gamma_m \tag{3.2}$$

where λ is the strength reduction factor due to slenderness, A is the horizontal cross-sectional area of the wall, f_d is the design compressive strength of the masonry wall, f_k is the characteristic compressive strength of the masonry wall and γ_m strength reduction factor for masonry material. Strength reduction factor λ is assumed as 0.51, the minimum value in the TSC (2007), for slenderness ratio values greater than 15. The parameter f_k has been taken as the minimum value in the study by Bozyigit *et* al. (2024), which is 3.4 MPa. The parameter f_d is calculated as 1.7 MPa by considering γ_m=2. The comparison of the vertical design loads with the vertical load demands acting on the walls is presented in Table 3.5. The same information is visualized in Figures 3.10-3.12 in colored format on the floor plans. The green and red colors stand for the safe and unsafe walls under vertical loads, respectively according to the vertical load check by the TBSC (2018). The critical walls under vertical load analysis are observed to be the ones with reduced thickness due to the placement of niches and also the column-like masonry walls between openings of the south facade in the ground floor of the building.

Table 3.5 Vertical force control for the walls under critical loading condition

Compression Check						
No	**Floor**	**Elevation**	**Wall No**	**NRd**	**Ned**	**|Ned| < Nrd**
				kN	**kN**	
1	**Basement**	**North Wall**	B_N_01	1877	-356	CHECK
2			B_N_02	124	-106	CHECK
3			B_N_03	1510	-262	CHECK
4			B_N_04	1397	-264	CHECK
5			B_N_05	1734	-204	CHECK
6			B_N_06	231	-40	CHECK
7			B_N_07	1224	-92	CHECK
8			B_N_08	898	-48	CHECK
9			B_N_09	612	-86	CHECK
10			B_N_10	938	-124	CHECK
11			B_N_11	765	-260	CHECK
12		**West Wall**	B_W_01	1768	-600	CHECK
13			B_W_02	510	-270	CHECK
14			B_W_03	2652	-428	CHECK
15		**South Wall**	B_S_01	673	-430	CHECK
16			B_S_02	867	-474	CHECK
17			B_S_03	95	-172	FAIL
18			B_S_04	2162	-206	CHECK
19			B_S_05	138	-82	CHECK
20			B_S_06	612	-31	CHECK
21			B_S_07	3325	-360	CHECK
22			B_S_08	104	-110	FAIL
23			B_S_09	694	-372	CHECK
24			B_S_10	816	-380	CHECK
25		**East Wall**	B_E_01	7115	-610	CHECK
26		**Partiton West**	B_PW_01	908	-254	CHECK
27			B_PW_02	2458	-214	CHECK
28		**Partiton East**	B_PE_01	2519	-146	CHECK
29			B_PE_02	918	-440	CHECK

Table 3.5 (cont'd) Vertical force control for the walls under critical loading condition

Compression Check						
No	**Floor**	**Elevation**	**Wall No**	**NRd**	**Ned**	**|Ned | < Nrd**
				kN	**kN**	
30			G-N-01	506	-218	CHECK
31			G-N-02	121	-138	FAIL
32			G-N-03	726	-312	CHECK
33			G-N-04	685	-254	CHECK
34			G-N-05	114	-112	CHECK
35			G-N-06	873	-170	CHECK
36			G-N-07	128	-96	CHECK
37		**North Wall**	G-N-08	636	-166	CHECK
38			G-N-09	129	-112	CHECK
39			G-N-10	604	-166	CHECK
40			G-N-11	128	-100	CHECK
41			G-N-12	987	-134	CHECK
42			G-N-13	145	-92	CHECK
43			G-N-14	1444	-168	CHECK
44			G-N-15	145	-144	CHECK
45			G-N-16	832	-240	CHECK
46			G_W_01	608	-394	CHECK
47		**West Wall**	G_W_02	136	-130	CHECK
48			G_W_03	179	-230	FAIL
49	**Ground Floor**		G_W_04	2493	-188	CHECK
50			G_S_01	305	-960	FAIL
51			G_S_02	218	-1120	FAIL
52			G_S_03	218	-1220	FAIL
53			G_S_04	218	-1130	FAIL
54			G_S_05	261	-1150	FAIL
55			G_S_06	218	-1170	FAIL
56		**South Wall**	G_S_07	218	-1150	FAIL
57			G_S_08	218	-1180	FAIL
58			G_S_09	505	-1980	FAIL
59			G_S_10	218	-1160	FAIL
60			G_S_11	218	-1180	FAIL
61			G_S_12	218	-1170	FAIL
62			G_S_13	418	-1210	FAIL
63			G_E_01	477	-416	CHECK
64			G_E_02	138	-208	FAIL
65		**East Wall**	G_E_03	1353	-228	CHECK
66			G_E_04	563	-176	CHECK
67			G_E_05	424	-240	CHECK

Table 3.5 (cont'd) Vertical force control for the walls under critical loading condition

Compression Check						
No	**Floor**	**Elevation**	**Wall No**	**NRd**	**Ned**	**|Ned |< Nrd**
				kN	**kN**	
68			F_N_01	1233	-66	CHECK
69			F_N_02	111	-28	CHECK
70			F_N_03	3658	-38	CHECK
71		**North Wall**	F_N_04	108	-28	CHECK
72			F_N_05	6271	-38	CHECK
73			F_N_06	126	-32	CHECK
74			F_N_07	1134	-70	CHECK
	First Floor					
75		**West Wall**	F_W_01	5536	-4	CHECK
76		**East Wall**	F_E_01	5517	-92	CHECK
77		**Gable West**	F_G_W_01	4590	-2	CHECK
78		**Gable East**	F_G_E_01	5185	-16	CHECK

Figure 3.10 Vertical strength control shown in the basement floor

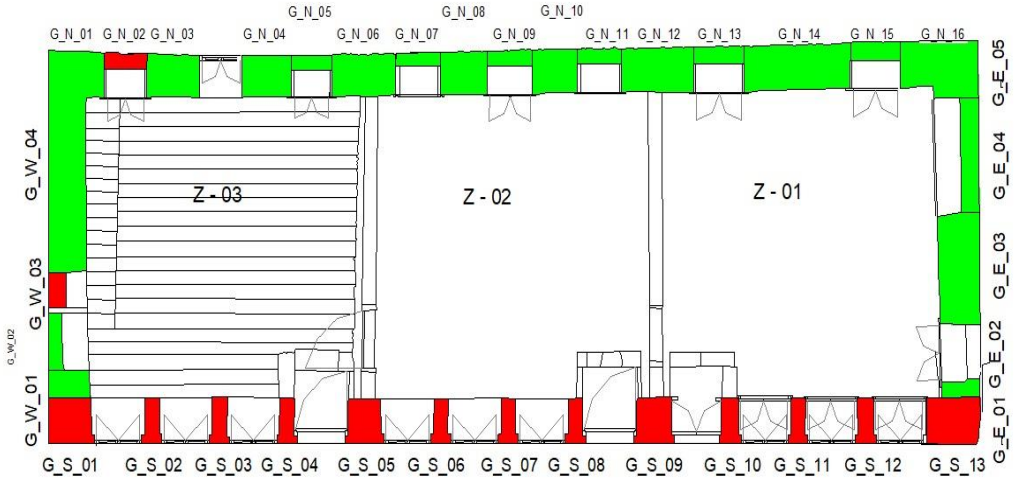

Figure 3.11 Vertical strength control shown in the ground floor

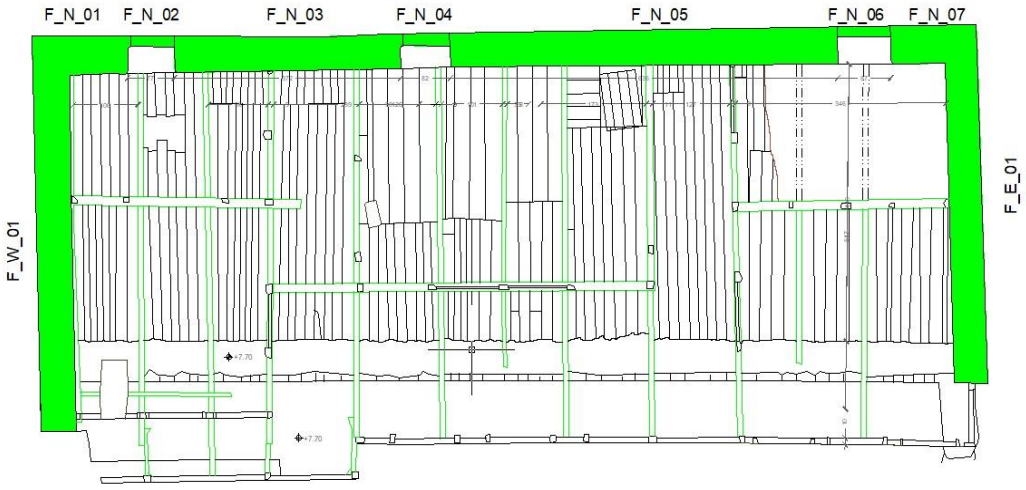

Figure 3.12 Vertical strength control shown in the first floor

In addition, the spatial distribution of vertical (compressive) stress contours within the mesh of the building under critical loading conditions is shown in Figure 3.13. The distribution of the compressive stresses within the building mesh seems to be in accordance with the vertical force check results.

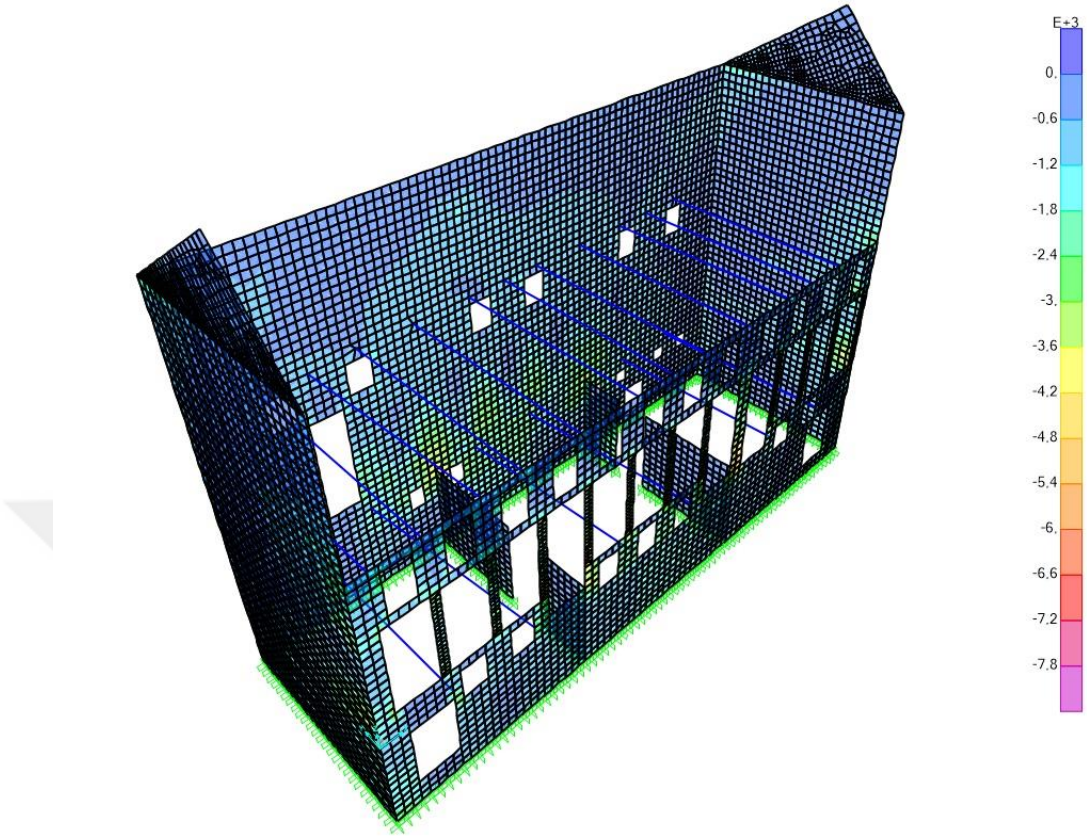

Figure 3.13 Maximum compression stress distribution within the building model under critical loading condition

3.3.2.2 Shear Force Control for the Structural Model

According to TBSC (2018), design shear force strength in load-bearing masonry walls (V_{Rd}), should be greater than the design shear force acting on the wall (V_{Ed}). The wall shear force resistance can be taken as the smaller of the values calculated with Equations 3.3 and 3.4.

$$V_{Rd} = f_{vd}\, t\, \ell_c \tag{3.3}$$

$$V_{Rd} = \ell t\, \frac{1.5 f_{vdo}}{b} \sqrt{1 + \frac{N_{Ed}}{1.5 \ell t f_{vdo}}} \tag{3.4}$$

where f_{vd} is the wall design shear strength, f_{vdo} is the design shear strength at zero vertical stress, ℓ is the wall length, ℓ_c is the wall length under compression, t is the wall thickness and b is the stress distribution shape coefficient. Accordingly, the shear force checks for all the walls under design-basis (DD2) earthquake spectrum are presented in Table 3.6. The spatial distribution of wall shear stresses in plan for all the floors are provided in Figures Figure 3.14-Figure 3.16. Again, the green and red colors stand for the approval and failure of the shear force check for the walls, respectively. The results reveal that most of the walls in basement floor and all the walls in ground floor do not qualify the shear stress check dictated by the equations in TBSC (2018). On the first floor, the walls with reduced thickness seem to be critical.

Table 3.6 Shear force control for the walls under critical loading condition

SHEAR CHECK									
No	Floor	Elevation	Wall No	VRd (1)	VRd (2)	VRd	VEd	SHEAR CHECK (VEd < VRd)	FAIL PATTERN
				kN	kN	kN	kN		
1	Basement	North Wall	B_N_01	175	100	100	110	FAIL	Diagonal Tension
2			B_N_02	24	14	14	99	FAIL	Diagonal Tension
3			B_N_03	194	60	60	124	FAIL	Diagonal Tension
4			B_N_04	192	55	55	128	FAIL	Diagonal Tension
5			B_N_05	204	54	54	136	FAIL	Diagonal Tension
6			B_N_06	51	13	13	104	FAIL	Diagonal Tension
7			B_N_07	150	41	41	122	FAIL	Diagonal Tension
8			B_N_08	105	30	30	123	FAIL	Diagonal Tension
9			B_N_09	63	28	28	110	FAIL	Diagonal Tension
10			B_N_10	83	47	47	118	FAIL	Diagonal Tension
11			B_N_11	68	57	57	112	FAIL	Diagonal Tension
12		West Wall	B_W_01	229	153	153	158	FAIL	Diagonal Tension
13			B_W_02	66	54	54	206	FAIL	Diagonal Tension
14			B_W_03	225	253	225	162	CHECK	-
15		South Wall	B_S_01	99	81	81	72	CHECK	-
16			B_S_02	121	93	93	227	FAIL	Diagonal Tension
17			B_S_03	14	22	14	94	FAIL	Sliding Shear
18			B_S_04	293	150	150	104	CHECK	-
19			B_S_05	16	19	16	40	FAIL	Sliding Shear
20			B_S_06	61	41	41	56	FAIL	Diagonal Tension
21			B_S_07	532	259	259	134	CHECK	-
22			B_S_08	16	22	16	82	FAIL	Sliding Shear
23			B_S_09	76	74	74	130	FAIL	Diagonal Tension
24			B_S_10	115	82	82	84	FAIL	Diagonal Tension
25		East Wall	B_E_01	996	541	541	140	CHECK	-
26		Partition Wes	B_PW_01	76	75	75	136	FAIL	Diagonal Tension
27			B_PW_02	219	196	196	196	FAIL	Diagonal Tension
28		Partition East	B_PE_01	203	182	182	136	CHECK	-
29			B_PE_02	122	89	89	218	FAIL	Diagonal Tension

Table 3.6 (cont'd) Shear force control for the walls under critical loading condition

SHEAR CHECK									
No	**Floor**	**Elevation**	**Wall No**	**VRd (1)**	**VRd (2)**	**VRd**	**VEd**	**SHEAR CHECK (VEd < VRd)**	**FAIL PATTERN**
				kN	**kN**	**kN**	**kN**		
30	**Ground Floor**	**North Wall**	G-N-01	29	36	29	106	FAIL	Sliding Shear
31			G-N-02	13	17	13	100	FAIL	Sliding Shear
32			G-N-03	71	59	59	80	FAIL	Diagonal Tension
33			G-N-04	75	45	45	76	FAIL	Diagonal Tension
34			G-N-05	16	9	9	94	FAIL	Diagonal Tension
35			G-N-06	116	32	32	110	FAIL	Diagonal Tension
36			G-N-07	17	8	8	114	FAIL	Diagonal Tension
37			G-N-08	70	23	23	110	FAIL	Diagonal Tension
38			G-N-09	16	8	8	96	FAIL	Diagonal Tension
39			G-N-10	59	22	22	118	FAIL	Diagonal Tension
40			G-N-11	16	8	8	108	FAIL	Diagonal Tension
41			G-N-12	105	36	36	116	FAIL	Diagonal Tension
42			G-N-13	20	18	18	114	FAIL	Diagonal Tension
43			G-N-14	121	69	69	120	FAIL	Diagonal Tension
44			G-N-15	18	20	18	114	FAIL	Sliding Shear
45			G-N-16	54	52	52	116	FAIL	Diagonal Tension
46		**West Wall**	G_W_01	130	66	66	94	FAIL	Diagonal Tension
47			G_W_02	21	19	19	77	FAIL	Diagonal Tension
48			G_W_03	17	22	17	116	FAIL	Sliding Shear
49			G_W_04	242	110	110	118	FAIL	Diagonal Tension
50		**South Wall**	G_S_01	63	58	58	268	FAIL	Diagonal Tension
51			G_S_02	51	71	51	176	FAIL	Sliding Shear
52			G_S_03	51	71	51	204	FAIL	Sliding Shear
53			G_S_04	51	71	51	204	FAIL	Sliding Shear
54			G_S_05	93	78	78	204	FAIL	Diagonal Tension
55			G_S_06	77	71	71	204	FAIL	Diagonal Tension
56			G_S_07	78	71	71	204	FAIL	Diagonal Tension
57			G_S_08	78	74	74	232	FAIL	Diagonal Tension
58			G_S_09	219	133	133	178	FAIL	Diagonal Tension
59			G_S_10	59	69	59	166	FAIL	Sliding Shear
60			G_S_11	59	69	59	166	FAIL	Sliding Shear
61			G_S_12	59	69	59	166	FAIL	Sliding Shear
62			G_S_13	112	101	101	334	FAIL	Diagonal Tension
63		**East Wall**	G_E_01	179	69	69	122	FAIL	Diagonal Tension
64			G_E_02	55	32	32	96	FAIL	Diagonal Tension
65			G_E_03	225	99	99	120	FAIL	Diagonal Tension
66			G_E_04	84	55	55	132	FAIL	Diagonal Tension
67			G_E_05	44	53	44	110	FAIL	Sliding Shear

Table 3.6 (cont'd) Shear force control for the walls under critical loading condition

SHEAR CHECK									
No	**Floor**	**Elevation**	**Wall No**	**VRd (1)**	**VRd (2)**	**VRd**	**VEd**	**SHEAR CHECK (VEd < VRd)**	**FAIL PATTERN**
				kN	**kN**	**kN**	**kN**		
68			F_N_01	101	57	57	78	FAIL	Diagonal Tension
69			F_N_02	22	13	13	66	FAIL	Diagonal Tension
70			F_N_03	313	179	179	28	CHECK	-
71		**North Wall**	F_N_04	31	10	10	12	FAIL	Diagonal Tension
72			F_N_05	531	295	295	32	CHECK	-
73			F_N_06	29	15	15	64	FAIL	Diagonal Tension
74			F_N_07	88	53	53	88	FAIL	Diagonal Tension
	First Floor								
75		**West Wall**	F_W_01	619	287	287	90	CHECK	-
76		**East Wall**	F_E_01	162	248	162	88	CHECK	-
77		**Gable West**	F_G_W_01	135	204	135	14	CHECK	-
78		**Gable East**	F_G_E_01	153	236	153	16	CHECK	-

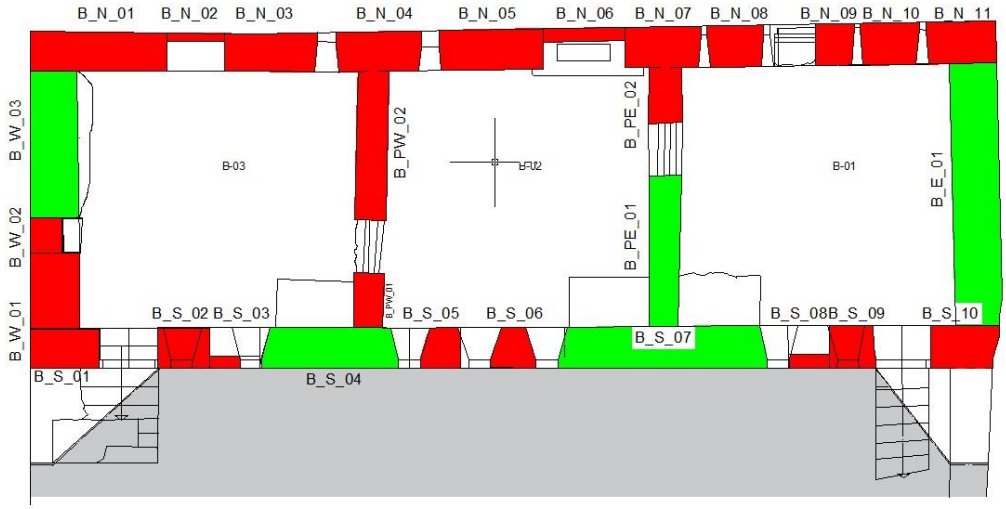

Figure 3.14 Shear force control shown in the basement floor

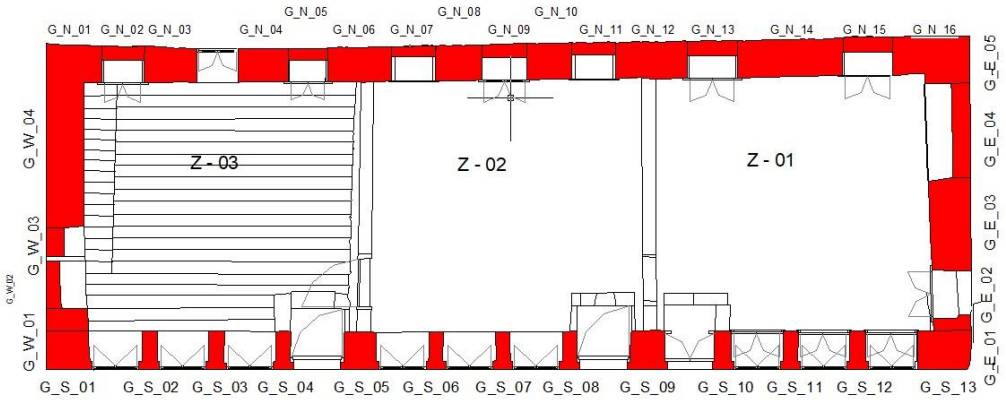

Figure 3.15 Shear force control shown in the ground floor

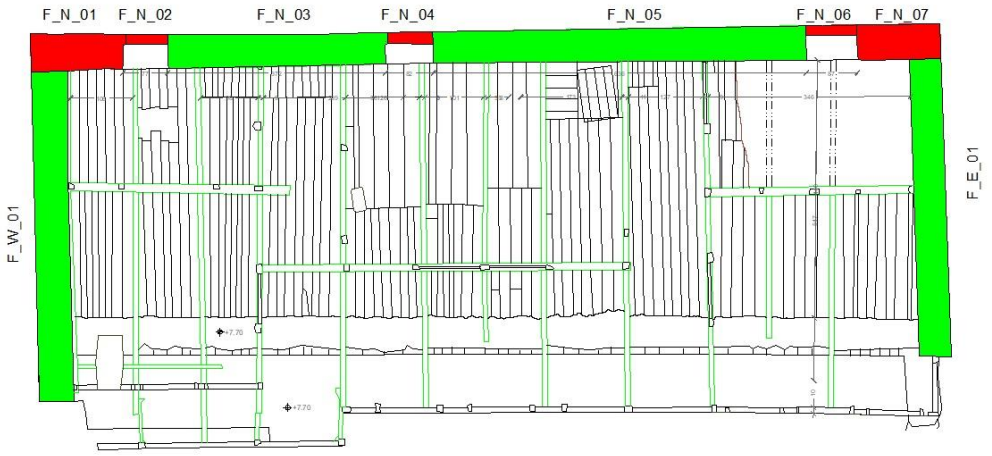

Figure 3.16 Shear force control shown in the first floor

In addition, the spatial distribution of shear stress contours within the mesh of the building under critical loading conditions is shown in Figure 3.17.

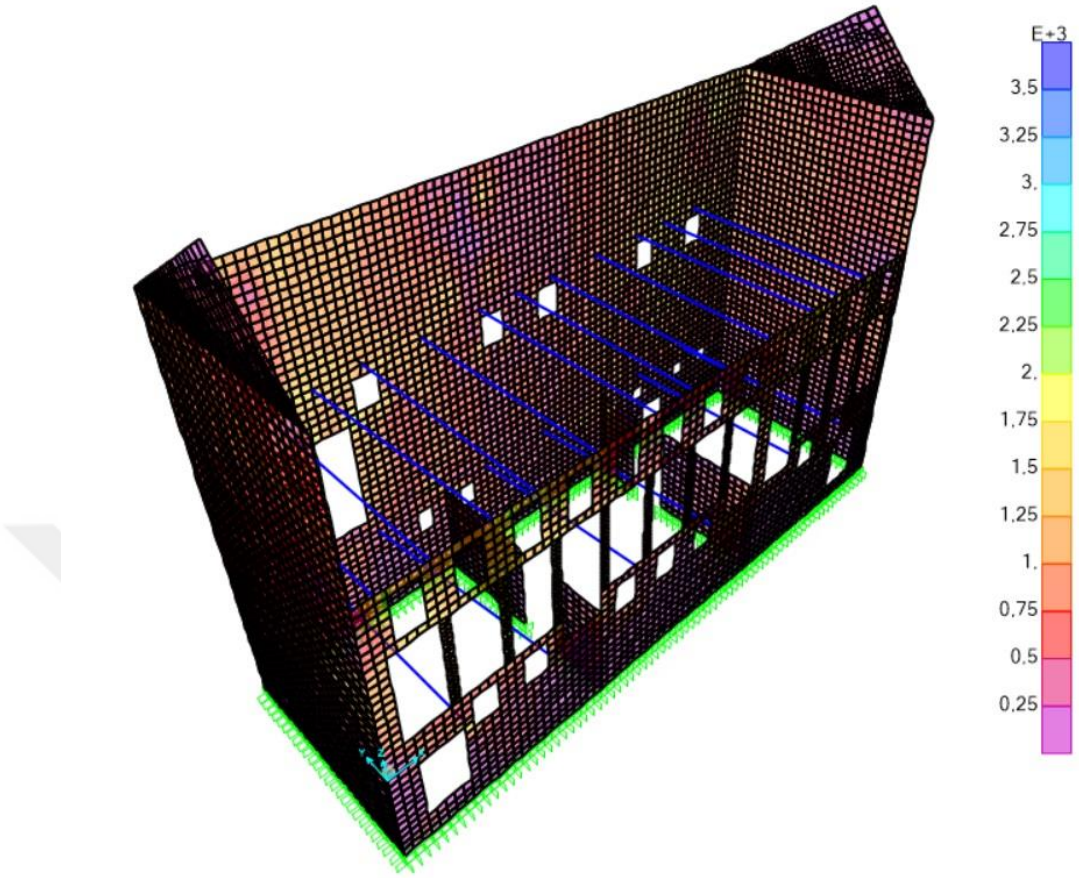

Figure 3.17 Maximum shear stress distribution within the building model under critical loading condition

3.3.3 Mechanism Based Control of the Structural Model

An alternative method for checking the out-of-plane rigid body motion of masonry walls is the mechanism-based calculation method. Out-of-plane failure of a wall can occur in many different ways as shown in Figure 3.18 (D'Ayala, 2003) and Figure 3.19 (GERMHS, 2017). Mechanism analysis defined in GERMHS, 2017 is performed for the north wall of the first floor, which has been observed as critical during the structural analysis and actually collapsed in the 2023 earthquake sequence. This analysis is performed for two possible overturning mechanisms. The

first one is the overturning action from the foundation level, and the second one is the overturning action from first floor slab level.

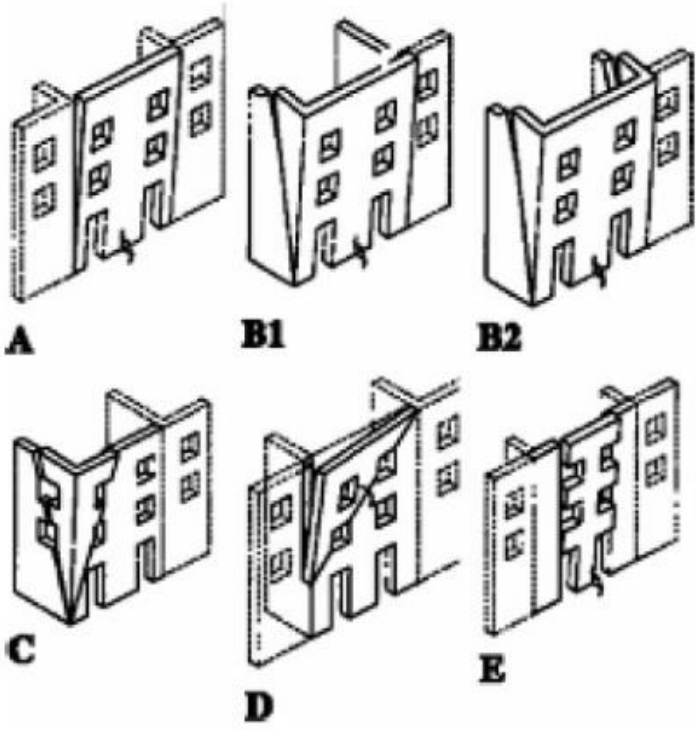

Figure 3.18 Mechanisms for overturning failures (D'Ayala, 2003)

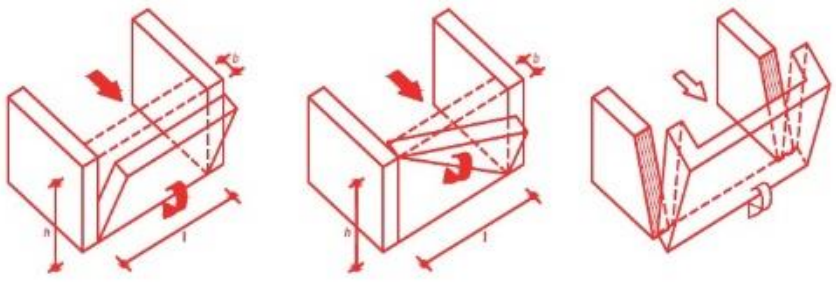

Figure 3.19 Failure mechansims of the facade walls (GERMHS, 2017)

Two mechanism states calculated below according to the GERMHS (2017) Section 6.5.5. where t is the thickness of the wall, α_0 is the load factor, M^* is the effective modal mass, e^* is the mass participation ratio and a^* is the spectral acceleration.

Mechanism State:1

Basement floor wall weight (W_b) : 351 kN

Load from the basement floor slab (P_b): 200 kN

Ground floor wall weight (W_g): 552 kN

Load from the ground floor slab (P_g): 150 kN

First floor wall weight (W_1): 487 kN

Load from the first floor slab (P_1): 0

Moment created by the forces keeping the wall in balance:

$(P_1+W_1+P_z+W_z+P_b+W_b)$ t/2: 522 kNm

Moment for overturning the wall:

$\alpha_0 \times W_b \times h_b / 2 + \alpha_0 \times P_b \times h_b + \alpha_0 \times W_z \times (h_b + h_z / 2) + \alpha_0 \times P_z \times (h_b + h_z) + \alpha_0 \times W_1 \times (h_b + h_z + h_1 / 2) + P_1 \times (h_b + h_z + h_1) = 522$ kNm

α_0 : 0.062

Storey displacements: δ_{wb}: 1.00, δ_{pb}: 0.84, δ_{wz}: 0.67, δ_{pz}: 0.46, δ_{w1}: 0.24, δ_{p1}: 0.12,

$M^* = [(W_b \times \delta_{wb} + W_z \times \delta_{wz} + W_1 \times \delta_{w1}) + (P_b \times \delta_{pb} + P_z \times \delta_{pz} + P_1 \times \delta_{p1})]^2$

M^* = 336 kNs2/m

e^*= 0.19

Spectral acceleration that causes the collapse mechanism:

$a^*_{capacity} = \alpha_0 \, g / e^* = 0.32 \, g$

$a^*_{demand} = 0{,}4 \times g \times S_{DS} = 0.51 \, g$

$$\frac{a * demand}{a * capacity} = 1.59 > 1$$

Then, the north wall of the first floor fails to satisfy the mechanism state one which is overturning from the foundation level.

Mechanism State 2:

Moment created by the forces keeping the wall in balance:

$(P_1+W_1)\ t / 2 = 146$ kNm

Moment for overturning the wall:

$\alpha_0 \times P_1 \times h_1 + \alpha_0 \times W_1 \times h_1 / 2 = 146$ kNm

$\alpha_0 = 0.19$

δ_{w1}: 0.50 δ_{p1}: 1.00

$M^* = [(W_b \times \delta_{wb} + W_z \times \delta_{wz} + W_1 \times \delta_{w1}) + (P_b \times \delta_{pb} + P_z \times \delta_{pz} + P_1 \times \delta_{p1})]^2$

$e^* = gM^* / (W_1 + P_1) = 0.25$

Spectral acceleration that causes the collapse mechanism:

$a^*_{capacity} = \alpha_0\ g / e^* = 0.75\ g$

$a^*_{demand} = Sae(T1)\Phi(z / H)\ \Gamma = 1.10g$

$$\frac{a * demand}{a * capacity} = 1.47 > 1$$

Then, the north wall of the first floor fails to satisfy the overturning from the level of first floor slab.

3.3.4 Evaluation of Analysis Results

After performing response spectrum analysis under design basis earthquake (10% probability of exceedance in 50 years or 475 years return period), the analysis results have been evaluated in terms of drift ratio, vertical and horizontal strength and kinematic rigid body mechanism of the walls (i.e. out-of-plane behavior). Performance assessments of the case study building for drift and kinematic mechanism are carried out according to the GERMHS (2017) whereas safety checks for vertical and horizontal strength capacities are done according to the criteria in the TBSC (2018).

Although linear elastic analysis approach is considered in this study, some of the major structural deficiencies of the case study building has been addressed by the analysis results. For instance, the absence of rigid floor diaphragm within the building causes some of the walls to experience critical in-plane deformation, especially the long north on the first floor. This is the only wall that resists the in-plane horizontal forces on the first floor since the wall in the south facade is absent. However, it should be mentioned that the structural model of the building is assumed to be detached and standing-alone. In reality, the case study building is constrained from the east and west facades by adjacent structures, so it is not possible for the real building to exhibit similar lateral drift ratios to the ones that have been obtained during the analysis.

Assessment of structural performance due to vertical and horizontal forces reveal that the reduced wall sections due to niches cause weak zones within the structure in terms of both compressive and shear force capacities. In addition, the south facade in the ground floor is another weak zone with many openings and small sections of slender masonry walls in between, like masonry columns. Hence the wall cross sections are not adequate to carry either vertical nor horizontal forces. Furthermore, the analysis results illustrate that the corners of the north wall in the first floor seem to be critical in terms of shear strength. This may be due to the irregular distribution

of masonry walls on the first floor, causing localized stress concentrations and also due to the adjacent position of the niches and the walls with reduced thickness.

Mechanism control described in the GERMHS, 2017 was done for the north wall of the first floor. Two mechanism state are checked. One, overturning from the level of foundation, the other is the overturning from the level of floor. In both, overturning of the north wall is shown.

CHAPTER 4

EVALUATION

Beştek House, a traditional house built with unreinforced masonry (URM) technique in the historical city center of Antakya, is modeled with macro modelling technique. It is analyzed by using Response Spectrum Analysis method using SAP2000 software using finite element method. Analysis results were interpreted with the conditions of Turkish Building Seismic Code (2018) and Guideline for Earthquake Risk Management of Historical Structures (GERMHS, 2017). Analysis results are compared with the observed damage in the building after 2023 Türkiye Earthquake Sequence.

4.1 Comparison of Analysis Results with Observed Damage in the Beştek House after the 2023 Türkiye Earthquake Sequence

The observed damage state of the Beştek House after the earthquake sequence has been explained in Section 2.4. In this section, the analysis results are compared with the observed damage of the building reported after the earthquake sequence. Eventually, there are cases where the numerical results and the observed damage overlap and differ from each other. These cases are discussed in detail in the following paragraphs.

Before making the comparison, it is important to remember the assumptions and limitations considered during the modelling and analysis stages of the case study building. First, the building is actually adjacent to other structures on the east and the west facades. While it is adjacent to a building with similar mass properties to the west, the building to the east is both smaller and has a smaller surface area in touch. The adjacent structures have not been modelled in this study. The building has been assumed as a stand-alone structure and all the results have been obtained

accordingly. Second, the Beştek House has a partial basement. Since the required information to model this basement part is not sufficient, the analytical model has been developed without the partial basement. Third, since rigid diaphragm action of the floors is missing, some simplifications have been used in order to realize the connection between some elements, especially between the steel beams and masonry walls. These simplified connections may simulate the actual load transfer, and in turn the internal forces of the members to some limited extent when compared with the actual behavior. Fourth, macro modelling approach has been considered for the walls by the use of shell element in the form of homogenized masonry walls.

Contrary to micro-modelling approach, the considered simplified approach does not enable the simulation of different masonry layers like crushed stone or rubble stone together with the characteristics of mortar in between the units. However, in order to use the micro modelling approach, all material parameters related to masonry units, mortar and the interface in between should be determined by using extensive experimental research, which is absent in the case of Beştek House. It is also a fact that workmanship quality cannot be incorporated into the material model although it might affect the behavior of masonry walls due to lack of information and the limitations of the idealized model used in this study. Therefore, the simplified macro model has been employed in structural modelling by accepting the loss of accuracy involved in the seismic evaluation of masonry walls.

For the last but not the least, linear elastic approach has been employed to analyze the building model. This choice brings the advantage of carrying out simple, practical and straight-forward analysis tools that are also commonly used in the seismic design of building structures. On the other hand, the linear elastic approach does not reflect the inelastic behavior, or in other words damage in the members. In addition, linear elastic method always yields more conservative results than the nonlinear methods due to its simplicity and approximate nature. Hence, it may not be possible to capture the actual damage mechanism of the structure, especially the local failures.

Keeping these assumptions and simplifications in mind, it can be stated that the wall collapse observed in the first floor of the building (Figure 4.1) is consistent with the analysis results. The drift ratio of the north wall of the first floor is calculated beyond the limits given in the GERMHS (2017). More importantly, this wall seems to be critical in the out-of-plane direction as shown in the mechanism calculation explained in Section 3.3.3. The east and west walls of the first floor that collapsed with the earthquake are in a limited damage state according to the drift analysis results. The difference real and simulated behavior of the east and west walls may be due to the fact that in actual case the building cannot move is the east-west direction due to adjacent structures whereas the numerical model simulates a stand-alone dynamic behavior. This may cause a significant difference in the in-plane behavior of the east and west perimeter walls, which are constrained in their out-of-plane direction but free to move in the in-plane direction. In addition, the assessment of shear strength capacity of the walls reveals that shear damage may occur in the corner wall elements where east and west walls intersect with the north wall. These walls may have collapsed because of the collapse of the north wall or they may have collapsed due to the hammering effect of the adjacent buildings with different dynamic characteristics.

Both the finite element analysis and the kinematic mechanism analysis results indicate that the north wall is vulnerable to out-of-plane action and has a high potential to collapse. This is one of the analysis results which has complete match with the observed damage as it can also be seen in Figure 4.1-Figure 4.3.

Figure 4.1 Out-of-plane collapse of the north wall on the first floor

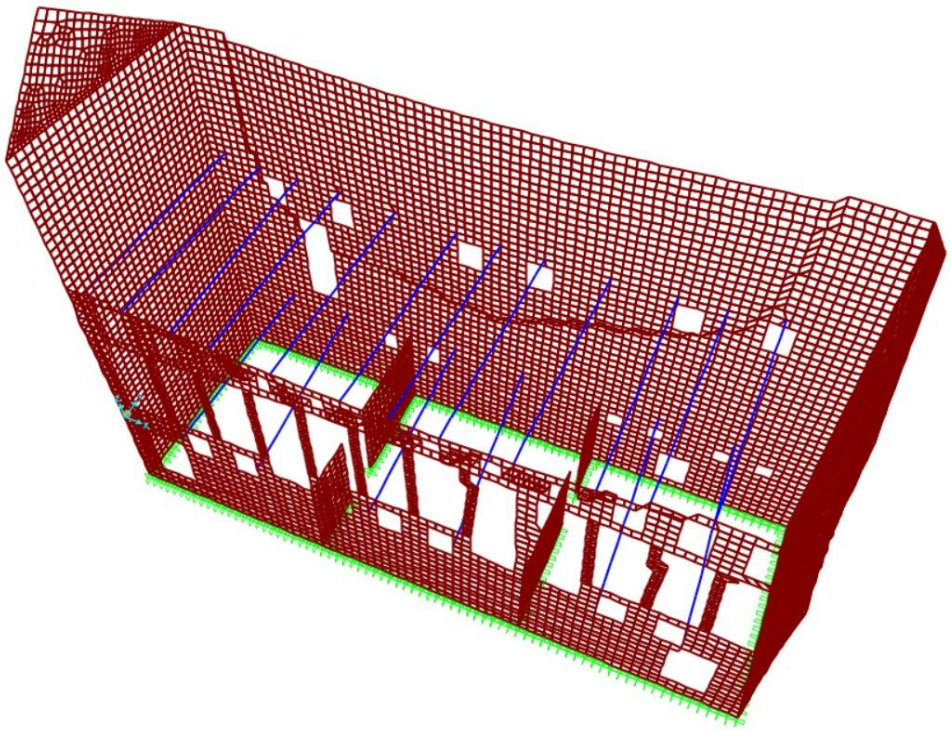

Figure 4.2 Deformed shape in the finite element model under critical loading condition

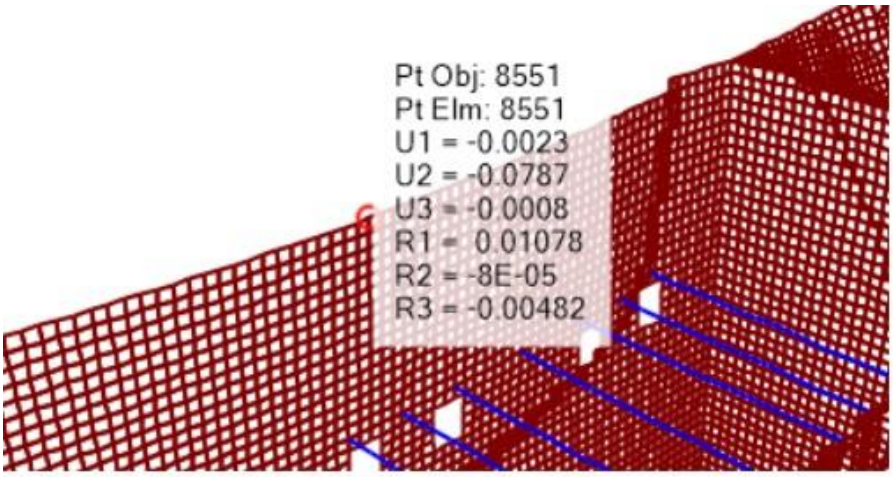

Figure 4.3 Drift in the north wall of the first floor according to the analysis results (U2=7.9 cm)

The ground floor walls have remained standing despite in-plane and out-of-plane damage. On the other hand, in the structural analysis, none of the ground floor walls seem to satisfy the shear strength criterion. When the drift analysis results of the north and south walls are examined, these walls are on the verge of collapse with a drift ratio of 0.95%. When these two analyses are evaluated together, it is expected that significant damage leading to collapse would occur in the ground floor walls. However, the actual damage is relatively lower compared to the analysis results. The main reason of this difference may be attributed to the existence of the adjacent buildings. These adjacent buildings limit the horizontal drift and change the damage state of the walls in both directions. As shown in Figure 4.4-Figure 4.5, in-plane wall damages are expected due to stress concentrations at the corners of the openings on the south facade of the ground floor, which has many openings. As shown in Figure 3.11 and Figure 3.15, the walls in this facade seem to violate the compression and shear strength checks under the effect of combined vertical and horizontal loads. In the post-earthquake damage, it is observed that the expected damage occurred at the corners of the doors of the rooms G01 and G02 opening to the courtyard (Figure 4.6). However, it is also necessary to mention the effect of the briquette wall separating

these two rooms. Although it is only taken into account as loads in the analysis, it is thought that this wall has considerable rigidity and forces the south facade out of plane. It is thought that the damage observed in Figure 4.6 is the result of a joint effect governed by in-plane and out-of-plane effects mentioned above. Another expected damage in the corners of upper window opening in the south wall of the ground floor was observed to have occurred after the earthquake (Figure 4.7-Figure 4.8).

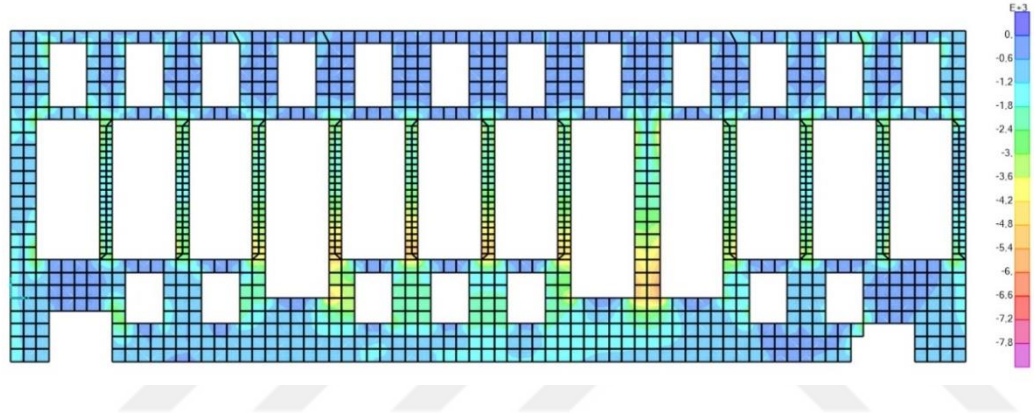

Figure 4.4 Compression stress distribution for the south wall in the ground floor

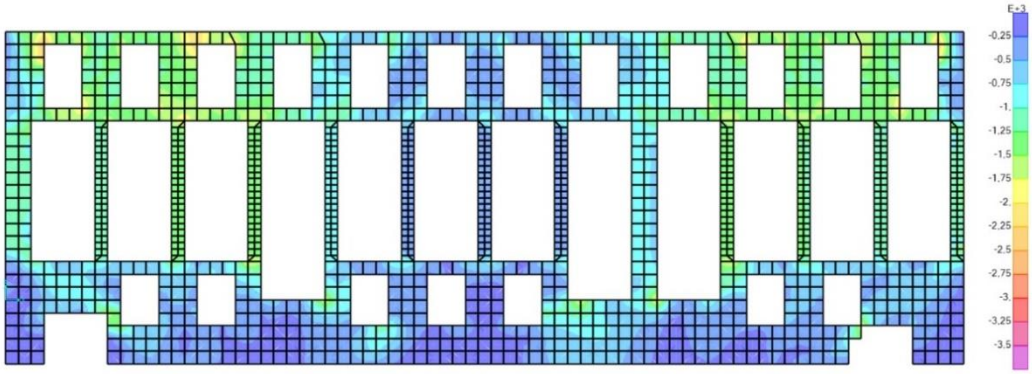

Figure 4.5 Shear stress distribution for the south wall of the ground floor

Figure 4.6 Observed earthquake damage for the south wall (METU TAÇDAM, 2023)

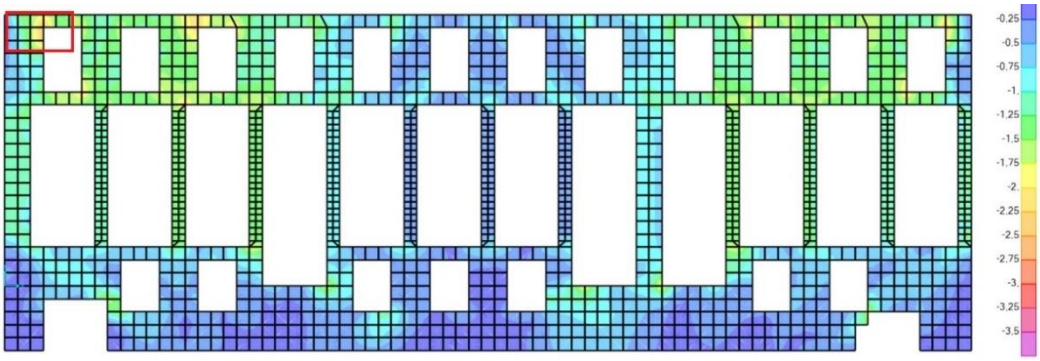

Figure 4.7 Expected shear failure in the upper corner of the openings in the south wall of the ground floor

Figure 4.8 Observed damage in the upper corner of the openings in the south wall of the ground floor (METU TAÇDAM, 2023)

The damage state of the basement floor could not be observed in detail after the earthquake due to security reasons (Figure 2.50). However, considering the member connections at the floor level adjacent to the basement, it is observed that there is no significant out-of-plane damage in the load-bearing walls. According to the results concerning the shear strength checks, it is expected from the north wall of the basement to suffer significant damage (Figure 4.9). This difference can be explained by the fact that the floor is partially under the ground in reality and therefore it is exposed to lower earthquake forces than assumed in the free-standing numerical model. The constraining effect of the adjacent buildings is valid also on this floor as well as in the entire building.

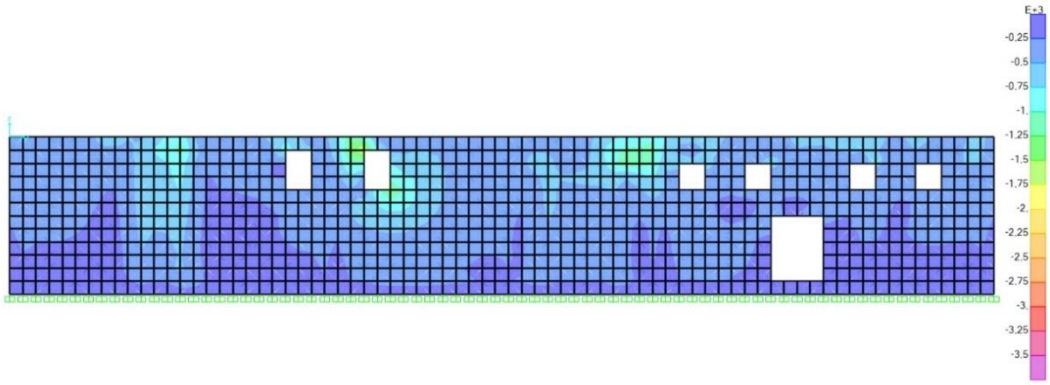

Figure 4.9 Shear stress distribution for the north wall of the basement floor

A recent study regarding the performance of traditional Antakya houses after the 2023 earthquake sequence (Rifaioglu *et* al. 2024) states that the presence of niches and timber frames embedded into masonry walls enhanced the seismic behavior of these buildings and stood intact even if the surrounding wall was heavily damaged or collapsed (Figure 4.10).

Figure 4.10 The superior performance of niches and timber frames embedded into masonry walls during the 2023 earthquakes (Rifaioğlu *et* al. 2024)

On the other hand, the analysis results show that the regions of niches where the wall section is reduced exhibit inferior performance in the case of both vertical and

horizontal load analysis (Figure 4.11). It is not easy to make definite statements regarding the actual performance of these regions after the earthquake since the real damage had been concentrated in some other regions with more critical deficiencies. However, Rifaioğlu *et* al. (2024) are right in the sense that if these timber prisms embedded in the niches on the wall are connected to each other by timber tie beams at the lintel and plinth level and form a framed structure for additional resistance to horizontal forces, then they can contribute to overall strength of the structure in addition to the load-bearing walls just like a confined masonry structure.

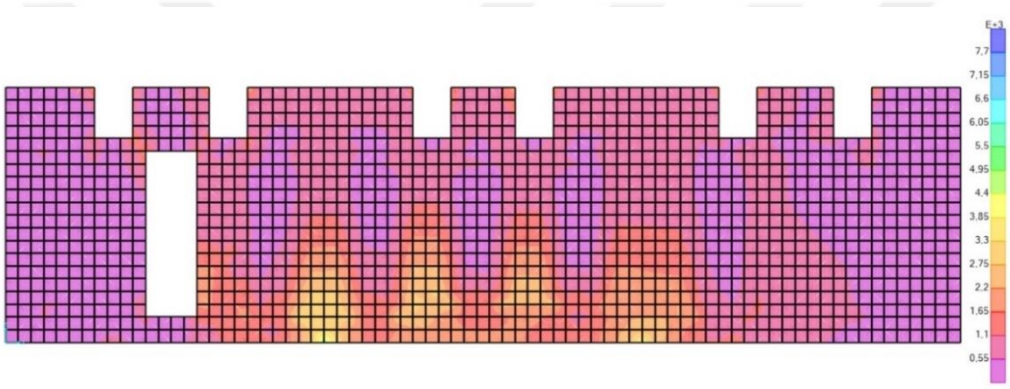

Figure 4.11 Stress concentration in the niches in the north wall of the ground floor

4.2 Intervention Strategies for the Beştek House

As explained in detail in the sections above, the structural weaknesses of the Beştek House can be reasoned as low strength of the load-bearing masonry walls, the inadequacy of the wall sections especially in the niches, the lack of rigid diaphragm effect, the effect of the architectural design of the south facade on the structural behavior and the effects of partition walls. In addition to the stand-alone properties of the structure, according to the comparison of the results of the numerical analysis and the damages observed after the earthquakes, the adjacent structure effect both

contributed to the survival of the building by limiting the horizontal displacements and damaged the structure due to the different dynamic characters of the structures and the hammering effect.

In case a strengthening study is to be carried out for Beştek House, a structural analysis should be carried out in which the basement of the building and the adjacent buildings are modelled together must be taken into account. To do that, structural analyses should be supported by laboratory and field studies. The following evaluations presented can be taken into consideration for the strengthening strategies for Beştek House. The desired performance level should be achieved by minimum intervention to the structure while conserving the architectural character as far as possible. In the intervention, the floor levels, building heights and rigidity properties of the adjacent buildings should be considered together with Beştek House.

First of all, it can be stated that the low masonry wall strength was effective in the earthquake damage of the building. In the modelling, the modulus of elasticity was taken as 2.85 MPa which is the minimum value in the study of Bozyigit *et* al (2024). In case of taking this value as 4.6 MPa which is the maximum value in the same study, the drift ratios of the walls are given in Table 4.1

Table 4.1 Drift ratios of the walls having modulus of elasticity (E) equal to: 4.6MPa

Wall	Height of the Wall (m)	Displacement (m)	Displacement Ratio (%)	Check (Before Collapse) (%1)	Check (Controlled Damage) (%0,7)	Check (Limited Damage) (%0,3)
Basement North	2,40	0,003	0,13%	✓	✓	✓
Basement West	2,40	0,001	0,04%	✓	✓	✓
Basement South	2,40	0,002	0,08%	✓	✓	✓
Basement East	2,40	0,001	0,04%	✓	✓	✓
Basement Partition West	2,40	0,002	0,08%	✓	✓	✓
Basement Partition East	2,40	0,001	0,04%	✓	✓	✓
Ground North	6,60	0,025	0,52%	✓	✓	X
Ground West	6,60	0,010	0,21%	✓	✓	✓
Ground South	6,60	0,026	0,56%	✓	✓	X
Ground East	6,60	0,012	0,26%	✓	✓	✓
First North	9,80	0,045	0,63%	✓	✓	X
First West (with Gable)	11,80	0,023	0,25%	✓	✓	✓
First East(with Gable)	11,80	0,020	0,15%	✓	✓	✓

It is seen that limited damage occurs in the walls shown in yellow color code only with the increase in wall strength even without the effect of rigid diaphragm. It is known that mortar strength is important in masonry wall strength (Lenczner 1972, Sahlin, 1971, Schneider, 1980). If the walls are rebuilt with a stronger and compatible mortar with original units, the desired performance level can be achieved.

Another important factor is the lack of rigid diaphragm effect. Table 4.2 presents the drift values that occur in the walls under the same loadings when the slabs are modelled as rigid diaphragms. In this case, without increasing the modulus of elasticity in the masonry walls, no controlled damage or collapse prevention damage level is exceeded in any wall. It is seen that only the first-floor walls would have faced limited damage.

Table 4.2 Drift ratios of the walls with rigid floor diaphragm effect in both floors (E:2.85 MPa)

Wall	Height of the Wall (m)	Displacement (m)	Displacement Ratio (%)	Check (Before Collapse) (%1)	Check (Controlled Damage) (%0,7)	Check (Limited Damage) (%0,3)
Basement North	2,40	0,001	0,04%	✓	✓	✓
Basement West	2,40	0,001	0,04%	✓	✓	✓
Basement South	2,40	0,001	0,04%	✓	✓	✓
Basement East	2,40	0,001	0,04%	✓	✓	✓
Basement Partition West	2,40	0,001	0,02%	✓	✓	✓
Basement Partition East	2,40	0,001	0,04%	✓	✓	✓
Ground North	6,60	0,006	0,11%	✓	✓	✓
Ground West	6,60	0,005	0,10%	✓	✓	✓
Ground South	6,60	0,005	0,10%	✓	✓	✓
Ground East	6,60	0,006	0,11%	✓	✓	✓
First North	9,80	0,026	0,63%	✓	✓	X
First West (with Gable)	11,80	0,031	0,50%	✓	✓	X
First East(with Gable)	11,80	0,023	0,33%	✓	✓	X

If it would be desired to provide the rigid diaphragm effect in Beştek House, it should be considered to preserve the steel beams, which represents the transition from traditional construction techniques to new techniques introduced in the 19th century. The connections of these steel beams to the wall can be improved. In the slab, adding steel beams in the orthogonal direction to the existing beams with similar rigidity properties can be considered as an option. This can be provided by constructing surrounding steel beams at the slab level. As such, existing steel beams can be fixed to these new horizontal beams. In the improvement of steel elements, the inclined positioning of steel beams can also be corrected.

There are studies showing that the rigid diaphragm effect is provided by reinforcing existing timber floors with timber elements. According to the study of Mirra (2021), existing timber floors reinforced with timber elements perform better than a reinforced concrete floor. In Beştek House, the rigid diaphragm effect, which is critical in masonry buildings, can be achieved by reinforcing the existing timber slab elements with timber elements perpendicular to them. To do that cement-based floor coverings on the ground floor rooms G01 and G02 should be removed. Strengthening of the slabs by ensuring rigid diaphragm effect should be thought together with the

strengthening of the masonry walls. Strengthening of the slabs should not result in extra stress concentration in the walls which are already weak.

It can be asserted that the architectural design of the south facade of the building causes important weaknesses in structural behavior. Both the south wall of the ground floor with many openings and the timber facade of the first floor have a critical effect on the structural behavior of the building. The south facade of the ground floor makes the masonry piers and spandrels in this wall weak against both compression and shear, as explained in Section 3.3 and Section 4.1. If the elements in this area were constructed with solid cut stones along the section, this weakness can be reversed by ensuring that the elements in this area work like columns and beams as in the frame structures. Since the south facade of the first floor was designed as timber, the box-like behavior, which is important for masonry structures, cannot be provided on the first-floor walls. Walls of the first floor work as cantilever walls and are decisive in the building's behavior. In order to improve the load transfer mechanism and to improve the modal movement of the building timber beams connecting the first floor east and west walls continuing along the facade in the with vertical connections to the ground floor and roof can be used.

Another critical factor in the out-of-plane behavior of the building's facade walls is that the walls are not supported orthogonal to their axes. In the basement floor, the connections of the masonry partition walls to the north and south walls can be improved. The briquette partition walls on the ground floor, which have different rigidity properties with the facade walls, can be removed. Instead, masonry walls or lighter timber panel walls can be constructed. There is no partition wall on the first floor. Timber or masonry walls similar to the mentioned for the ground floor can be considered on this floor, as well.

4.3 Intervention Strategies for Historical Antakya Houses

Since Antakya has been a multicultural settlement region since ancient times, it possesses a highly specialized and traditional building construction experience. The Beştek House is a typical example of this traditional construction practice with its unique characteristics. The structural deficiencies of the Beştek House that have been explained in the previous sections can be handled by taking proper countermeasures. The primary aim of intervention strategies for historical structures is to protect them from harmful environmental conditions, impacts, and destructive earthquakes while adhering to the principles of conservation. In this context, structural safety of the Beştek House against seismic action focuses on two major goals: ensuring that the structure satisfies the specified performance level for its intended use and preserving its historical significance, including its original materials and character. Accordingly, the seismic performance of the Beştek House (and similar timber framed stone masonry buildings in the region) can be improved by focusing on the interventions to overcome the inherent deficiencies of the structure. For instance, the rigid floor diaphragm action can be maintained by improving the timber floors with additional timber elements that allows the load transfer to walls in both orthogonal directions. In addition to this, wall-to-floor connections can be improved by specific connection details in order to ensure the integrity of horizontal and vertical structural members. Another intervention alternative for this structural typology can be to improve the out-of-plane capacity of stone masonry walls by improving the existing wall-to-wall connections and placing additional walls in normal direction in order to reduce the unsupported length of the wall. Timber roof structures should also be improved by replacing the degraded timber members due to moisture and termite action and also improving the joints of the roof truss system. Finally, it should be mentioned that traditional timber prisms used as niches should be connected to each other by timber frame members at the lintel and plinth level in order to construct a timber frame within the stone masonry wall. This timber frame can assist the walls in carrying the lateral loads and also to keep the integrity of the structure just like in

the case of confined masonry buildings. The timber frames used for framing between the prisms should be checked regularly and replaced in the case of material deterioration.

CHAPTER 5

CONCLUSION

This thesis study focuses on a historical Antakya House, named as the Beştek House, which sustained heavy damage and experienced partial collapse during the 2023 Kahramanmaraş, Türkiye earthquake sequence. The Beştek House is a traditional building with unique architectural and structural characteristics. These specific construction features may affect the seismic performance of the structure in a positive or negative manner. The main target of this study is to examine the seismic performance of traditional Antakya buildings specific to the Beştek House as a case study building. In the first part of the thesis, the Beştek House is introduced with all its inherent architectural and structural features. Then the seismicity of the Antakya region is explained with a special emphasis to the 2023 Kahramanmaraş Türkiye earthquake sequence, which is an extraordinary earthquake disaster with multiple destructive events that produced very high seismic demands in the region. Next, the numerical modelling of the Beştek House is explained with all the assumptions and simplifications. The seismic analysis approach is presented together with the loading cases involved during the analysis. After that, the analysis results in terms of drift, strength and mechanism checks are demonstrated with a detailed comparison of the obtained response to the observed damage during the 2023 earthquake sequence. The last part of the study is devoted to a general evaluation regarding the seismic performance of the Beştek House in the context of the developed numerical model.

Briefly, it can be stated that the thesis study provides an important contribution to the literature by presenting the importance of pre-disaster and post-disaster documentation of cultural heritage, local structural deficiencies of traditional Antakya houses, their unique dynamic behavior and the intervention methods that can be applied to such historical structures.

Notwithstanding the limitations and gross assumptions that have been considered during the modelling and analysis stages, the following conclusions can be stated at the end of this study:

- The Beştek House is a historical building in Antakya with inherent traditional and local construction techniques. It is a hybrid structure with different construction techniques employed with multiple materials during the interventions at different periods in the past. Since the building was documented in great detail before the earthquake and after the earthquake as much as possible, the geometrical properties of the building are exactly conveyed to the idealized numerical model, which is a very important advantage for the success in structural modelling and the validity of the obtained numerical response compared to the actual behavior. Hence it can be concluded that for successful seismic performance evaluation of specific and traditional structures, detailed documentation of architectural and structural features is crucial.
- The Beştek House has important structural features that enhance or impair its seismic behavior. One of the major issues is the absence of rigid diaphragm action of the floors. This hinders the box-like behavior of the structure, proper distribution of the lateral loads from floors to the vertical structural members and especially the out-of-plane capacity of the masonry walls. Another negative aspect related to the structure is the too many openings along the south facade of the ground floor. Since load-bearing walls between these openings constitute only a limited portion of the total length of this facade, it is expected that these wall parts are critical in resisting both vertical and horizontal loads. Another important deficiency can be regarded as the reduced cross-sectional properties of the walls at the niches, which develop weak zones during load transfers. On the other hand, the adjacency of the Beştek House to nearby structures in the east-west direction seems to compensate for some part of the inferior behavior by constraining the structure and the wall components and not allowing them to drift as they

would have experienced in a stand-alone building and assuming that the hammering effect due to adjacency creates a minor issue. These observations are also supported by the analysis results.

- The results obtained from the analysis of the structural model seem to agree with the observed damage to some extent. For instance, the out of plane vulnerability of the north wall in the first floor, which had partially collapsed during the earthquake sequence, can be directly predicted from the results of the finite element and kinematic mechanism analyses. The insufficient vertical and shear force capacity of the slender wall parts between the openings in the ground floor can be realized during the performance assessment studies by using the analysis results. However, it should be mentioned that the linear elastic analysis method and the macro modelling approach for masonry walls possess many simplifications and assumptions, and it is not possible to capture the exact damaged behavior with these simplified tools, especially localized and specific damage modes that belong to different types of structural components and their connections. However, applied modelling and analysis seem to be successful in capturing the locations and types of major critical parts of the structure.
- As also stated above, the adjacency of the Beştek House to nearby structures seems to have a major effect on the seismic performance of the structure. However, the structural model is developed by assuming a stand-alone building that is free to translate in all directions. This eventually makes the comparison between the predicted and the observed damage difficult, but since there is no detailed information about the structural properties of the adjacent buildings, it is not possible to model these buildings as an aggregate block structure.
- The analysis results show that the regions of niches where the wall section is reduced exhibit inferior performance in the case of both vertical and horizontal load analysis. However, this niches in which timber prisms are embedded as a traditional construction feature of Antakya Houses, can

contribute to overall strength of the structure in addition to the load-bearing walls just like a confined masonry structure if these timber prisms embedded in the niches on the wall are connected to each other by timber tie beams at the lintel and plinth level and form a framed structure for additional resistance to horizontal forces.

- Although it cannot be evaluated as a data input for modelling and analysis, the workmanship quality and local applications in construction technology are very important parameters to be taken into consideration in structural condition assessment of historical structures. The performance of masonry structures is directly related to the wall coursing and local connections between members. The incorporation of such details to the analysis requires more information about the structure and a more detailed modelling approach but these features can lead to closer results to the actual behavior of the considered structure.
- The structural deficiencies of the Beştek House can be handled by taking proper countermeasures with the primary aim of protecting these structures from harmful environmental conditions, impacts, and destructive earthquakes while adhering to the principles of conservation. Accordingly, the seismic performance of the Beştek House (and similar timber framed stone masonry buildings in the region) can be improved by focusing on possible interventions (maintaining rigid floor diaphragm action by additional timber elements, enhancing wall-to-floor and wall-to-wall connection details, increasing the out-of-plane capacity of the stone masonry walls, improving the members and joints in timber roofs and forming timber frames embedded into walls by lintels and prisms as niches) to overcome the inherent deficiencies of the structure.
- This thesis study shows the importance of assessing the actual performance of historical and traditional buildings in earthquake prone regions to preserve cultural heritage and how challenging it is to obtain realistic seismic response through analysis since these structures are unique, have complex load transfer

paths with many different types of structural and non-structural members and the special connections between these members. Hence a trade-off between the accuracy of the model and the computational cost should be maintained for a successful performance assessment study. The structural analysis should be supported by field and laboratory tests to obtain specific geometrical and material properties of the investigated building since the validity of the developed model mainly depends on the realization of these parameters as input variables to the analysis platform.

- It is asserted that the great destruction in Antakya is related to the poor quality of mortars. Studies can be carried out that examine the change in the properties of mortars over time under atmospheric conditions of the city. These studies should also consider global climate change and possible effects on Antakya. Interventions to the historical buildings should consider these and similar academic studies.
- Due to the unique and complicated nature of historical structures, a wide range of expertise is required for condition assessment of such heritage. Therefore, all the related studies should be carried out in an interdisciplinary manner by including experts from different fields like architecture, conservation of cultural heritage, structural engineering, material engineering, geotechnical engineering and geological engineering (for earthquake-related issues). In addition, a methodological approach for pre-event and post-event data collection is crucial and invaluable to assess the actual behavior and performance of unique historical structures. For the specific case of Beştek House, these data have been collected in a very detailed manner before and after the 2023 Türkiye earthquake sequence. Hence, even if the building is demolished after the earthquake, pre-earthquake and post-earthquake documentation can be used for research purposes in the future.

This study has a limited scope as explained in the previous sections. Some recommendations can be stated for future research as follows:

- More detailed modelling techniques can be employed in order to get closer results to the actual behavior. Special features like connections between different members, niches with their timber elements can be incorporated to the model in order to model the load transfer paths within the building.
- Nonlinear static and dynamic analysis can be applied to the structural model in order to examine the damage mechanisms under seismic action and then compare them with the observed damage.
- The effect of the underground historical layer on the seismic performance of the structure can be examined by modelling the foundation in a more detailed manner by using the pre-event documentation of the building.
- The building under consideration can be modelled as an aggregate with the adjacent buildings to examine the unified dynamic behavior of these buildings as a block. In order to achieve this task, all the geometrical and material properties of the adjacent structures should be obtained.
- The numerical models for the strengthened building with different intervention techniques can be modelled and the results can be compared with the existing condition of the building to evaluate the effectiveness of each intervention technique.

REFERENCES

AFAD (Disaster and Emergency Management Presidency, Republic of Türkiye) - For strong ground motion records https://tadas.afad.gov.tr/

AFAD, 2023. 06 Şubat 2023 Pazarcık-Elbistan (Kahramanmaraş) Mw: 7.7 – Mw: 7.6 Depremleri Raporu. 140 s. (in Turkish)

Akyuz, HS., Altunel E., Karabacak V., Yalciner C.C. (2006). Historical earthquake activity of the northern part of the Dead Sea Fault Zone, southern Türkiye, Tectonophysics 426 (3-4), 281-293

Ambraseys, N. (1989): Temporary seismic quiescence: SE Turkey, Geophys. J., 96, 311-331.

Ambraseys, N. (2009). Earthquakes in the Mediterranean and Middle East, Cambridge Press

Arya A, Boen T, Ishiyama Y, Martemianov A, Meli R, Scawthorn C, Vargas J, Yaoxian Y. (1986). Guidelines for earthquake resistant non-engineered construction. The International Association for Earthquake Engineering, Tokyo.

Askan, A., Altindal, A., Aydin, M.F., Erberik, M.A., Koçkar, M.K., Tun, M., Balaban, M.S., Uygucgil, H., Kop, A., Karimzadeh, S. and Mutlu, S., (2024). Assessment of urban seismic resilience of a town in Eastern Turkiye: Turkoglu, Kahramanmaras before and after 6 February 2023 M 7.8 Kahramanmaras earthquake. Earthquake Spectra.

Beyen K., Erdik M., Mazmanoğlu C., Ekmekçioğlu, Z. (2003). Antakya'nin Geçmişten Günümüze Sismik Aktivitesi ve Yapilmasi Gerekenlerin Bir Uluslararasi Konferansin Işığında Değerlendirilmesi Türkiye Mühendislik Haberleri, Sayı 423 (in Turkish)

Bozyigit, B., Ozdemir, A., Donmez, K., Dalgic, K. D., Durgut, E., Yesilyurt, C., ... & Acikgoz, S. (2024). Damage to monumental masonry buildings in Hatay

and Osmaniye following the 2023 Türkiye earthquake sequence: The role of wall geometry, construction quality, and material properties. Earthquake Spectra.

D'Ayala D., Speranza E. (2003). Definition of collapse mechanisms and seismic vulnerability of historic masonry buildings. Earthquake Spectra, No. 19, pp. 479-509.

Demir, A. (2004). "The urban Pattern of Antakya: Streets and Houses, Topoi Supplement 5: Antioche de Syrie Histoire, Images et Traces de la ville antique, 221-238.

Downey, G. (1961). A History of Antioch in Syria: From Seleucus to the Arab Conquest, Princeton University Press.

EERC (2023). Preliminary Reconnaissance Report on February 6, 2023 Kahramanmaras Pazarcık (Mw= 7.7) and Elbistan (Mw=7.6) Earthquakes. Ankara: Middle East Technical University.

EMS98 - Grünthal, G. (editor) (1998). European macroseismic scale 1998. Cahiers du Centre Européen de Géodynamique et de Séismologie. Conseil de l'Europe. Luxembourg, 1998.

Ersoy, Ş. (2009). Doğu'nun Kraliçesi Antakya'da Depremler Devam Edecek mi? (1. Bölüm Jeolojik Yapı ve Tarihsel Depremler). Hatay Keşif (Aylık Kültür ve Keşif Dergisi) (in Turkish)

Guideline for Earthquake Risk Management of Historical Structures. (GERMHS, 2017). Directorate General of Foundations

Hendry AW, Sinha BP, Davies S.R. (2006). Design of masonry structures. Taylor and Francis, London.

ITU, 2023. 6 Şubat Depremleri Nihai Rapor, İstanbul Teknik Üniversitesi (in Turkish) https://haberler.itu.edu.tr/docs/default-source/default-document-library/2023_itu_subat_2023_deprem_son_raporu.pdf?sfvrsn=1583fe76_2

KOAERI, 6 February 2023 (04:17) Kahramanmaraş - Gaziantep Türkiye M7.7 Earthquake, 6 February 2023 (04:17 GMT+03:00) Strong Ground Motion and Building Damage Estimations Preliminary Report (v6)

Lenczner, D. (1972). Elements of Loadbearing Brickwork. Pergamon Press.

Lourenco, P. B. (1996). Computational Strategies for Masonry Structures. (PhD Thesis). Delft Technical University, Holland

Lourenco, P. B. (2008). Structural masonry analysis: recent developments and prospects, University of Newcastle, Australia

METU CONS 506 – Design in Architectural Conservation Studio Course, (2019-2020). METU Department of Architecture, Graduate Program of Conservation of Cultural Heritage

METU TAÇDAM (2023) Antakya'nın Çok Katmanlı Kültürel Mirasının Deprem Sonrası Belgelenmesi, Hasar Tespiti ve Değerrlendirilmesi. Ankara: Middle East Technical University. (in Turkish)

Mirra, M, Ravenshort, G. (2021). Optimizing Seismic Capacity of Existing Masonry Buildings by Retrofitting Timber Floors: Wood-Based Solutions as a Dissipative Alternative to Rigid Concrete Diaphragms, Buildings, 11, 604

Pamir, H. (2009). Alalakh'dan Antıokheıa'ya Hatay'da Kentleşme Süreci/Urbanization Process in Hatay From Alalakh To Antioch. Mustafa Kemal Üniversitesi Sosyal Bilimler Enstitüsü Dergisi, 6(12), 258-288. (in Turkish)

Pinon, P. (2004). "Survivances Et Transformations Dans La Topographie D'Antioche Apres L'Antiquite", Topoi, Suppl. 5, pp. 191-219.

Rifaioğlu, M.N. (2012) An Enquiry Into the Definition of Property Rights in Urban Conservation: Antakya (Antioch) From 1929 Title Deeds and Cadastral Plans, PhD Thesis, METU

Rifaioğlu, M. N., Hurol, Y., & Şahali, Ö. (2024). Traditional Know-How for Earthquake Resistance: The Logical Framework of Coffered Wall and Ceiling Systems in Historical Antakya Houses. International Journal of Architectural Heritage, 1-20.

Roca, P., Cervera, M., Gariup, G., and Pela, L. (2010). Structural Analysis of Masonry Historical Constructions. Classical and Advanced Approaches. Archives of Computational Methods in Engineering; 17: 299-325

Sahlin, S. (1971). Structural Masonry. Prentice Hall, Englewood Cliffs, NJ.

Sandalcı, M. (2005). İskenderun Dekovil Hattı, Osmanlı Bilimi Araştırmaları, 6.2, 287-297. (in Turkish)

SAP2000 (v21.1.0). Integrated Software for Structural Analysis & Design, Knowledge Base, Computers and Structures Inc. California, USA.

Sauvaget, J. (1935). Le Plan de Laodicee-Sur-Mer, Institut Francais de Damas, Bulletin d'etudes Orientales, vol4, Cairo,

Sbeinati, M. R., Darawcheh, R., & Mouty, M. (2005). The historical earthquakes of Syria: an analysis of large and moderate earthquakes from 1365 BC to 1900 AD. Annals of Geophysics.

Schneider R.R., Dickey W.L. (1980). Reinforced Masonry Design. Prentice Hall Inc., Englewood Cliffs, New Jersey.

Turkish Building Seismic Code (2018). Ankara: Turkish Ministry of Interior Disaster and Emergency Management Presidency.